NOAA Technical Memorandum OAR PMEL-118

Long-Term Studies of Particulate Flux On and Near the Juan de Fuca Ridge

D.A. Tennant[1], E.T. Baker[1], A.J. Paulson[2], R.A. Feely[1], and G. Lebon[3]

[1]Pacific Marine Environmental Laboratory
7600 Sand Point Way NE
Seattle, WA 98115-6349

[2]NE Fisheries Science Center/NMFS
James J. Howard Laboratory
74 Magruder
Highlands, NJ 07732

[3]Joint Institute for the Study of the Atmosphere and Ocean (JISAO)
University of Washington
Box 351640
Seattle, WA 98195

January 2001

Contribution 2118 from NOAA/Pacific Marine Environmental Laboratory

NOTICE

Contribution No. 2118 from NOAA/Pacific Marine Environmental Laboratory

For sale by the National Technical Information Service, 5285 Port Royal Road
Springfield, VA 22161

Contents

List of Figures

List of Tables

Long-Term Studies of Particulate Flux On and Near the Juan de Fuca Ridge

D.A. Tennant[1], E.T. Baker[1], A.J. Paulson[2], R.A. Feely[1], and G. Lebon[3]

Abstract. Sequentially sampling sediment traps were deployed in the region of the Cleft segment of the Juan de Fuca Ridge from 1984 to 1991 to gain a better understanding of the vertical flux of particles from hydrothermal plumes. Most traps collected ten sequential subsamples spanning a total deployment time of nearly a year. Data from four of the moorings (V18, V24, V26, and V43) were binned and averaged by trap depth to estimate the mean total flux from above and below the hydrothermal plume. Total flux in traps above 2100 m was 25.6 ± 44.6 mg m^{-2} day^{-1}; below 2100 m the mean flux was 30.4 ± 37.1 mg m^{-2} day^{-1}. The flux of hydrothermal particles enriched in Fe, Mn, P, V, S, and Cu at North Cleft moorings near Monolith and Pipe Organ vents showed a greater increase as a function of depth than did the total flux. Flux of these elements was 2 to 5 times greater below the plume than above but their combined flux was not great enough to account for the total flux increase at the bottommost traps. A combination of hydrothermal input and resuspended sediments may account for the near-bottom flux increase. Total and elemental fluxes generally increased at all depths during the spring and fall surface plankton blooms. Typical fluxes during non-bloom periods were 10 to 25 mg m^{-2} day^{-1}, while peak fluxes during blooms were generally 40 to 150 mg m^{-2} day^{-1}. Al, Si, P, Fe, and Mn fluxes increased by factors of 3 to 9 during bloom periods. Microscopic examination of trap samples indicated that organic aggregates were a common constituent. We suggest that organic aggregates produced in the euphotic zone account for the increase in hydrothermal sedimentation following surface blooms because these aggregates scavenge hydrothermal particles from the plume during the vertical descent and transport them to the seafloor.

1. Introduction

Seafloor hydrothermal venting on the Juan de Fuca Ridge (JDFR) has been observed, measured, and documented over the last several years by many investigators. Initial research and discovery was reported by Delaney *et al.* (1981), Normark *et al.* (1983), and Lupton *et al.* (1985).

Pacific Marine Environmental Laboratory (PMEL) began broad-based scientific investigations of hydrothermal venting on and near the JDFR in 1984. The JDFR is located approximately 500 km off the northwestern coast of the United States between the Blanco and Sovanco fracture zones (Fig. 1). One area of research PMEL has concentrated on has been the elucidation of the chemical and physical nature of the hydrothermal plumes associated with active seafloor vents. This study focused on hydrothermal plumes on the Cleft segment (Fig. 1), one of the most hydrothermally active tectonic segments on the JDFR (Baker and Hammond, 1992). High velocity (~0.1 to ~1.0 m s^{-1}) hot water, rich with dissolved minerals, discharges from deep-sea hot springs and produces clouds of fine-grained sulfide and sulfate precipitates. Edifices formed by the precipitated sulfides and sulfates

[1]NOAA/Pacific Marine Environmental Laboratory, 7600 Sand Point Way NE, Seattle, WA 98115

[2]NE Fisheries Science Center/NMFS, James J. Howard Laboratory, 74 Magruder Highlands, NJ 07732

[3]Joint Institute for the Study of the Atmosphere and Ocean (JISAO), University of Washington, Box 351640, Seattle, WA 98195

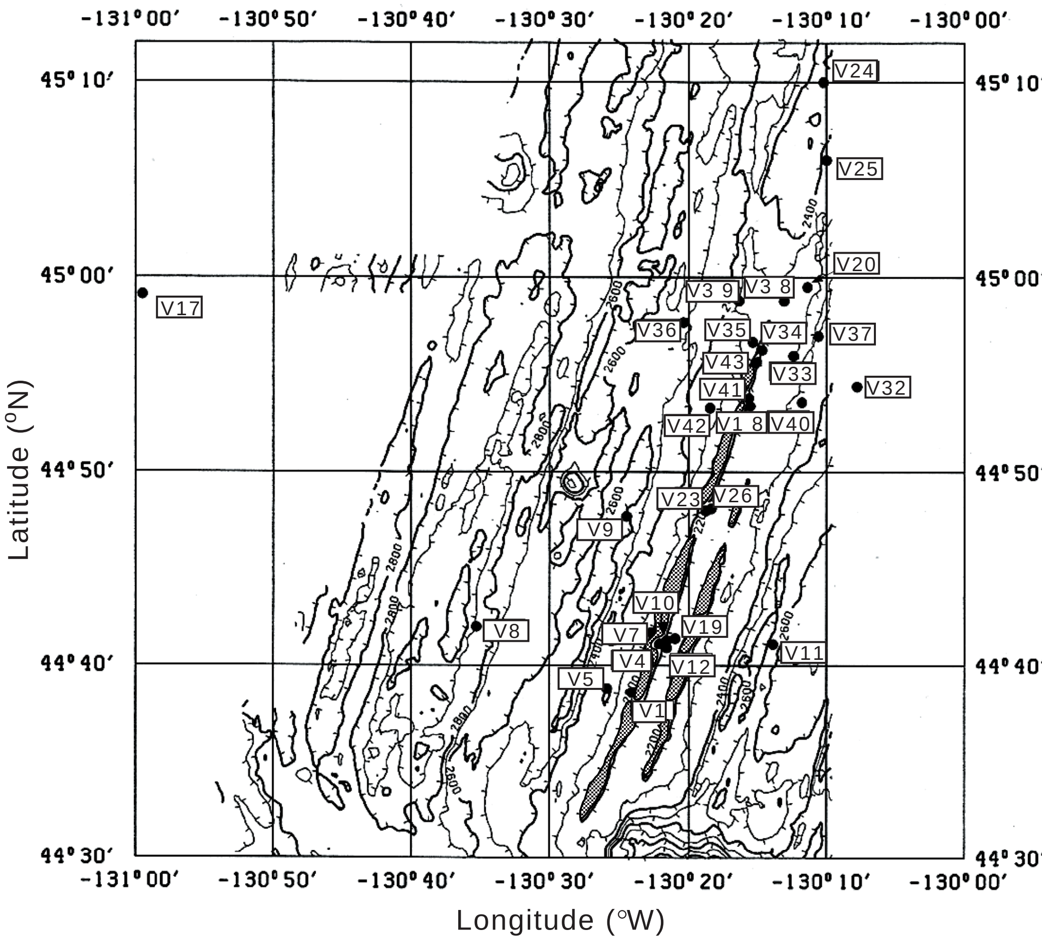

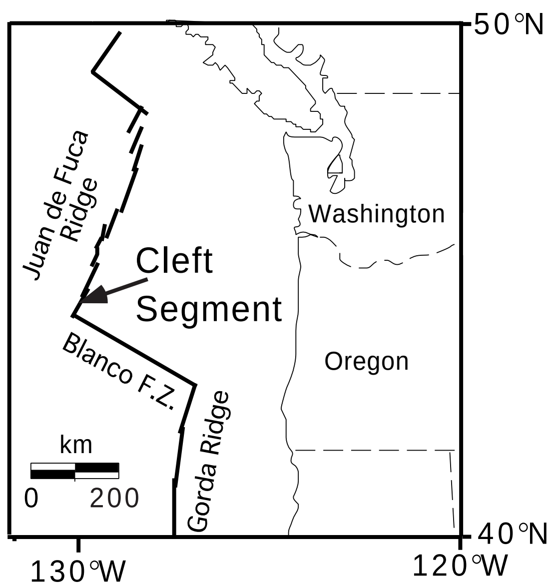

Figure 1: (Top) Bathymetry (100 m contour interval) and locations of sediment trap moorings. (Bottom) Location of Cleft segment on the Juan de Fuca Ridge. Note that the grey shaded area of the bathymetric map denotes the walls of the ridge with the axial valley between.

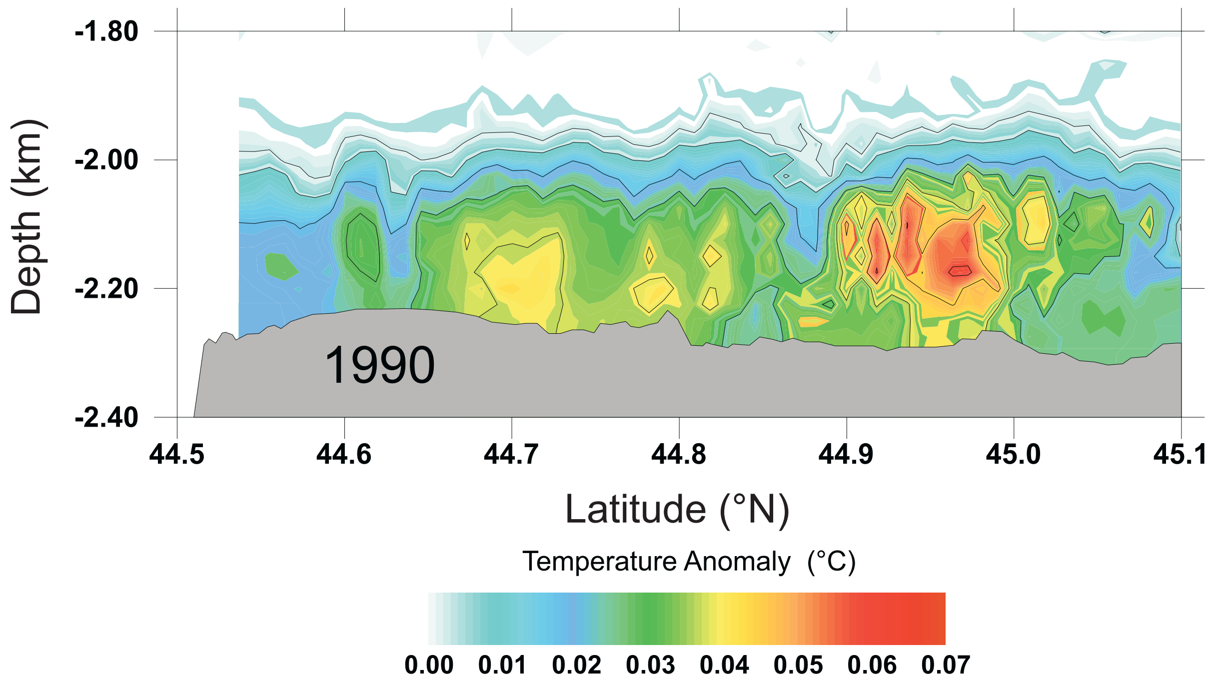

Figure 2: CTDT transect of hydrothermal temperature (°C) anomalies along the Cleft segment axial valley during summer 1990.

are commonly called black and white smokers, respectively. Hydrothermal particulates vented at Cleft segment of the JDFR characteristically include sphalerite, pyrite, sulfur, pyrrhotite, barite, cubanite, Fe oxyhydroxides, and chalcopyrite (Feely *et al.*, 1987). The elemental composition of the common minerals includes Cr, Cu, Zn, Mn, Fe, Al, Si, S, and P. The hot discharge mixes with ambient seawater and rises to a level of neutral buoyancy (Fig. 2) where the water and entrained particles are dispersed by the regional flow.

Two principal discharge areas are known on the Cleft segment. The south Cleft site is centered near 44°41′N and was discovered in 1981 (Normark *et al.*, 1983). The north Cleft site is centered near 44°57′N and was discovered in 1986 (Baker *et al.*, 1987). PMEL has been mapping the plume at south Cleft since 1984 (Baker *et al.*, 1985; Baker and Massoth, 1986; Baker, 1994; Feely *et al.*, 1994; Massoth *et al.*, 1994). Since 1986 our surveys extended to, and in most cases concentrated on, plumes associated with north Cleft vent fields (Baker, 1994). Plume mapping was accomplished by towing a CTD and beam transmissometer (CTDT) in a saw-tooth pattern through the bottom 400–800 m of water so that continuous measurements of hydrography and light attenuation were made. These up-down tows (Tow-yos) were conducted along and across axis; thus it was possible to produce a three-dimensional representation of the hydrothermal plume. Although there is interannual variation of the hydrothermal temperature and attenuation signals (both spatially and in magnitude), typically the Cleft hydrothermal plume temperature and attenuation anomaly maxima were about 100 ± 50 meters above bottom (mab). The maximum plume rise height is typically

~200 m at south Cleft and ~300 m at north Cleft (Baker, 1994). Plumes emanating from the Cleft segment tend to be entrained by regional flow along the strike of the axial valley from north to south and spread several kilometers east and west of the axial valley (Baker *et al.*, 1985; Cannon *et al.*, 1991).

This study was initiated to answer several questions regarding the vertical flux of particles within and above the hydrothermal plume. Specifically, the research had the following objectives:

1. To determine the vertical mass flux (VMF) of hydrothermal particulates at JDFR hydrothermal plume sites,

2. To characterize the chemical and physical nature of the hydrothermal plume particulates,

3. To determine whether there is a periodicity associated with the vertical flux of hydrothermal plume particles, and if so,

4. To determine what mechanisms regulate the periodicity.

Sequentially sampling sediment traps (Baker and Milburn, 1983) on taut wire moorings were placed above, within, and beneath the hydrothermal plumes at Cleft segment for periods of days to months to determine the VMF of the plume particles. Mooring deployment data is listed in Table 1.

Moorings were located within the axial valley and on the outer and inner flanks of the Cleft Segment; off-axis deployments were placed both east and west of the ridge (Fig. 1).

2. Methods

2.1 Predeployment Preparations

Sequentially sampling traps, which collect up to 10 samples per deployment at predetermined time intervals, were used in this study (Fig. 3). The traps have a teflon funnel (~0.2 by 0.5 m) which feeds into the opening of the sample jars. The plate into which the sample jars fit contains 11 holes to accommodate 10 sample jars and a blank space which is open to the funnel during deployment and recovery; such a configuration prevents the brine solution in the jars (see next paragraph) from washing out during deployment and recovery. This plate and sample jars comprise a carrousel which rotates via an attachment to a motor/timer. The funnel, sample jar carrousel, and motor/timer are housed within a 1.0 by 0.20 m PVC tube; the sample jars are 3.2 by 22.2 cm acrylic cylinders of ~200 ml capacity. Subsurface moorings fitted with acoustic releases were employed in all cases.

Prior to deployment the sample jars are filled with a dense brine to prevent the diffusion of preservative (formalin) from the sample jars when they are open to the funnel. A preservative is required to kill biota which alter the collected particulates (Knauer *et al.*, 1984; Wakeham *et al.*, 1993). Because our sediment trap collections were to be analyzed for metalliferous

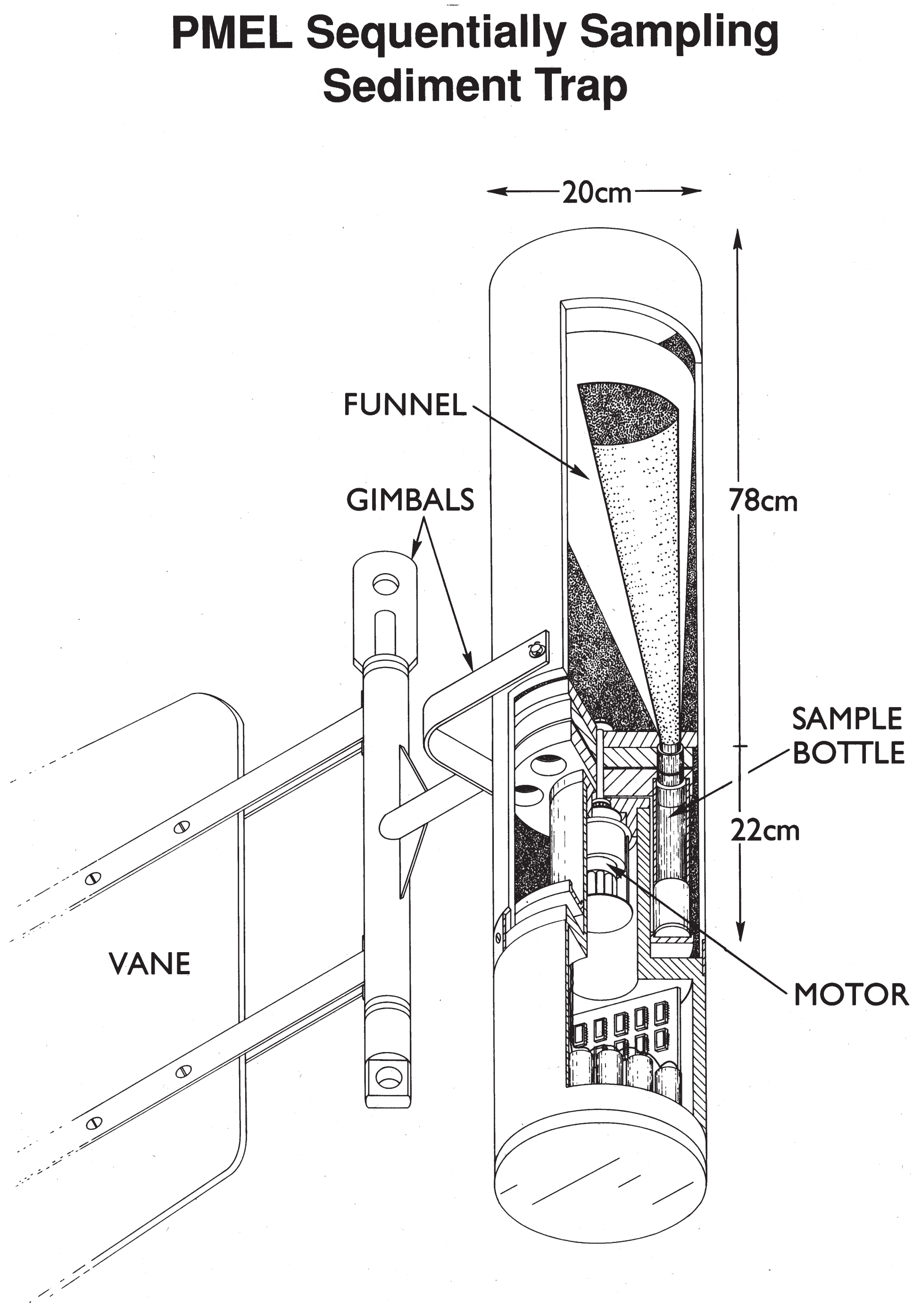

Figure 3: Diagram of sequentially sampling sediment trap used in this study. The vane orients the sediment trap upstream of the mooring line which attaches to the top and bottom of the vane gimbal (rearward of the two gimbal pivots shown).

precipitates, a careful cleaning procedure was carried out on the sediment trap brine/preservative solution to ensure freedom from contamination. A bed of Chelex-100 was first cleaned by rinsing it with 1 N HCl, adding several rinses of particle free water and adjusting it to pH 8 with 1 N NaOH. The sea water and formalin to be used as the sediment trap fill solution was then put through the Chelex-100 bed using slightly positive pressure. The salinity of the solution was then adjusted to approximately 85 ppt and enough $CaCl_2$ was added (0.76 g l^{-1}) to saturate the solution with calcium to prevent calcareous particulates from premature dissolution. The reagents used were Merck Suprapur®.

2.2 Deployment and Collection Strategies

Sediment traps were moored at several depths to determine the vertical flux of particles: (a) in ambient water above the hydrothermal plume; (b) at several locations within the hydrothermal plumes (~100 m above bottom), (c) close beneath the plume core, and (d) near bottom.

Several different experiments were conducted to observe vertical flux over short-term (hours to days) and long-term (year-long) periods. Most collections were long term to obtain continuous flux data over a year; a few short-term deployments were conducted to observe high-frequency flux trends.

2.3 Sample Storage

Recovered samples were retained in the sediment trap collection jars and stored in refrigerated picnic coolers in the cold box of the ship and then transferred to laboratory cold boxes until processing could begin. In some cases (Mooring V43) the supernate was sampled immediately upon trap recovery. Prior to processing, samples of the supernate of the sampling jars were collected for salinity, nutrient, and metal analyses.

2.4 Vertical Mass Flux Determination

Sediment trap samples were prefiltered through acid cleaned (24 hrs in 6N HCl bath) 406 mm mesh polyethylene screen to eliminate swimmers (see Knauer *et al.*, 1984; Wakeham *et al.*, 1993). During the first several years subsamples were produced with a Folsom splitter; in subsequent years with a Walker splitter (Tennant *et al.*, 1987) to provide more aliquots. The Folsom splitter is a binary splitter; if more than two aliquots are required, the initial ones must be resplit. As many as ten aliquots are provided with the Walker splitter. In almost all cases at least two aliquots were produced for vertical flux measurements and elemental analyses. Mass determinations were done by vacuum filtering a known fraction of the sample through preweighed 47 mm 0.4 μm pore Nuclepore membranes that were subsequently dried and reweighed. Vertical mass flux (VMF) (mg m^{-2} day^{-1}) was calculated from the following relationship:

m = Measured mass of cylinder contents (mg)
a = Collection area of the sediment trap (m^2)
t = Collection period (days)
VMF = m/ta

The Si concentrations in the supernates of the sampling jars after recovery indicated the opal had dissolved into the sampling jar solution between collection and processing. We were able to approximate the amount of this loss in some cases. When possible (during the processing of the V34 mooring samples only), the VMF was corrected by adding back to the VMF value the amount of Si which we determined had dissolved. This method for accounting for the sample loss due to dissolution into the brine solution is described below.

2.5 Microscopic Examination

Several samples of each sediment trap were given a cursory microscopic examination under a Wild dissecting microscope (120×–1000×) to obtain an impression of the nature of the particles.

2.6 Biogenic Silica Determination

Beginning in 1988, we measured opal concentrations in sediment trap samples to evaluate the role that sinking surface diatoms might play in mediating the vertical flux of particles from the hydrothermal plumes. The sample from the mass flux filter was used for the silica analysis after the mass analysis was completed. A hot NaOH extraction (Krausse *et al.*, 1983; Paasche, 1973) was used for the analysis.

2.7 Elemental Flux

2.7.1 Particle Flux

The total elemental fluxes were calculated from concentrations of the elements in the sediment trap samples as well as the amounts of elements remobilized during deployment, storage, and processing. Particles from some of the sample aliquots produced during splitting were analyzed for several hydrothermal elements by X-ray primary and secondary emission spectrometry using a Kevex Model 8000-770 X-ray energy spectrometer with a rhodium X-ray source and Zr, Se, and Co secondary targets. A nondestructive thin film technique was used (Feely *et al.*, 1991). The aliquot of the sediment trap particles allotted to elemental analysis was carefully concentrated, ground, and loaded onto 37-mm filters with the appropriate loading mass (250–400 μg). The split of sediment trap material allotted to metal determination was first centrifuged in 250-ml wide-mouth centrifuge bottles at 7500 RPM. After sampling the splitting solution, most of the remaining splitting solution was removed by vacuum suction. The sediment trap particles were resuspended in the small volume of remaining liquid and transferred to a 15-ml conical centrifuge tube. After centrifuging at 15,000 RPM, the splitting solution was removed by vacuum suction and the slurry containing the particles was transferred to a 2.5-ml acrylic ball-mill vial. The particles and the accompanying splitting solution, which contained salt, were freeze dried. A 5-mm acrylic ball was added to the ball-mill vial and the mixture of particles and salt was ground for 15 min. Based on the mass of particles obtained from the mass flux split, all or a fraction of the dried ground particles was transferred to a 2-ml spectrophotometer cuvette. After adding 1.9 ml of distilled water and resuspending the particles, the absorbance of the suspension was measured at 750 nm. Based on an empirical calibration curve, the mass of the particles contained in the cuvette was estimated. Depending on the results of this calculation, all or a portion of the volume in the cuvette was pipetted into 30 ml of pH 8 water overlying an acid-cleaned, pre-weighed, 37-mm, 0.4-μm polycarbonate filter. This slurry was then vacuum filtered, and the filter was rinsed with pH 8 water. The fluxes of elements that were associated with the analyzed particles were calculated by multiplying the mass fraction of each element in the particles (mg of element/per mg of suspended matter) by the VMF.

2.7.2 Remobilized Flux

Metals on particles can be remobilized (a) into the supernate of the collection jar during deployment, (b) into the supernate of the jar during storage between recovery and splitting, (c) into the diluted splitting aliquots between the splitting of and processing on split aliquots, and (d) during the centrifuging of the splitting aliquot, freeze-drying, grinding, and resuspending the particles onto the final filters. The variable manner in which each of the four sets of recovered samples was processed dictated that the remobilized flux be calculated differently for each sample set (Appendix Table A1).

Analyses of some solutions needed to accurately calculate the remobilized flux were not performed because of budgetary or sample storage limitations. The instances in which the remobilized fluxes could not be determined because of missing data are noted.

2.7.2.1 Remobilization During Deployment and Storage. In general, the salinity of the supernate in the recovered sample jar was considerably less than the salinity of the fill solution, but higher than the salinity of open ocean water. This observation indicated that a considerable volume of the fill solution added to the collection jars before deployment was replaced by ambient seawater. Given the salinity of the supernate in a sampling jar upon recovery (S_{su}), the salinity of the fill solution (S_f) and the salinity of the ambient water at the depth of the trap (S_a), the fraction of ambient seawater present in the sampling jars at recovery (Fr_a) and the fraction of fill solution present in the sampling jars at recovery (Fr_f) can be calculated using the conservation of volume:

$$Fr_a + Fr_f = 1 \tag{1}$$

and salt:

$$S_{su} = (Fr_a * S_a) + (Fr_f * S_f). \tag{2}$$

Combining equations 1 and 2, the fraction of ambient water in the sampling jars (Fr_a) can be calculated as:

$$Fr_a = (S_f - S_{su})/(S_f - S_a). \tag{3}$$

Fr_f can be calculated by difference using eq. 1. The excess elemental concentration of Si and P that was generated from the remobilization from the particles (C_{ex}) can be calculated using the following mass balance:

$$C_{ex} = C_{su} - [(Fr_f * C_f) + (Fr_a * C_a)] \tag{4}$$

where C_{su} is the measured elemental concentration in the supernate in the full sampling jars, C_f is the elemental concentration of the fill solution, and C_a is the elemental concentration of seawater at depth obtained from field data (Appendix Table A2a–d).

In the case in which the supernate is sampled at recovery, the elemental flux attributable to remobilization in the supernate solution (RF_{su}) during deployment is calculated as:

$$Rf_{su} = (C_{ex} * V_{su})/(A * t) \tag{5}$$

where V_{su} is the volume of the sampling jar (0.18 l), A is the area of the trap opening (0.0314 m^2) and t is the time during which the sampling jar was collecting material. Equation 5 can be used to calculate remobilization during both deployment and storage only when the full volume of original supernate in the jar is first sampled at some time after recovery, i.e., just prior to splitting of traps from moorings V23, V26, and V34 (Rf_{su} in Appendix Table 1). We have assumed that the Fe and Mn concentration in the fill solution, which was pre-extracted, and in seawater at the depth of the sediment trap were low compared to the Fe and Mn concentrations found in the supernate solution. Therefore, we assume that all Fe and Mn in the sampling jar supernates originated from the particles (i.e., $Mn_{su} = Mn_{ex}$), and that the fluxes of Fe and Mn attributable to remobilization in the supernate solution (RF_{su}) can be calculated according to equation 5.

The salinity and nutrient data from the supernate can also provide additional information used for quality control purposes. In some cases in which there was significant replacement of the fill solution in the collection jars by ambient seawater, the excess Si and P concentrations calculated from eq. 4 (C_{ex}) were negative. Si and P must have been stripped from the supernate by the particles, if all the assumptions on which eqs. 1–4 were based are correct. While adsorption of P onto Fe-rich particles in the collection jars is plausible, significant amounts of Si are unlikely to precipitate. The inorganic N data provides the answer to this dilemma. If total inorganic N is lower than that expected from the replacement of the fill solution by deep ocean water and is in the form of nitrate, then the seawater that replaced the fill solution must have been surface water. If the seals between the jar and the rotating plate or the seal between the stationary plate and the rotating plate were leaking, low-nutrient surface water could have leaked into the collection jar during recovery. This set of conditions is especially plausible if an upside-down trap is bobbing in and out of the water right before being brought onboard. If the aqueous contents of the collection jar are exchanging with surface water, then sediment particles could also have escaped from the collection jar and the total and elemental fluxes from this collection jar should be scrutinized for errors. If the total inorganic nitrogen is low and in the form of ammonia, then denitrification could also be responsible for the low inorganic nitrogen concentration. The chemical form of the inorganic nitrogen can also be used to assess whether the degree of Fe and Mn remobilization is consistent with the progression of reactions for organic matter remobilization (Froelich *et al.*, 1979). The reduction of Fe and Mn oxides on the particles should only occur after all the nitrate has been converted to ammonia.

In contrast to moorings V23, V26, and V34, the four traps on mooring V43 were sampled immediately after recovery for salinity, nutrients, and metals. The remobilization (RF_{su}) in the full supernate volume during only the time of deployment can be calculated using eqs. 1–5. The samples were then stored in a reduced volume (~70 ml) at 4°C for 10 weeks. Before splitting, the volume of supernate (V_2) was measured and additional supernate samples were collected. This supernate sample was analyzed for Fe and Mn concentrations (C_2), but was not analyzed for Si or P. The changes in Fe and Mn concentrations of supernates ($C_2 - C_{su}$) during the 10-week storage period were used to calculate a separate storage remobilization term (RF_{st}) in the reduced storage volume.

$$Rf_{st} = [(C_2 - C_{su}) * V_2]/(A * t). \tag{6}$$

2.7.2.2 Remobilization During Storage in the Diluted Splitting Solution and Resuspension. A preliminary experiment on the remobilization of elements during storage in the splitting solution and during processing was conducted on four samples from mooring V24. After the particles had been stored in the diluted splitting solution aliquot for 18 months, the particles were processed as described above, and the splitting solution aliquots were sampled and analyzed. The amounts of Si, P, Fe, and Mn in excess of that expected from dilution of the original supernate were calculated, and compared to the amounts remaining on the particles. In this experiment, less than 2% of the total Mn fluxes and less than 1% of the total Fe fluxes were found to have been remobilized over the 18-month period in which the particles were in contact with the diluted splitting solution aliquot. In contrast, between 4% and 12% of the total Si fluxes were remobilized in the splitting solution. The amount of P remobilized in the splitting solutions ranged between 1% and 58% of the total P fluxes. Unless P remobilization can be calculated during storage in splitting solution, caution is suggested when interpreting P fluxes. Less than 2% of the mass of Si, P, V, Fe, and Mn of the particles was remobilized during the process of freeze drying, grinding, and resuspending onto filters.

The determinations of salinity, Si, and P in the splitting solutions from mooring V34 collected in August 1991 (Appendix Table A2c) allowed calculations of remobilization while the particles were in the splitting solution (RF_{spl}). The total volumes of liquid in all fractions of the split fractions

(V_{spl}) were measured. The splitting solutions allotted to element analysis were sampled after the initial centrifugation. The ratio of the salinity in the splitting solution (S_{spl}) to the salinity in the supernate (S_{su}) allows calculation of dilution by the splitting process. Excess elemental concentration (C_{ex-spl}) in the splitting solution not attributable to dilution of the supernate is calculated as follows:

$$C_{ex-spl} = C_{spl} - [(S_{spl}/S_{su}) * C_{su}] \tag{7}$$

where C_{spl} is the elemental concentration in the split. The flux attributable to dissolution during storage in the splitting solution (RF_{spl}) is calculated as follows:

$$RF_{spl} = (C_{ex-spl} * V_{spl})/(A * t) \tag{8}$$

2.7.2.3 Mooring V23. The supernates of the full collection jars were sampled 17 months after recovery and analyzed. Equations 1–5 were used to calculate Si, P, Mn, and Fe remobilization (Appendix Table A3) during both deployment and storage (RF_{su} in Appendix Table A1). The salinities of the supernates (38.7–47.6 ppt) were low compared to the salinity of the fill solution added to the traps before deployment (88.3 ppt). These calculations indicated that the liquid in the sampling jars at recovery contained between 76% and 92% ambient seawater. Eight of the nine concentrations of Si and P in the supernate solutions (Appendix Table A2a) were higher than the concentrations of fill solution, which were obtained from sampling jars that were not opened at depth due to malfunctions. There were measurable amounts of Mn in all nine sampling jars and measurable Fe concentrations in supernates from two sampling jars. The lower amounts of nitrate in the sampling jars compared to the fill solutions suggest that nitrate was the dominant electron acceptor for organic matter oxidation.

The samples of the splitting solutions taken after 19 months of storage were not analyzed. Therefore, the extent of remobilization of Si, P, Fe, and Mn while the particles were stored in the splitting solution is not known.

2.7.2.4 Mooring V26. The supernates of the full collection jars were sampled 7.5 months after recovery and analyzed (Appendix Table A2b). Equations 1–5 were used to calculate Si, P, Mn, and Fe remobilization (Appendix Table A3) during both deployment and storage (RF_{su} in Appendix Table A1). Because of limited amounts of supernate, not all sampling jars were sampled for salinity. For missing salinity data, the average value of the available salinity data from the appropriate trap was used. Like the trap on mooring V23, the extent of replacement of the fill solution ranged between 77% and 96%. The lower amounts of nitrate in the sampling jars compared to the fill solution suggest that nitrate was the electron acceptor for organic matter oxidation.

The samples of the splitting solutions taken after storage of 6 months were not analyzed. Therefore, the extent of remobilization of Si, P, Fe, and Mn while the particles were stored in the splitting solution is not known.

2.7.2.5 Mooring V34. The supernates of the full collection jars were sampled 7.5 weeks after recovery and analyzed (Appendix Table A2c). Equations 1–5 were used to calculate Si, P, Mn, and Fe remobilization (Appendix

Table 3c) during both deployment and storage (RF_{su} in Appendix Table 1). The salinity data from sampling jars from this mooring were generally between 45 and 60 ppt (Appendix Table A2c), which indicated that an average of 35% of the fill solution was replaced by ambient waters. In this set of traps, the lesser degree of replacement of fill solution by ambient seawater is consistent with the shorter collection time. Moderate amounts of Fe and Mn were found in the supernate. The nutrient data suggest that oxygen was the electron acceptor for organic matter remobilization in all sampling jars on mooring V34. This observation is consistent with the short collection time and the immediate recovery of the mooring.

The determinations of salinity, Si, and P in the splitting solutions (Appendix Table A2c) allowed calculations of remobilization while the particles were stored in the splitting solution (RF_{spl} in Appendix Table A1) for 10 months. The amount of Si remobilized in the splitting solution averaged 75% of the total remobilized Si flux, and ranged between 30% and 100% of the remobilized Si flux. The amounts of P remobilized in splitting solution were low and highly variable.

2.7.2.6 Mooring V43. Supernates in the full collection jars for traps on mooring V43 were sampled immediately after recovery. Remobilization of Si, P, Mn, and Fe during deployment only (RF_{su} in Appendix Table 1) was calculated using the salinity, nutrients, and metal data (Appendix Table A2d) and eqs. 1–5. The remaining supernate ($\sim$70 ml) was stored for 3 months and analyzed immediately before processing. Equation 6 was used to calculate remobilization during storage (RF_{st} in Appendix Table A1) for only this set of traps on mooring V43. The low nitrate, high ammonia (not presented), and the high Fe and Mn concentrations in the supernate of sampling jars 1 and 4 of the trap at 2150 m on mooring 43 indicate that Fe and Mn were the electron acceptors for organic matter remobilization. In these two cylinders, the remobilized Mn flux was greater than 90% of the total Mn flux. For all other sampling jars from traps on mooring V43, oxygen appeared to be the electron acceptor for organic matter remobilization. The Fe and Mn remobilized flux listed in Appendix Table A3 includes remobilization during both deployment and storage. Unfortunately, the samples collected from the supernate in contact with the particles during storage were not analyzed for nutrients. Therefore, only the Si and P remobilized flux during deployment (RF_{su}) is reflected in Appendix Table A3.

Within 2 days, the splitting solutions allotted to the determination of metals were centrifuged and freeze dried. Under these circumstances, it is unlikely that any particulate Si, P, Mn, or Fe were remobilized into the splitting solution.

2.8 Current Velocity Measurements

Aanderaa current meters were deployed on all moorings. These data are available at PMEL.

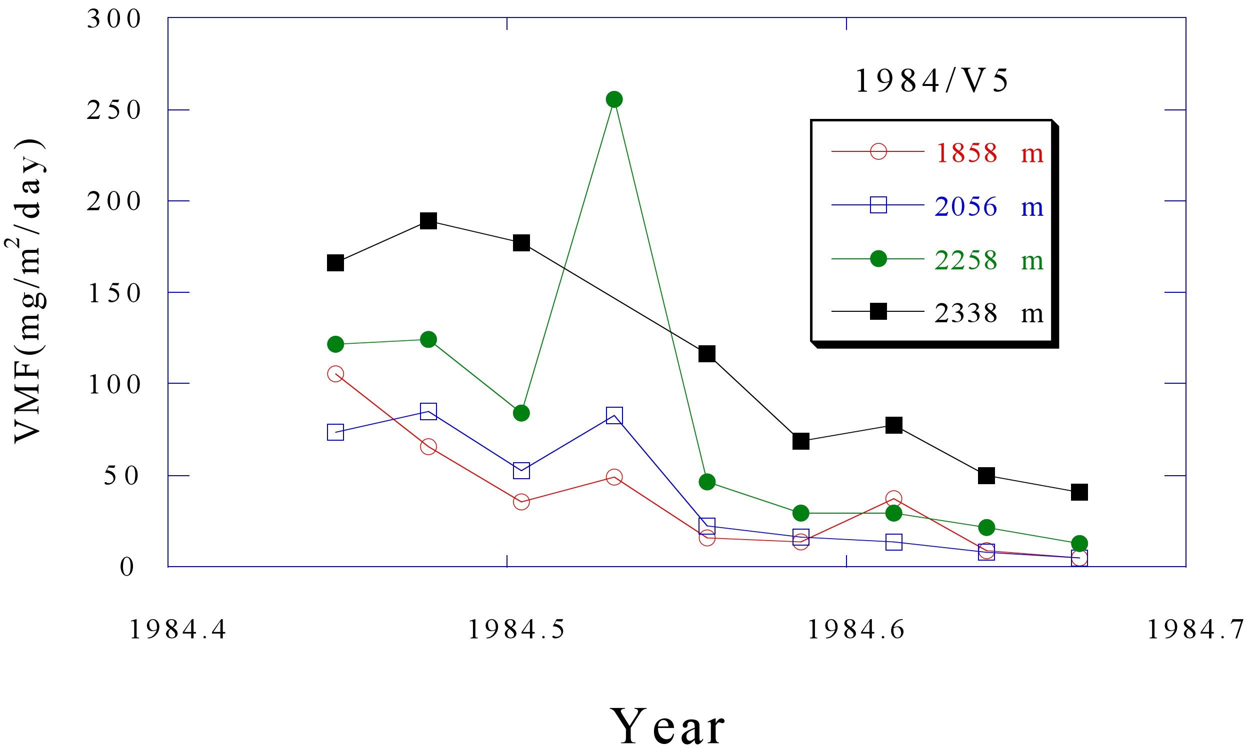

Figure 4: Vertical mass flux as a function of time at mooring V5.

3. Results

Compilations of total VMF and elemental fluxes are given in Tables 2–6. Below we summarize the results on a yearly basis.

3.1 1984 (V1, V4, V5)

VMF (Table 2) was measured at three on-axis locations (moorings V1, V4, and V5) at south Cleft during the 1984 field season. The original data from V1 and V4 have been lost but the mean flux from the single sediment trap at 2178 m on V4 was 110 ± 40 mg m^{-2} day^{-1} for 10 2-day samples (Baker *et al.*, 1985).

The VMF at mooring V5 (Fig. 4) trended from high in June to low in September 1984 and increased with increasing depth. Mean flux at 1858 m and 2338 m was 37 and 111 mg m^{-2} day^{-1}, respectively. The spike observed during the fourth collection period is anomalous.

3.2 1985

3.2.1 (V7) 3.5-Day Collections; On-Axis

Mooring V7 sediment traps (Fig. 5) collected particles at south Cleft from 7 June to 12 July 1985, in 3.5-day intervals, at approximately mid-axis of the Cleft Segment, at 2195 m, 2230 m, and 2245 m. The three traps were located from directly below the top of the hydrothermal plume to 5 mab. Two

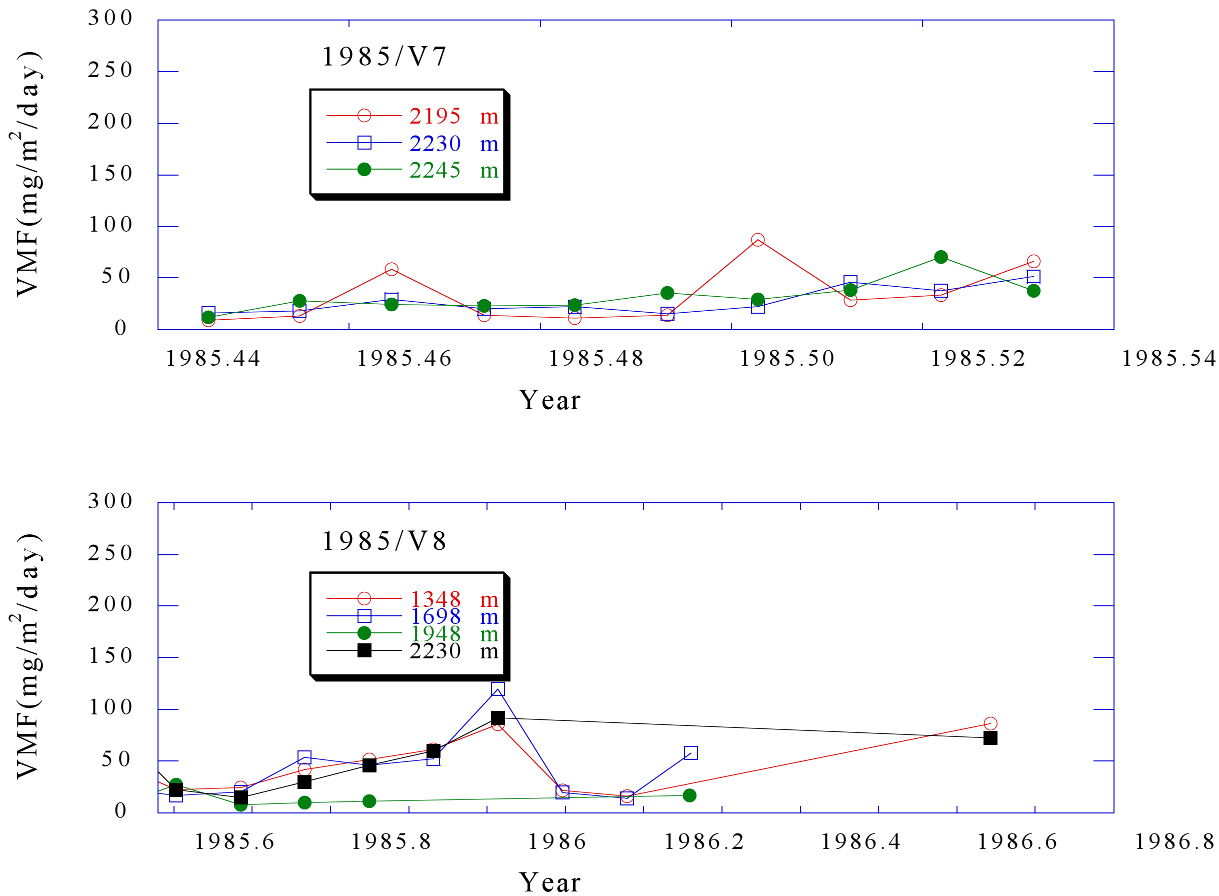

Figure 5: Vertical mass flux as a function of time at moorings V7 and V8.

additional traps at 1950 m and 2240 m malfunctioned. Of the functioning traps, the mean VMF was similar at the three depths (33, 30, and 29 mg m^{-2} day^{-1}). In general, the sedimentation rate was unvaried throughout the collection period at all depths except for the two spikes observed at 2195 m.

3.2.2 (V8) 30-Day Collections; Off-Axis

Mooring V8 was located approximately 14 km due west of the south Cleft vent field in 2250 m of water from 8 June 1985 to 22 August 1986. Of the four moored sediment traps (at 1348 m, 1698 m, 1948 m, and 2230 m) only one operated properly; the others stopped at various times in the normal rotational sequence which was set to be completed by 4 April 1986. In general, the flux appeared similar at all depths except at 1948 m and increased gradually to a peak during January 1986 (Fig. 5).

3.3 1986

During 1986–1987, four moorings were deployed; two were on-axis (V10: short term experiment, V12) and two were off-axis (V9, V11).

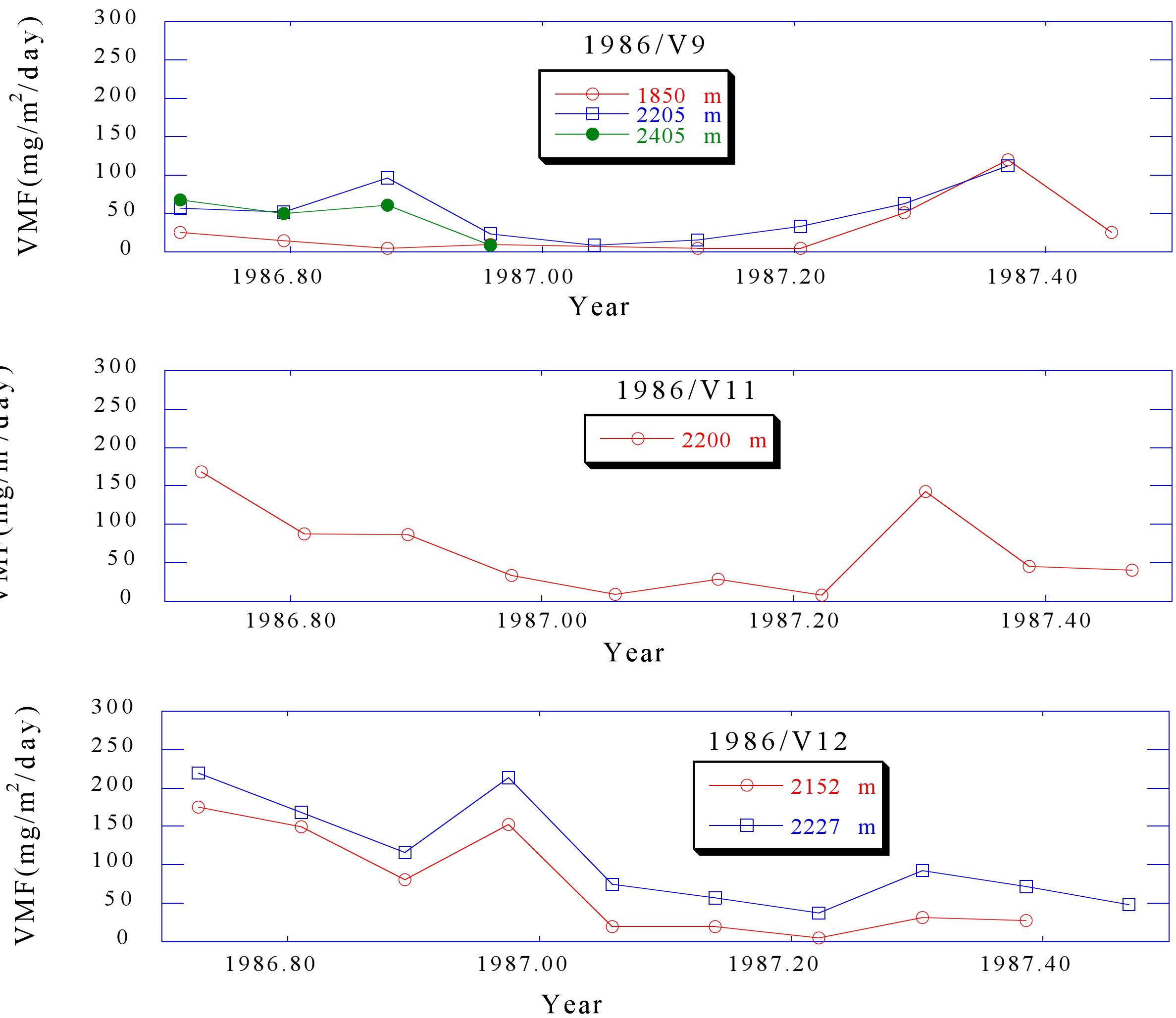

Figure 6: Vertical mass flux as a function of time at moorings V9, V11, and V12.

3.3.1 (V9, V11, V12) 30-Day Collections; Off- and On-Axis

3.3.1.1 Off-Axis. Mooring V9 was moored off axis ~11 km NNW of the south Cleft vents; each sample was a 30-day interval. Sediment traps were placed at 1850 m, 2205 m, and 2405 m. Results (Fig. 6) show that VMF was sharply increased during late fall–early winter 1986 and again during the following spring. Flux magnitudes were similar at all three depths except that the VMF was somewhat lower during the first three collection intervals at 1850 m.

Mooring V11 was located ~10 km due east of the south Cleft site and had one sediment trap at 2200 m (50 mab). Sedimentation maxima of about 150 mg m^{-2} day^{-1} during late summer and the following spring were apparent (Fig. 6).

3.3.1.2 On-Axis. Mooring V12 held two sediment traps at 2152 m and 2227 m and was moored in the axial valley at south Cleft. The VMF at

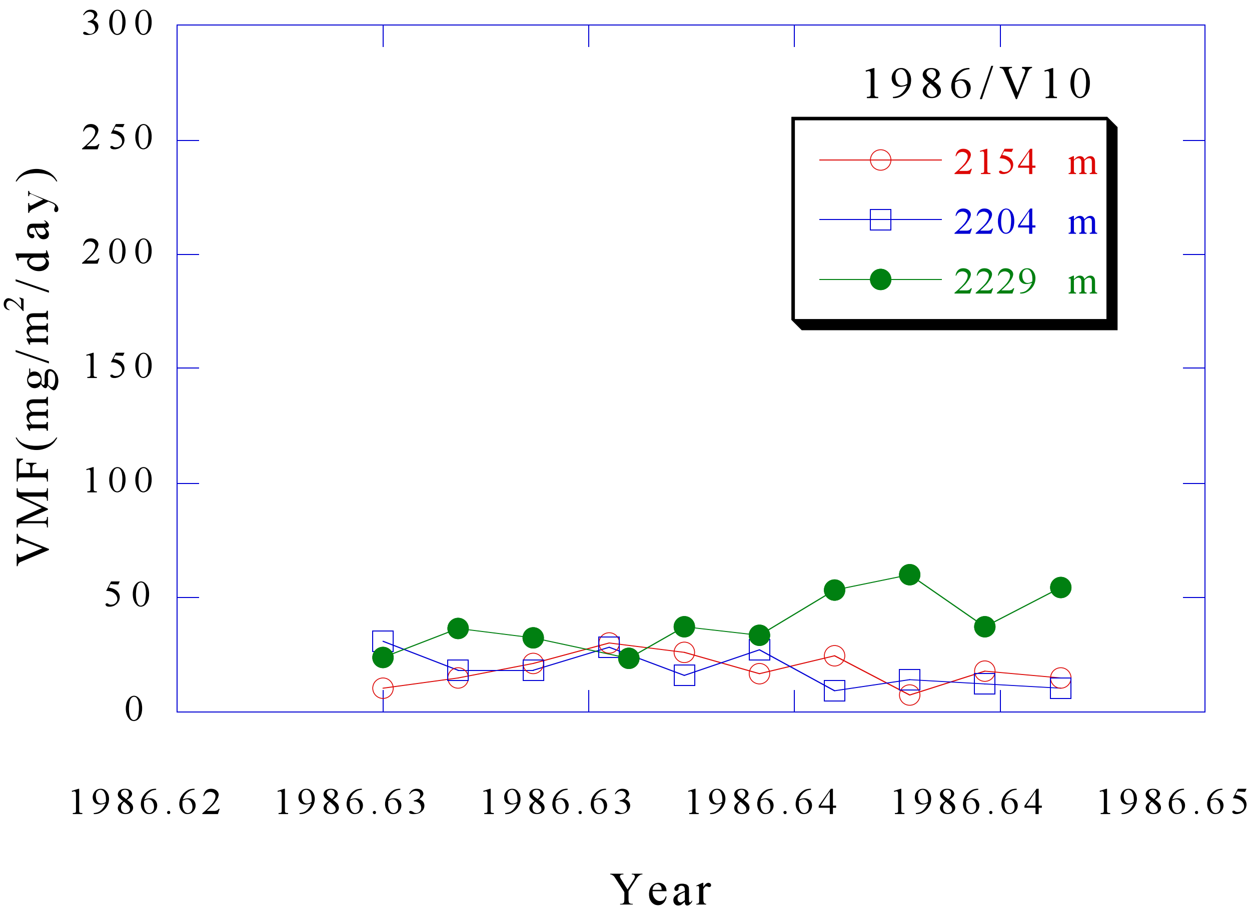

Figure 7: Vertical mass flux as a function of time at mooring V10.

both depths trended similarly and the VMF temporal variation was similar to V9 and V11 (Fig. 6). The magnitude of the VMF at both depths was considerably elevated (150–250 mg m^{-2} day^{-1}) during the fall–winter of 1986 compared to the rest of the year.

3.3.2 (V10) 16-Hour Collections; On-Axis

A 7-day mooring (16-hour collection intervals), V10, was deployed at south Cleft segment. The VMF was about 10 to 50 mg m^{-2} day^{-1} throughout August 1986, the higher fluxes occurring at the deepest trap. It is noteworthy that the VMF at V12 was 3 to 4 times higher during the same time while being located only about 1 km distant (see Figs. 6–7).

3.4 1987

Five moorings were deployed between mid-July 1987 and mid-May 1988; V17 was moored off-axis about 45 km northwest of the south Cleft site, V18 in the region of the 1986 megaplume discovery (Baker *et al.*, 1987), and V19 at south Cleft. In addition, moorings V16 and V20 were deployed off-axis and at the megaplume site, respectively. Trap failures occurred during/after the fourth cycle at 2250 m at V17 and at 2248 m at V19. Thus, the last data point in both cases represents an integrated VMF, i.e., when the traps malfunctioned, the sequencing was stopped so that sedimentation continued only into one cylinder for the duration of the deployment. Thus the daily VMF was determined by dividing by the number of days each of the terminal cylinders were open. Trap failures also occurred on V16 and V20, rendering no usable samples from either mooring.

3.4.1 (V17) 30-Day Collections; Off-Axis

Mooring V17 was off-axis about 45 km northwest of the south Cleft site and had sediment traps at 1500 m, 2100 m, and 2500 m. The sediment traps had 30-day collection periods. Sedimentation rates (Fig. 8) were relatively low, steady, and similar during the first seven collection periods, then increased from less than 20 mg m^{-2} day^{-1} to 150 to 250 mg m^{-2} day^{-1}.

3.4.2 (V18) 30-Day Collections; Megaplume I Site

Mooring V18 was deployed at the 1986 megaplume site from July 1987 to May 1988 with sediment traps at 1500 m, 2100 m, and 2285 m. The temporal and quantitative VMF variations observed (Fig. 8) were very similar to those observed at both V17 and V19.

3.4.3 (V19) 30-Day Collections; South Cleft Site

Mooring V19, deployed at south Cleft, had sediment traps at 2000 m and 2245 m, the former of which failed after mid-November.

3.5 1988

Two moorings, V23 and V24, were deployed in the mid-axial valley, near the sites of megaplumes I and II, respectively (see Baker *et al.*, 1989). Collections were made from mid-June 1988 to mid-May 1989. Subsamples were collected in 30-day intervals. Opal analyses were done on all of the 1988 samples (Table 2).

3.5.1 (V23) 30-Day Collections; Megaplume I Site

3.5.1.1 VMF. Of four sediment traps on mooring V23, only the 2050 m trap produced usable samples for determination of VMF and opal concentrations (Fig. 9). Traps at 1850 m, 2125 m, and 2195 m malfunctioned. The measured VMF of the first subsample (mid-July to mid-August 1988) at 2050 m was anomalously high (526 mg m^{-2} day^{-1}) and was not plotted. Otherwise the particle flux trend was uniformly low from throughout the year and then increased sharply the following spring.

3.5.1.2 Opal. The contribution to the VMF from opal particles was about 20% by weight and except for the low opal concentration during August–September (2.3%), was fairly consistent; the highest concentration (30%) was observed during the January–February 1989 interval.

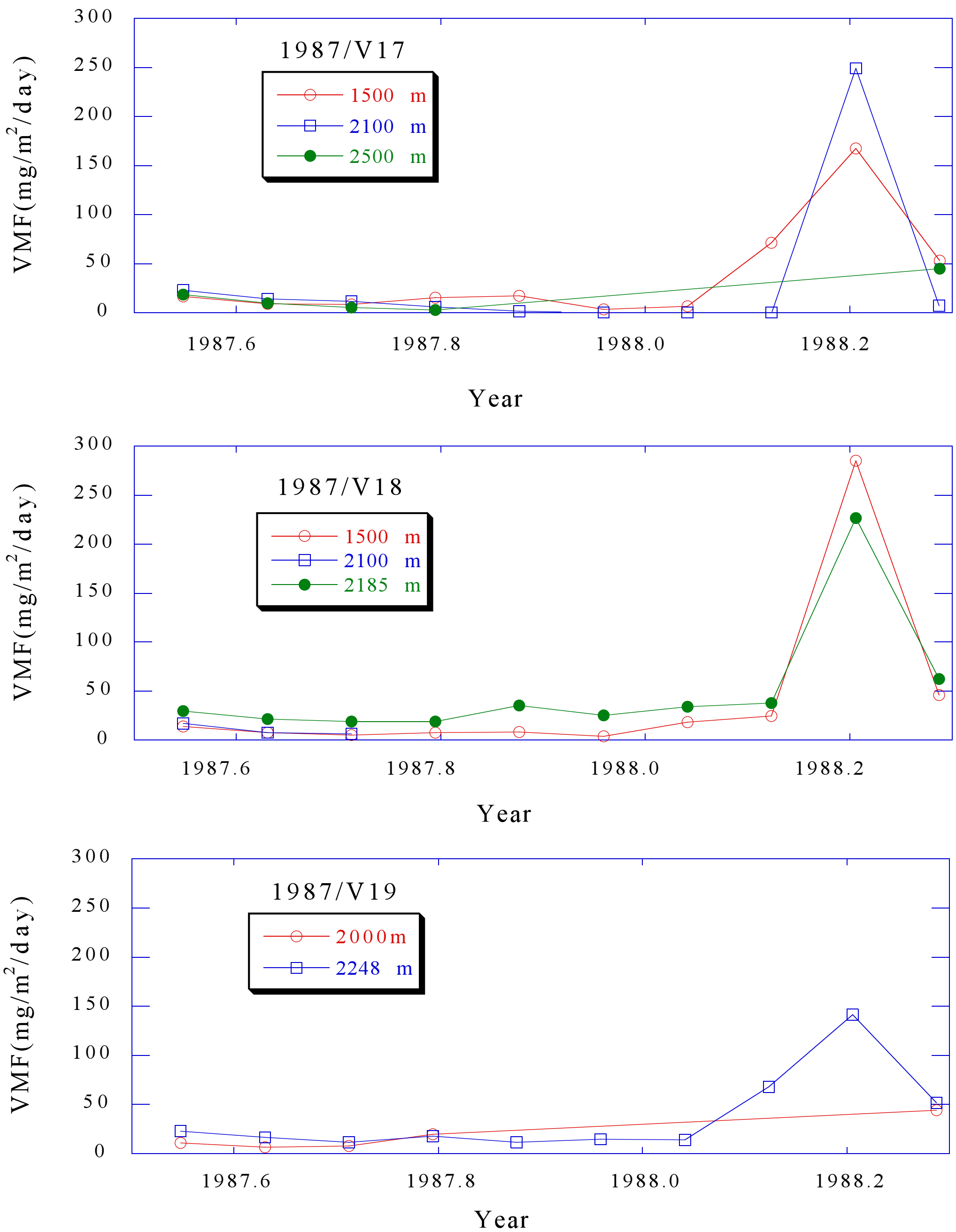

Figure 8: Vertical mass flux as a function of time at moorings V17, V18, and V19.

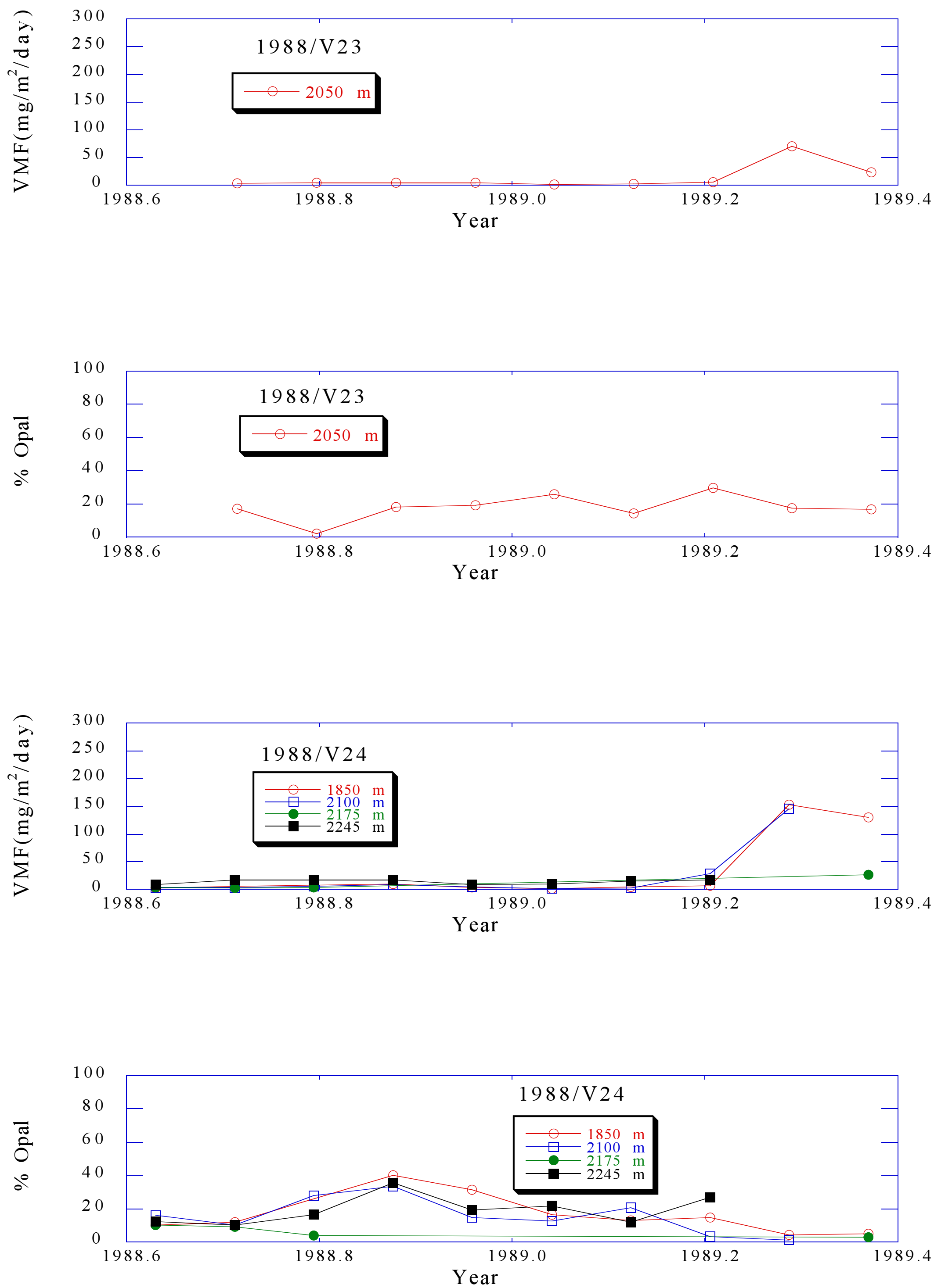

Figure 9: Top to bottom: vertical mass flux and % opal at mooring V23, and vertical mass flux and % opal at V24 as a function of time.

3.5.1.3 Elemental Fluxes. The V23 samples were analyzed to determine the flux of several elements associated with hydrothermal systems including Fe, P, Mn, Zn, S, Cu, and Cr.

The corrected flux of the elements (Table 3) analyzed are shown in Fig. 10 as a function of time. A plot of the total VMF is at the top of each panel for comparison. Several of the elements (Fe, S, Zn, Cr, and Si) exhibited temporal signatures very similar to that exhibited by the total VMF, i.e., very low sedimentation rates during the first six to seven collection periods with a sharp increase during the spring months of 1989. The Cu and P flux was highly variable throughout the year with a sharp spring increase; the Mn flux was highest in late summer 1988, decreasing steadily until late winter 1989 and then increasing sharply during the spring.

3.5.2 (V24) 30-Day Collections; Megaplume II Site

3.5.2.1 VMF. Mooring V24 had sediment traps at 1850 m, 2100 m, 2175 m, and 2245 m. Several VMF subsamples were not reported; the tenth sample from the 2100 m trap was lost; the fourth through ninth samples of the 2175 m trap were unusable; the ninth and tenth 2245 m samples were absent due to trap malfunction. The VMF trend (Fig. 9) was similar to that at V23: low (2 to 30 mg m^{-2} day^{-1}), uniform sedimentation rate from mid-July 1988 through February and at 1850 m and 2245 m, well into March 1989. The VMF was highest ($\sim$150 m^{-2} day^{-1} at 1850 m and 2100 m) from March to April 1989.

3.5.2.2 Opal. Opal concentrations were greatest at 1850 m, 2100 m, and 2245 m (Fig. 9) during mid-October to mid-November 1988 and the opal concentrations at those depths were similar throughout the first 7 months. Opal concentrations were lowest (1% and 4%) at 1850 m and 2100 m when VMF was greatest during the April–May collection periods. Opal flux at 2175 m was considerably less than at the other three depths during the first three collection periods.

3.6 1989

Two moorings, V25 and V26, were deployed in 1989 at the northern and middle part of Cleft segment, respectively, each collecting 33-day subsamples. Samples from 1848 m and 2050 m were analyzed for a suite of elements associated with hydrothermal vent fluid.

3.6.1 (V25) 33-Day Collections; Megaplume II Site

Mooring V25 had sediment traps at 1848 m, 2100 m, 2175 m, and 2245 m. The two upper traps malfunctioned after four and three collection periods, respectively. While functioning, the VMF into these traps was similar (Fig. 11) and ranged between 5 and 11 mg m^{-2} day^{-1}. VMF at 2175 m and 2245 m was uniform and low until April 1990 when it increased to 433 and 83 mg m^{-2} day^{-1}, respectively, and then decreased to 6.5 mg m^{-2} day^{-1} by July–August 1990 at the 2245 m trap.

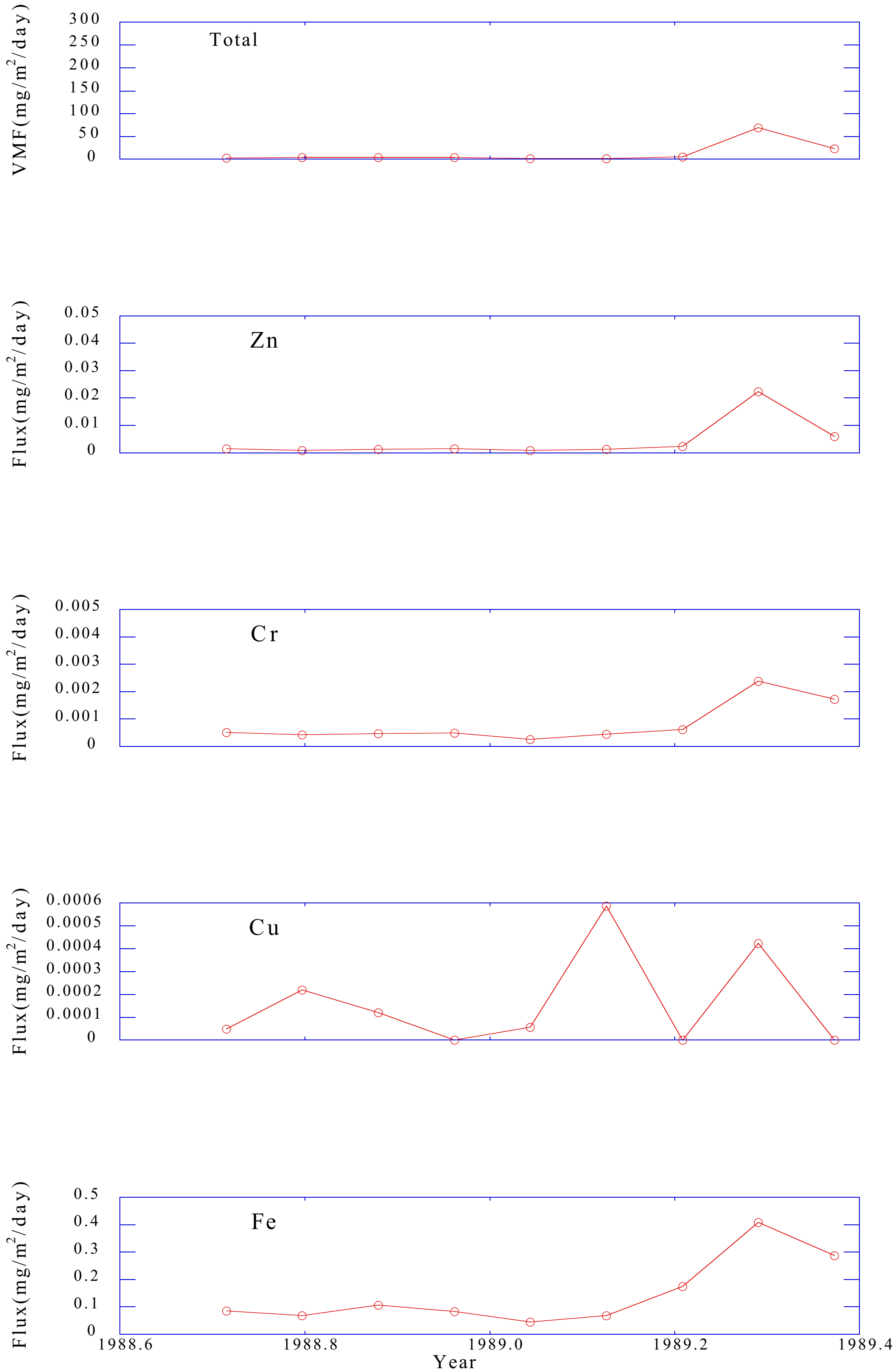

Figure 10a: Mean elemental flux (Zn, Fe, Cu, and Cr) and total flux as a function of time at the 2050 m trap on mooring V23.

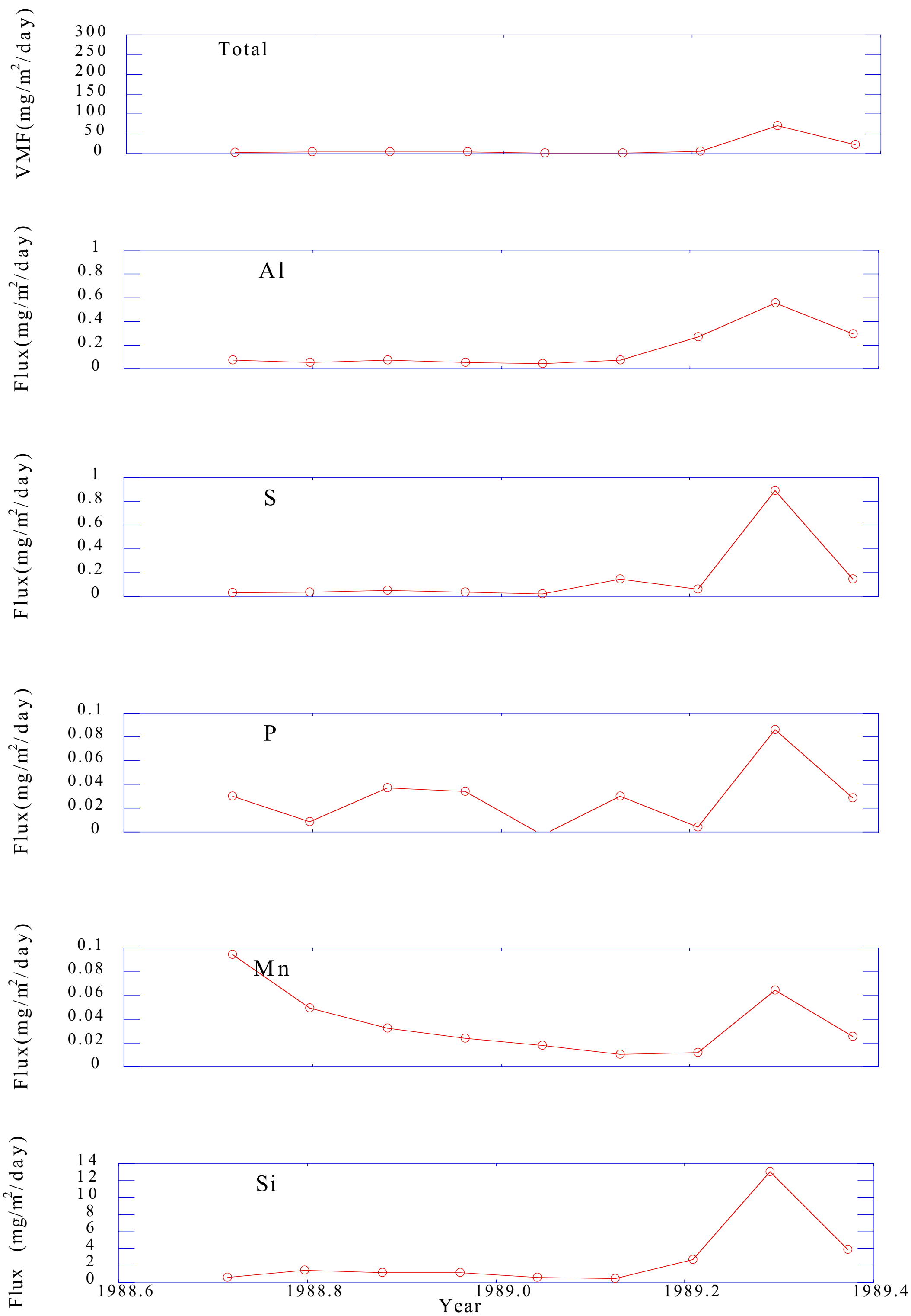

Figure 10b: Mean elemental flux (Al, Mn, Si, S, and P) and total flux as a function of time at the 2050 m trap on mooring V23.

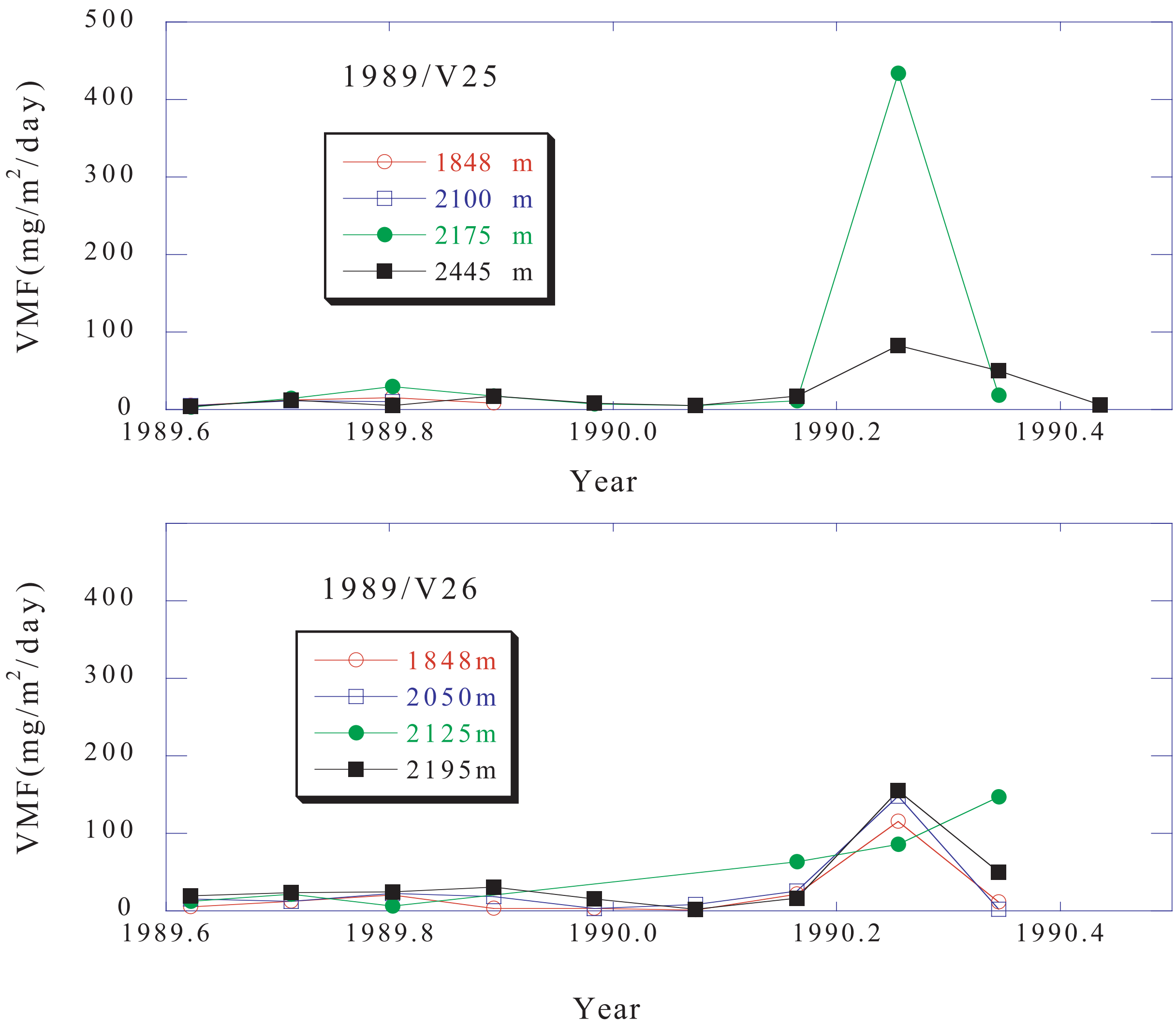

Figure 11: Vertical mass flux as a function of time at moorings V25 and V26.

3.6.2 (V26) 33-Day Collections; North Cleft

Mooring V26 had sediment traps at 1848 m, 2050 m, 2125 m, and 2195 m. Each trap collected nine 33-day subsamples; the tenth was lost because the traps were retrieved prematurely. The fourth through sixth samples of the 2125 m trap had insufficient mass for VMF determination.

3.6.2.1 VMF. The VMF at V26 trended similarly to that at V25 (Fig. 11) on an annual basis. The August 1989 to April 1990 VMF generally ranged between about 10 and 25 mg m^{-2} day^{-1} at the three lower traps. The VMF at the 1848 m trap was less, generally between 2 and 20 mg m^{-2} day^{-1}. The peak sedimentation rate ($\sim$100–160 mg m^{-2} day^{-1}) in all but the 2125 m trap occurred during April–May 1990. The peak rate at the 2125 m trap ($\sim$140 mg m^{-2} day^{-1}) occurred about a month later, by which time sedimentation at the other traps had fallen to between 2 and 50 mg m^{-2} day^{-1}.

3.6.2.2 Elemental Fluxes. Samples from 1848 m and 2050 m were available for elemental analysis (Table 3). The elemental temporal flux variations at mooring V26 are shown in Figure 12a and 12b. In general the temporal pattern of elemental flux mimicked the total VMF pattern, i.e., it was relatively low midsummer with increases during the fall and during the spring of the nearly year-long collection period. At plume depth (2050 m), notably sharp spring flux increases were observed by Fe (0.02 to 1.31 mg m^{-2} day^{-1}), Mn (0.008 to 0.155 mg m^{-2} day^{-1}), S (0.092–1.442 mg m^{-2} day^{-1}), and Zn (0.0007–0.0382 mg m^{-2} day^{-1}).

3.7 1990

During the 1990 field season, long-term and short-term VMF experiments were done. In the short-term experiment, 11 moorings holding a total of 20 sediment traps which collected subsamples every 6 days were deployed in a grid on the north end of Cleft segment (Fig. 1). These short-term moorings were recovered about 3 days prior to the deployment of the long-term mooring (V43) that held four sediment traps which subsampled every 27 days. Moorings V43 was placed in the same locations as was the short-term mooring V34, i.e., mid-axis approximately 2.8 km southwest of Pipe Organ vent (Embley *et al.*, 1991). Relatively complete data sets of elemental flux (uninterrupted, multi-depth) from both long- and short-term experiments were acquired during the 1990–1991 deployments. Consequently these data were examined more thoroughly than the elemental flux data from moorings V23 and V26.

3.7.1 (V43) 27-Day Collections; North Cleft

3.7.1.1 VMF. Mooring V43 had sediment traps at 1800 m, 2050 m, 2150 m, and 2250 m (Table 2). VMF was measured from 28 September 1990 to 26 June 1991. The VMF trended similarly and was of similar magnitudes at all depths (Fig. 13). The trend was notably different from past years because of an increase in VMF during late fall to the early winter months of 1990. The late fall increase in VMF was remarkably similar at all four depths; from shallow to deep the VMF measured 44, 45, 56, and 51 mg m^{-2} day^{-1}. The spring 1991 increase in VMF measured 80, 51, 77, and 87 mg m^{-2} day^{-1}, shallow to deep. Nominal background flux was about 10 to 20 mg m^{-2} day^{-1} and ranged from about 2 to 27 mg m^{-2} day^{-1}.

3.7.1.2 Elemental Fluxes. Four traps on mooring V43 were recovered on 10 June 1991. An aliquot of the solids of each cylinder from each of the four long-term traps was analyzed for elemental composition (including Al, P, Si, Ca, V, Cr, Mn, Fe, Cu, and Zn) by X-ray spectrometry (Table 4).

Hydrothermal particle flux vs. depth. Depth profiles of elemental flux (Fig. 14) show that Fe, Mn, Cu, P, Al, and V have increased flux at 2050 m and below compared with fluxes at the 1800 m. Cu flux increased about fourfold between the 1800 m and 2250 m trap, Mn increased fivefold,

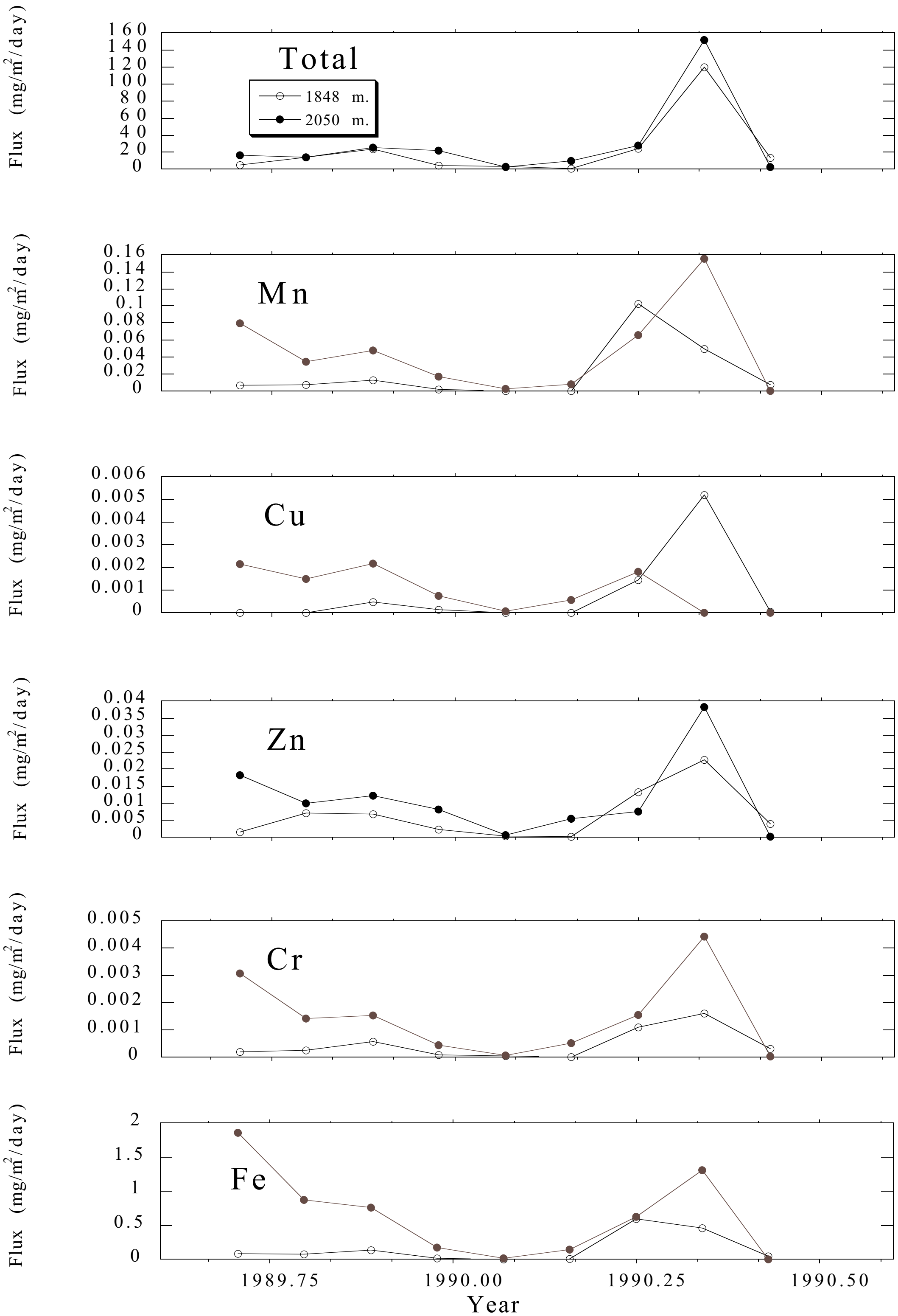

Figure 12a: Elemental (Mn, Cu, Zn, Cr, and Fe) and total flux as a function of time at mooring V26.

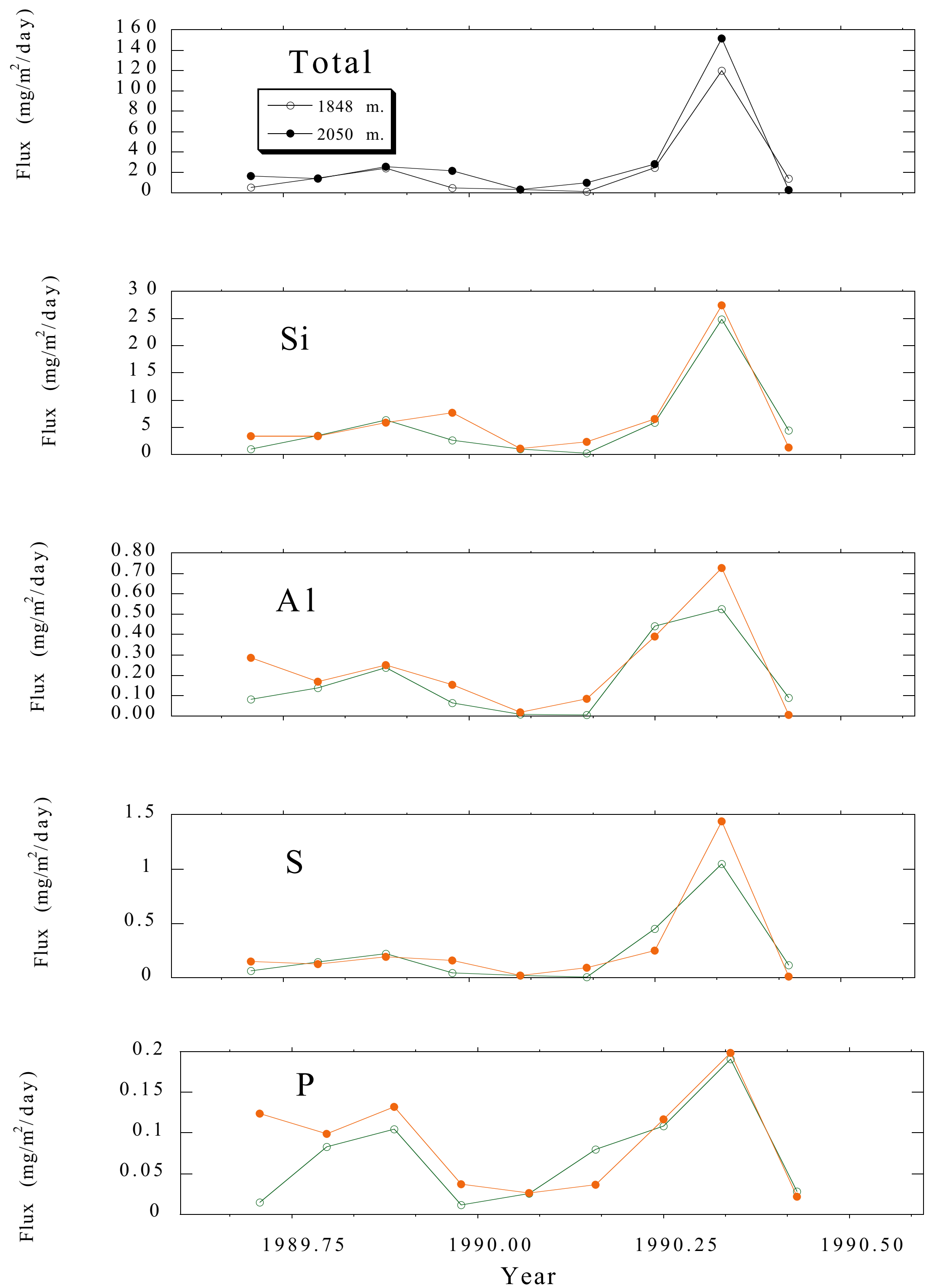

Figure 12b: Elemental (S, Si, Al, and P) and total flux as a function of time at mooring V26.

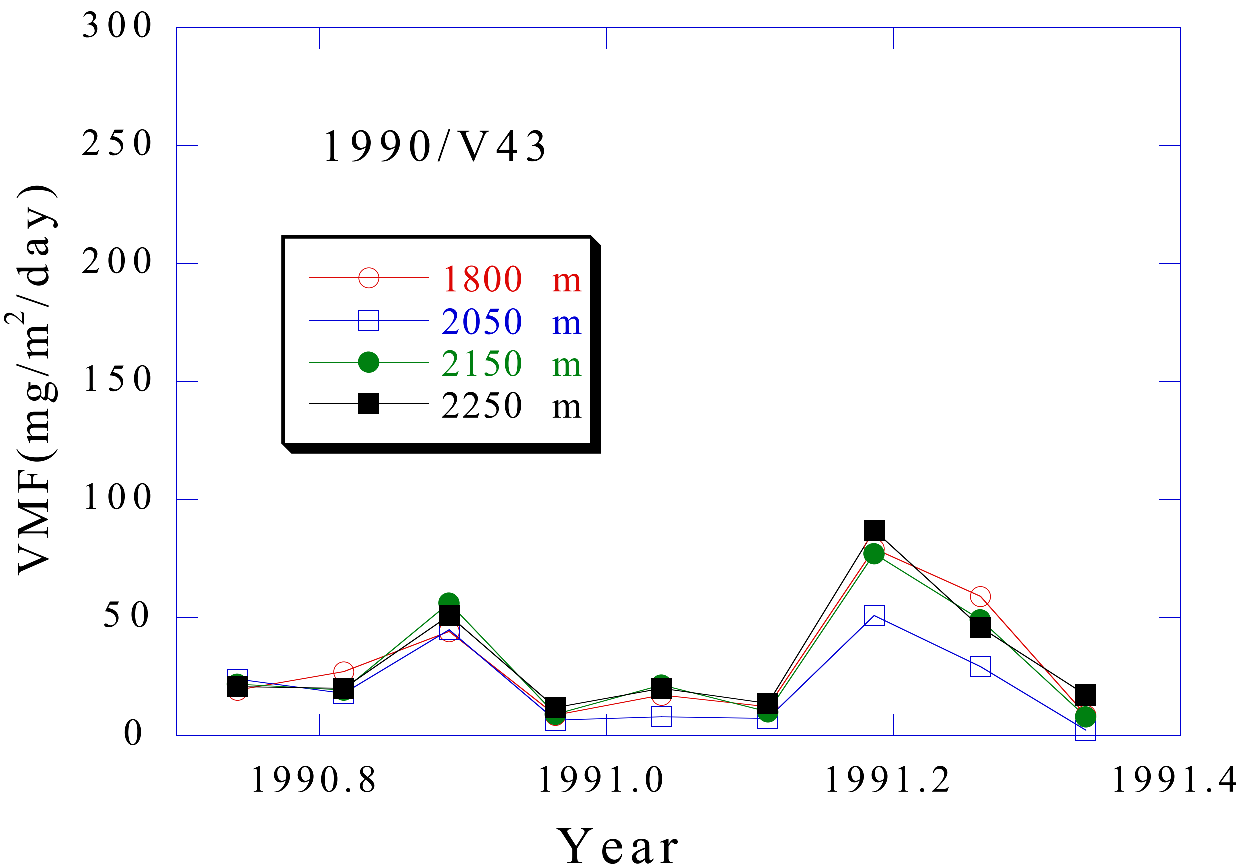

Figure 13: Vertical mass flux as a function of time at mooring V43.

V flux nearly doubled between 1800 m and 2250 m, P flux increased more than 4 times from the 2050 m trap to the 2250 m trap, and the 2150 m Fe flux was about 30 times higher than at the 1800 m trap.

Hydrothermal particle flux vs. time. The magnitude of elemental fluxes at the 2150 m and 2250 m depths varied considerably throughout the year and trended similarly to the total VMF (Fig. 15). In all cases at the two deepest traps, the flux of Al, Si, P, Fe, Mn, and V increased considerably above background in late fall to early winter 1990 and again during the spring months of 1991. Elemental fluxes at the 1800 m and 2050 m traps tended to be considerably smaller in most cases.

Al — Background particulate Al flux was about 0.1–0.3 mg m^{-2} day^{-1} during late summer 1990 and mid-winter 1990–1991 at all depths. Lower particulate Al flux trends were measured at the 1800 m and 2050 m depths and higher fluxes tended to occur at 2150 m and 2250 m with a few exceptions. The lowest particulate Al flux (~0.1 mg m^{-2} day^{-1}) was measured at the 2250 m trap during the fall of 1990 and at the 2050 m and 2250 m traps during early summer 1991. Highest particulate aluminum fluxes were recorded at the 2150 m and 2250 m traps (~0.4–0.6 mg m^{-2} day^{-1}) during the late fall and spring peak flux periods.

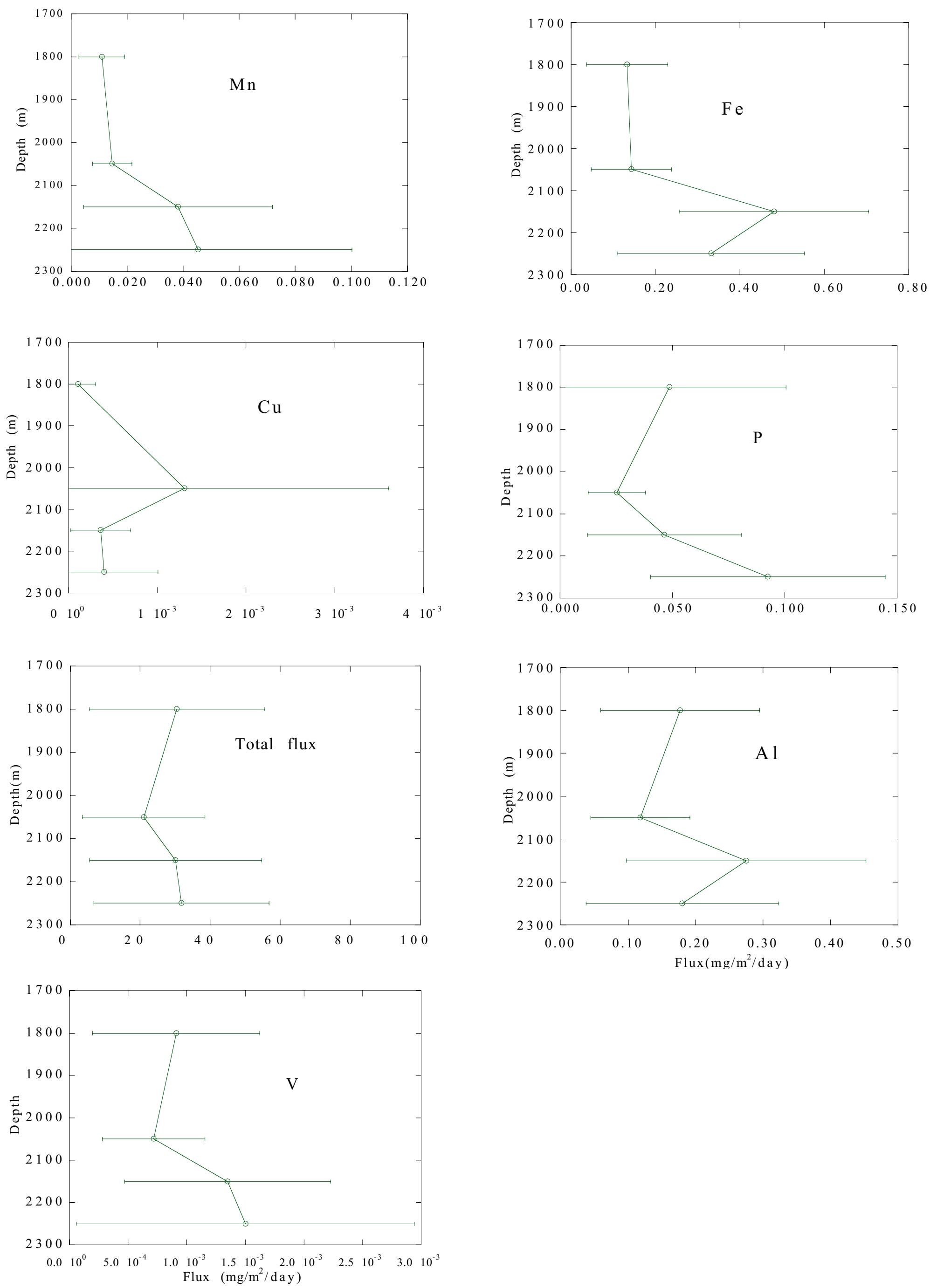

Figure 14: Elemental flux as a function of depth at mooring V43. Error bars denote one standard deviation.

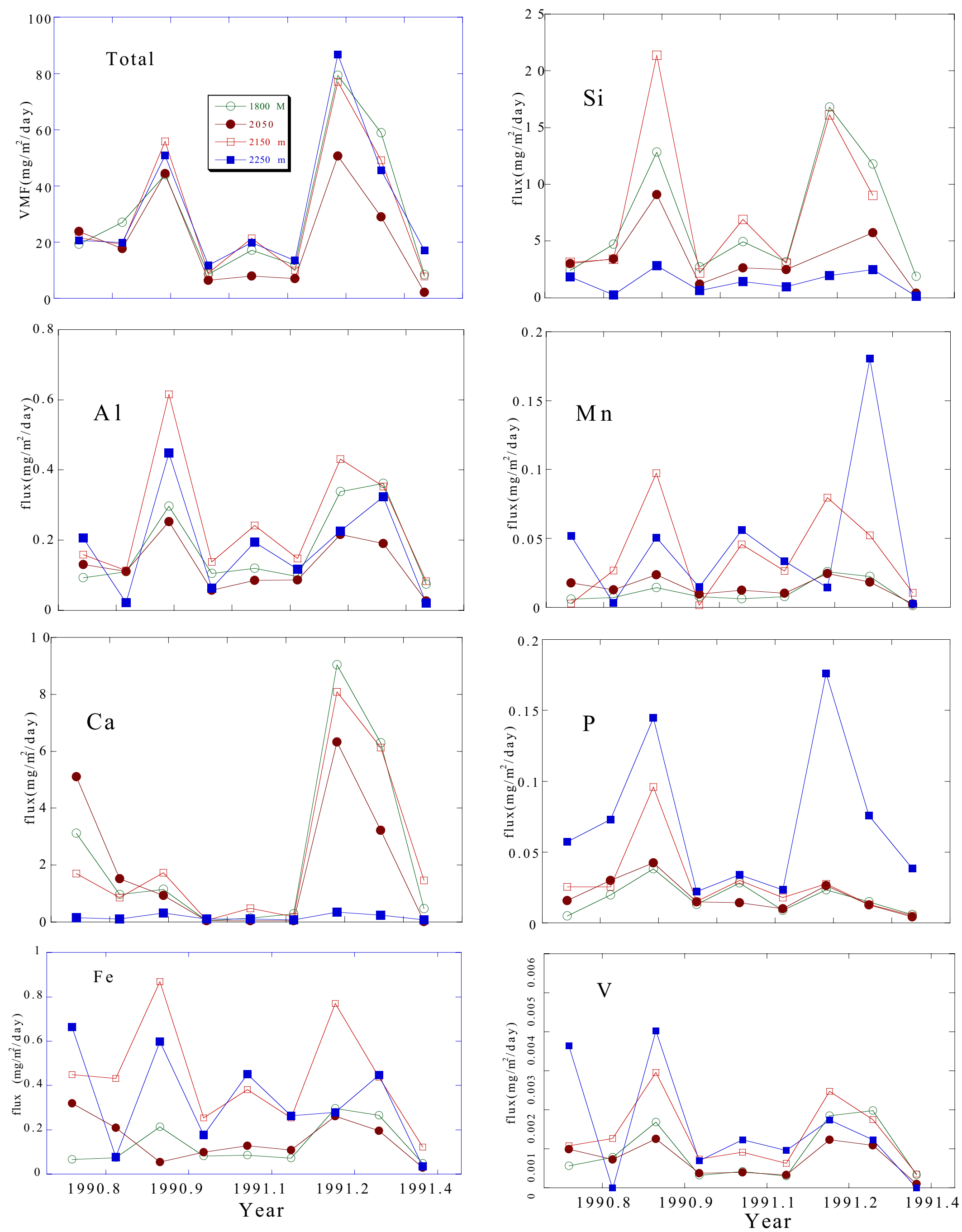

Figure 15: Elemental flux as a function of time at mooring V43.

Si — Particulate Si flux was lowest throughout the year at 2250 m (~1–3 mg m^{-2} day^{-1}). A maximum in particulate Si flux was measured during late fall 1990 at 2150 m. During spring 1991 Si fluxes were particularly elevated (~18 mg m^{-2} day^{-1}) at 1800 m and 2150 m.

P — Particulate P flux was lowest throughout the year in the upper three traps which collected about 0.05 mg m^{-2} day^{-1} or less except for the 2150 m trap which collected about 0.1 mg m^{-2} day^{-1} during one collection period late in 1990. The 2250 m trap collected substantially more particulate P, especially during the late fall and spring when P fluxes of 0.15 to 0.18 mg m^{-2} day^{-1} were recorded.

Fe — These fluxes were generally low in the upper traps at 1800 m and 2050 m ($\leq$0.3 mg m^{-2} day^{-1}) compared to the flux at the lower two traps and did not follow a noticeable trend. Fe flux at 2150 m was much higher throughout the year than at shallower depths and trended similarly to total VMF. The Fe flux at 2150 m ranged from about 0.2 to >0.5 mg m^{-2} day^{-1} with maxima in late fall 1990 and spring 1991. Fe flux at 2250 m trended somewhat differently than at 2150 m. The maximum flux (>0.5 mg m^{-2} day^{-1}) occurred 2 months earlier than at 2150 m and periods of relatively low flux alternated with periods of higher flux on a bi-monthly mode except during spring 1991. The spring 1991 maximum in particulate Fe flux was delayed by one interval relative to the 2150 m trap.

Mn — Particulate Mn flux was uniformly low (<0.02 mg m^{-2} day^{-1}) at the 1800 m and 2050 m traps compared to the 2150 m and 2250 m traps. The Mn flux at 2150 m was relatively uniform throughout the year and ranged from about 0.03–0.1 mg m^{-2} day^{-1}. At 2250 m the Mn flux was elevated compared to that at 2050 m but generally a bit lower than at 2150 m except for a dramatic increase during the spring of 1991 when it increased from a nominal background of about 0.05 mg m^{-2} day^{-1} to more than 0.15 mg m^{-2} day^{-1}.

V — Flux of particulate V trended similarly to the total VMF throughout the year. It was lowest in the upper traps (~.0005–.002 mg m^{-2} day^{-1}) and greatest (0.003–0.004 mg m^{-2} day^{-1}) during fall-early winter of 1990 at 2250 m.

3.7.2 (V32–V42) 6-Day Collections; North Cleft

3.7.2.1 VMF. The short-term experiment commenced mid-July and ended mid-September 1990. The moorings were placed in a grid over and around the north Cleft vent field (Fig. 1) such that five of the moorings (V34, V35, V38, V39, and V41) were located in the axial valley near Monolith and Pipe Organ vents. The other six moorings were located as much as ~8 km to the east and west of the axial valley. Three of the sediment traps, V32/2250 m, V34/2150 m (one of two replicate traps), and V38/2050 m, malfunctioned and returned no samples. All samples were measured for total VMF and opal concentration (Table 5).

The mean VMF measured in the axial valley was ~36 mg m^{-2} day^{-1}; the mean of the other traps was ~26 mg m^{-2} day^{-1}. In all cases 62% ± 10% of the VMF was attributable to opal (Figs. 16–18). The peak sedimentation rate occurred during August, during which the VMF increased from ~20 to ~50–60 mg m^{-2} day^{-1} in nearly all the traps and opal concentrations varied much the same as the VMF. On the other hand, the 2150 m trap on V34 collected much higher VMF, 110–140 mg m^{-2} day^{-1}, and a much lower opal contribution, 5%–40% (80% in the first subsample).

3.7.2.2 Elemental Fluxes. Samples from mooring V34 only were analyzed for hydrothermal elemental concentrations. The corrected fluxes are found in Table 6. The average elemental flux during the 60-day deployment was much higher in general than the average during the year-long deployment (see Figs. 15 and 19). Fe flux, for example, ranged from about 0.5 mg m^{-2} day^{-1} at 2050 m to nearly 5 mg m^{-2} day^{-1} at 2250 during the 60-day experiment. During the year-long deployment the Fe flux did not exceed 0.9 mg m^{-2} day^{-1}. The flux of Fe, Cu, P, Mn, and V were also considerably greater during the short-term experiment. While the elemental flux magnitude was greater during the short-term experiment, the flux/depth pattern was similar to that observed during the year-long deployment (Fig. 20).

Several elemental fluxes did mimic to some extent the total VMF variation pattern. The total VMF was in excess of 150 mg m^{-2} day^{-1} during the first collection period at 2150 m. The Al, Si, Fe, Mn, V, Cr, and S fluxes at 2150 m were notably high during the first collection period. By the second collection period the fluxes of these elements decreased significantly, in some cases to as little as one third of the original level, which was in general maintained throughout the duration of the experiment. The flux level of these elements at 2050 m and 2250 m were in general about the same as the 2150 m background level. The V, Cr, and Fe fluxes at 2150 m exhibited a secondary maximum during the sixth collection period while S and Fe fluxes exhibited secondary peaks during the same time span but at 2250 m. The S flux increased more than 4 times during the sixth collection interval at 2250 m. The flux of Mn, Zn, and P were variable. In general the elemental flux at 2050 m was much lower than at deeper depths.

4. Discussion

4.1 Total Vertical Mass Flux

4.1.1 Depth Variations

Several past investigations using sediment traps have found that particle flux as a function of depth is variable and that quantities measured can be a result of varying sources and mechanisms (Rowe and Gardner, 1979; Martin and Knauer, 1983; Gardner *et al.*, 1985; Walsh *et al.*, 1988; Dymond and Roth, 1988; Feely *et al.*, 1994). The major sources of settling particles in the ocean include organic detritus generated in the euphotic zone, airborne (dust and pollen primarily), hydrothermal, and resuspended sediments from the seafloor. The bulk of the surface source is organic carbon, $CaCO_3$, and opal, a large fraction of which does not reach the seabed because of dissolution and other recycling processes. Consequently, sediment trap catchment by a vertical regime of moored traps decreases with depth unless there are

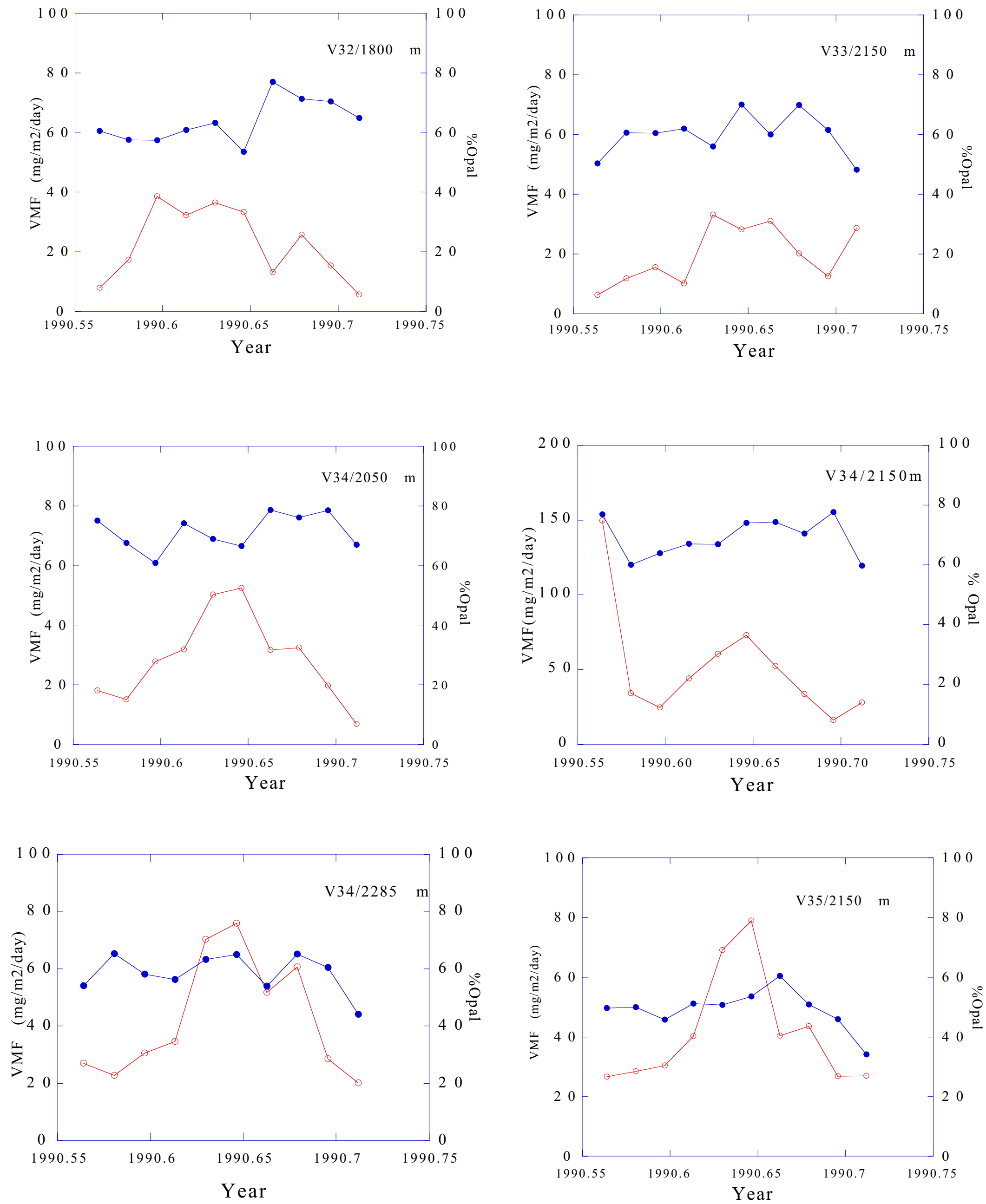

Figure 16: Vertical mass flux (open circles) and % opal (closed circles) as a function of time at moorings V32, V33, V34, and V35.

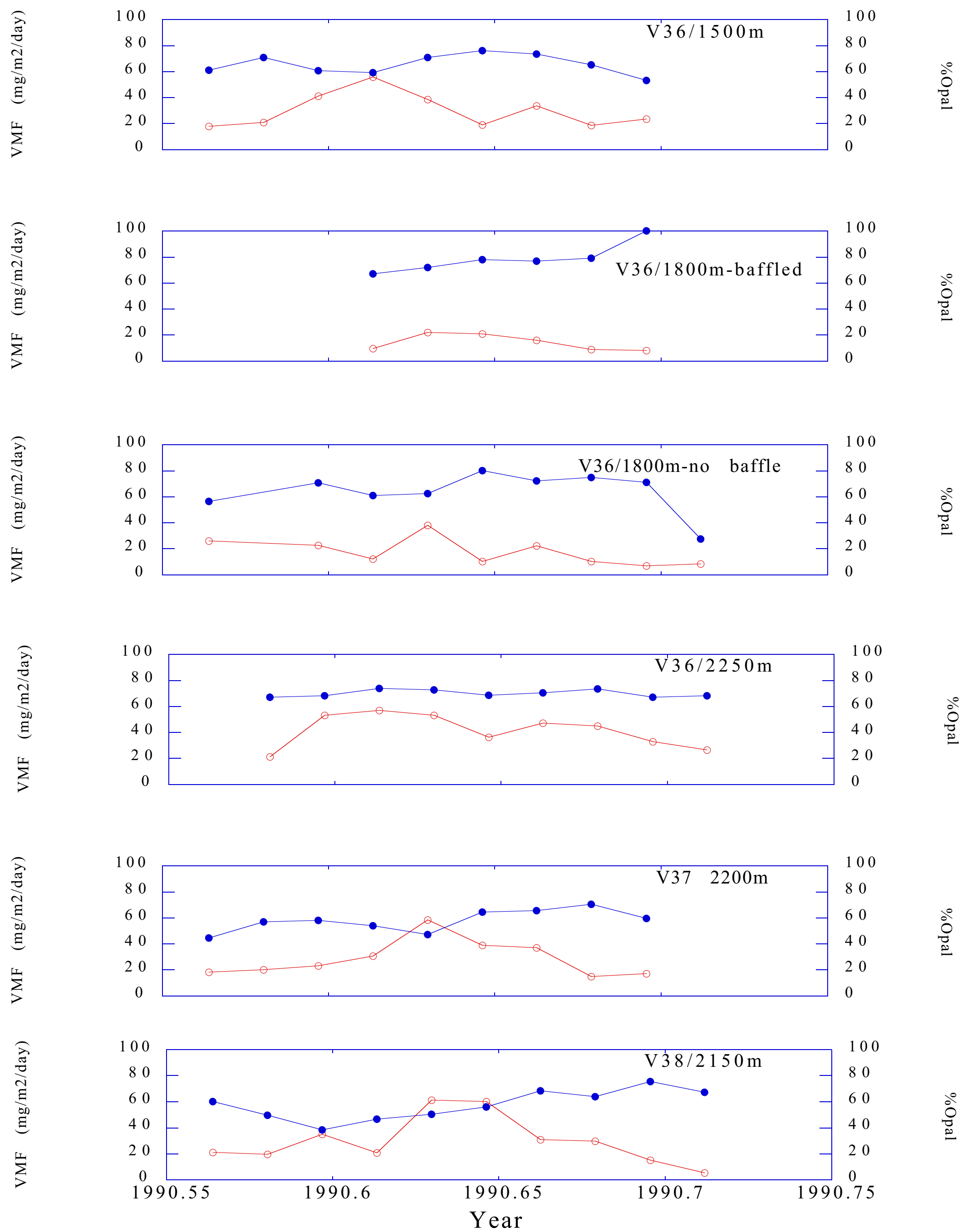

Figure 17: Vertical mass flux (open circles) and % opal (closed circles) as a function of time at mooring V36, V37, and V38.

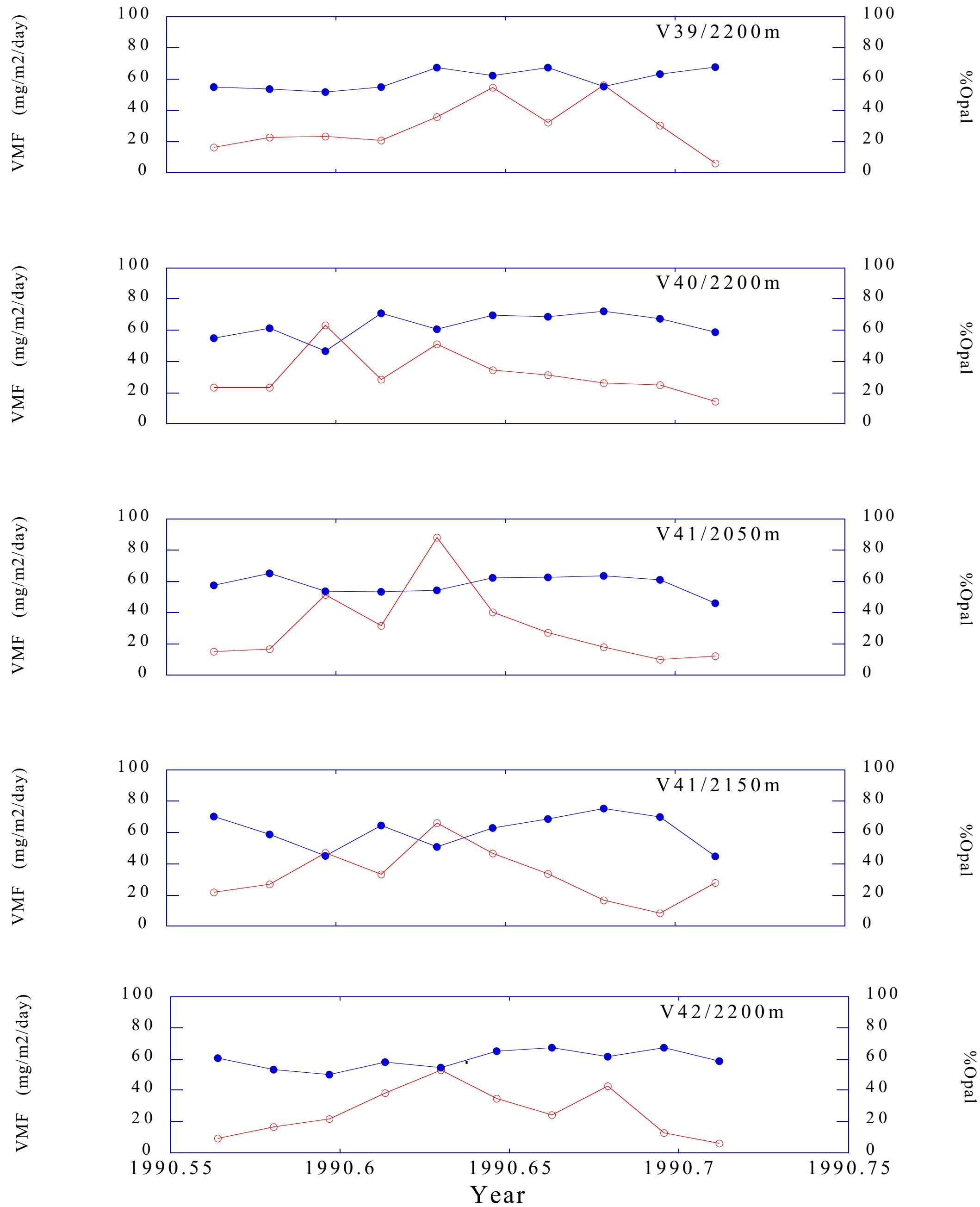

Figure 18: Vertical mass flux (open circles) and % opal (closed circles) as a function of time at mooring V39, V40, V41, and V42.

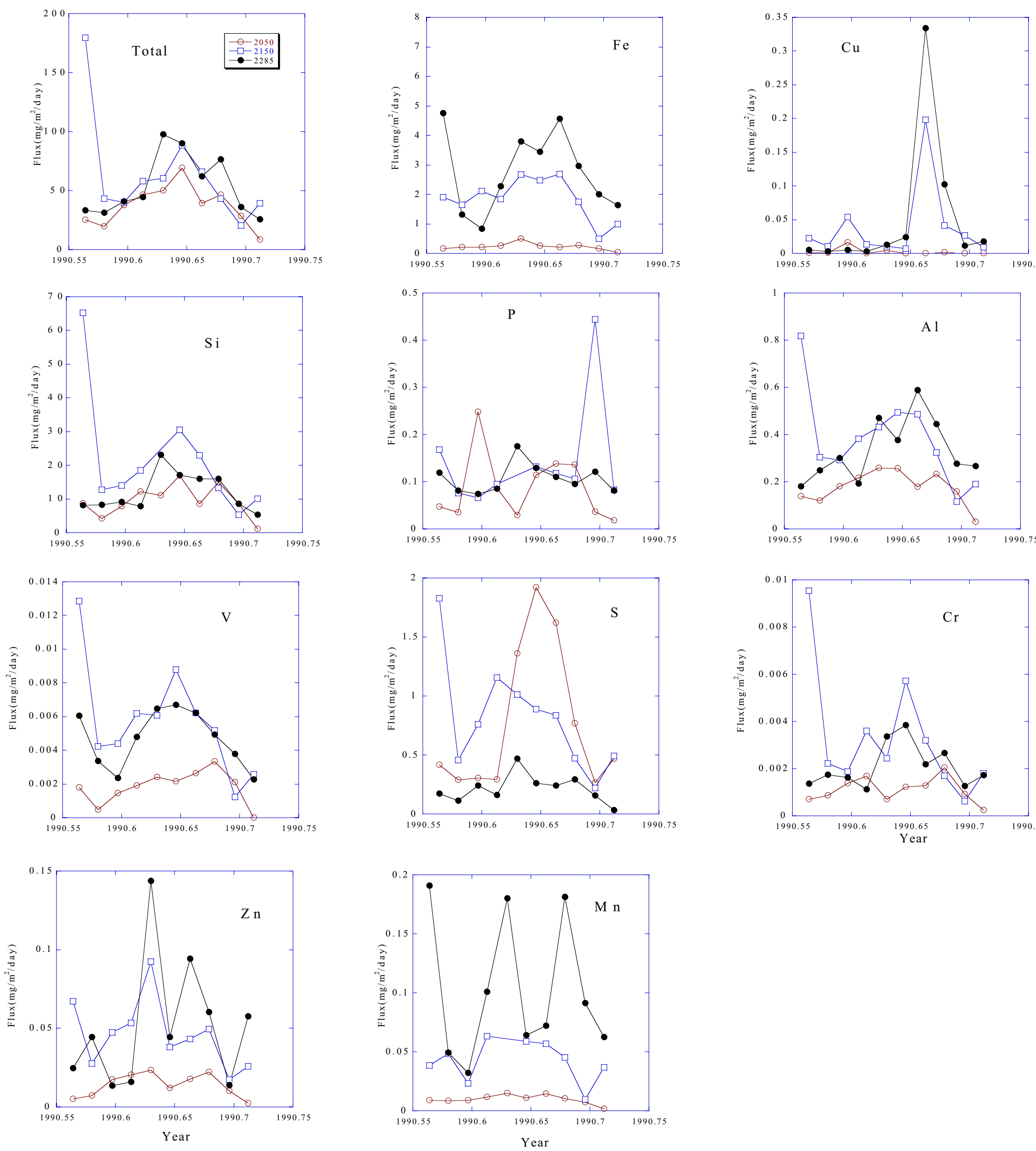

Figure 19: Elemental flux as a function of time at mooring V34.

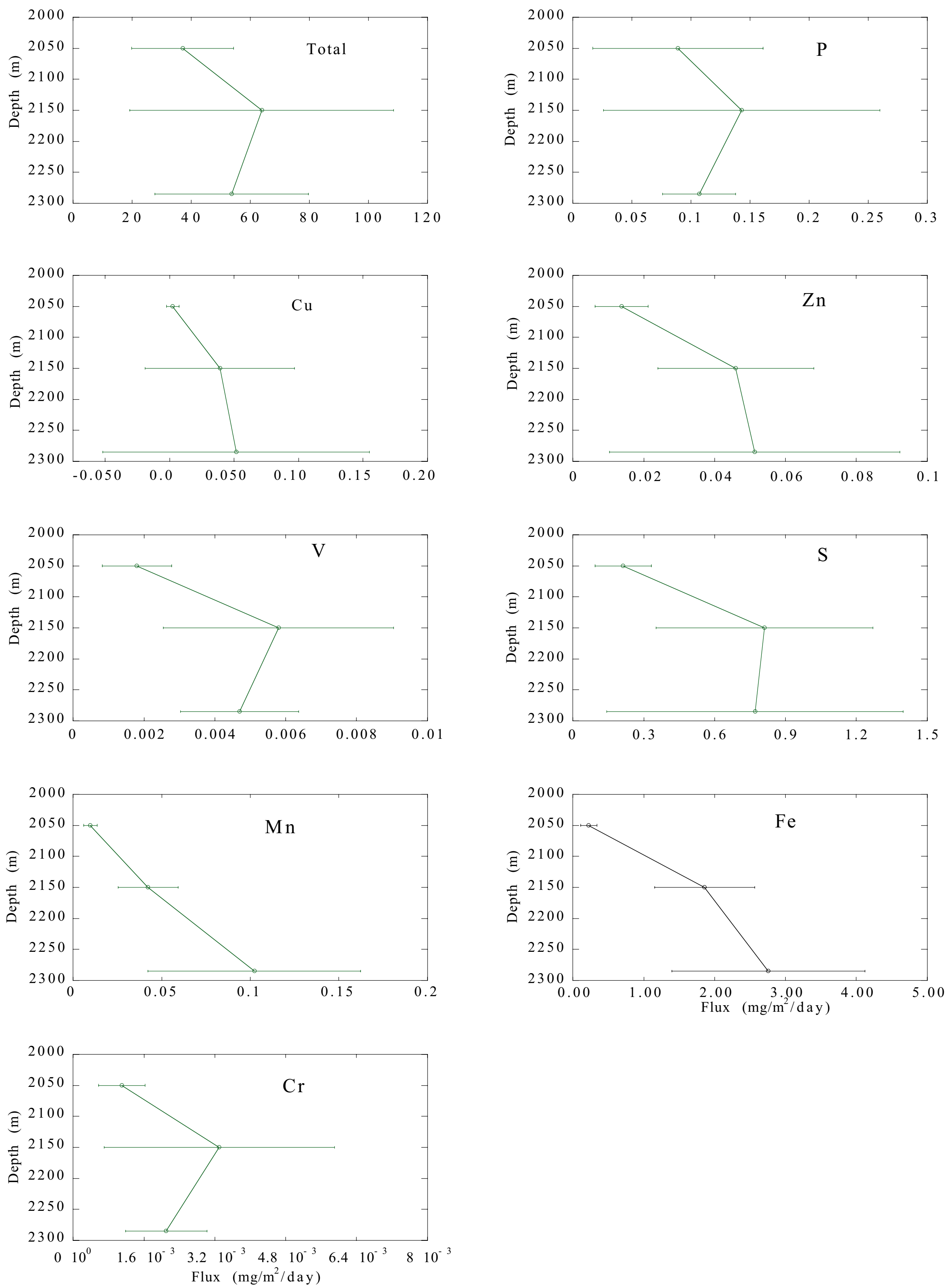

Figure 20: Elemental flux as a function of depth at mooring V34. Error bars denote one standard deviation.

additional particle sources to the deeper traps, e.g., hydrothermal input and/or resuspension of seabed material.

One of the primary strategies employed in this study was locating sediment traps above the plume, within the plume, and below the plume in an attempt to quantify the input of hydrothermal particles. Figure 21 is a comparison of the mean total flux at those depths. Data from only four moorings (V18, V24, V26, and V43) were used because they were the only ones with enough data to compare interdepth flux variations in a statistically valid manner, i.e., they were on-axis moorings that had nearly complete data sets (eight or more consecutive subsamples) from at least two of the depth regimes. Data from these moorings were selected for comparison such that subsamples from any given depth must have a corresponding subsample at a comparison depth. If subsamples from any deployment were missing *critical* subsamples, the data from that trap would not be used. Critical subsamples are those that were collected during spring bloom and mid-winter months, and are so designated because these times are probably the most critical in terms of regulating the amount of sedimentation into the sediment traps (see discussion below). The mean VMF measured at <2100 m traps was 25.6 ± 44.6 mg m^{-2} day^{-1}; at >2100 m the VMF was 30.4 ± 37.1 mg m^{-2} day^{-1}. Of the sediment trap samples collected only V43 had elemental data that corresponds to the above flux data. From the V43 data set (Table 4) it is clear that although there is a considerable increase in both Fe and S with increasing trap depth, the input of hydrothermally derived particles cannot account for more than 5% of the increased flux below 2100 m. It is possible that the increase of VMF with depth is a combination of hydrothermal and resuspended sediments. Although we do not have direct evidence of resuspended sediments, near-bottom Aanderaa current meter data from previous deployment periods (Cannon *et al.*, 1991) in the axial valley have measured bottom current velocities ≥ 7 cm sec^{-1} 36% and 53% of the time during the periods that VMF exceeded 100 mg m^{-2} day^{-1}. Southard *et al.* (1971) and Lonsdale and Southard (1974) have shown that current speeds of 7–10 cm sec^{-1} are required for resuspension of calcareous ooze.

4.1.2 Short-Term Temporal Variations—1990 Experiments

From 1990 to 1991 there were two separate deployment periods. During the first period, from mid-July to mid-September 1990, 6-day subsamples (60-day total) were collected at 11 mooring sites (V32–V42) at North Cleft. The second deployment period went from late September (1990) to late June (1991) during which 27-day subsamples were collected.

During the 1990 short-term experiment, total sedimentation rate increased significantly at most sediment trap locations and at several depths midway through the collection period (Figs. 16–18). VMF increased from $\sim$20 to $\sim$60 mg m^{-2} day^{-1} during the July segment of the collection period. Fifteen of seventeen traps deployed showed this trend. We have no firm explanation for the cause of this increase. Summer bottom currents were apparently not vigorous enough to cause resuspension. Nor were the flux increases due to increased sedimentation of hydrothermal particles and/or

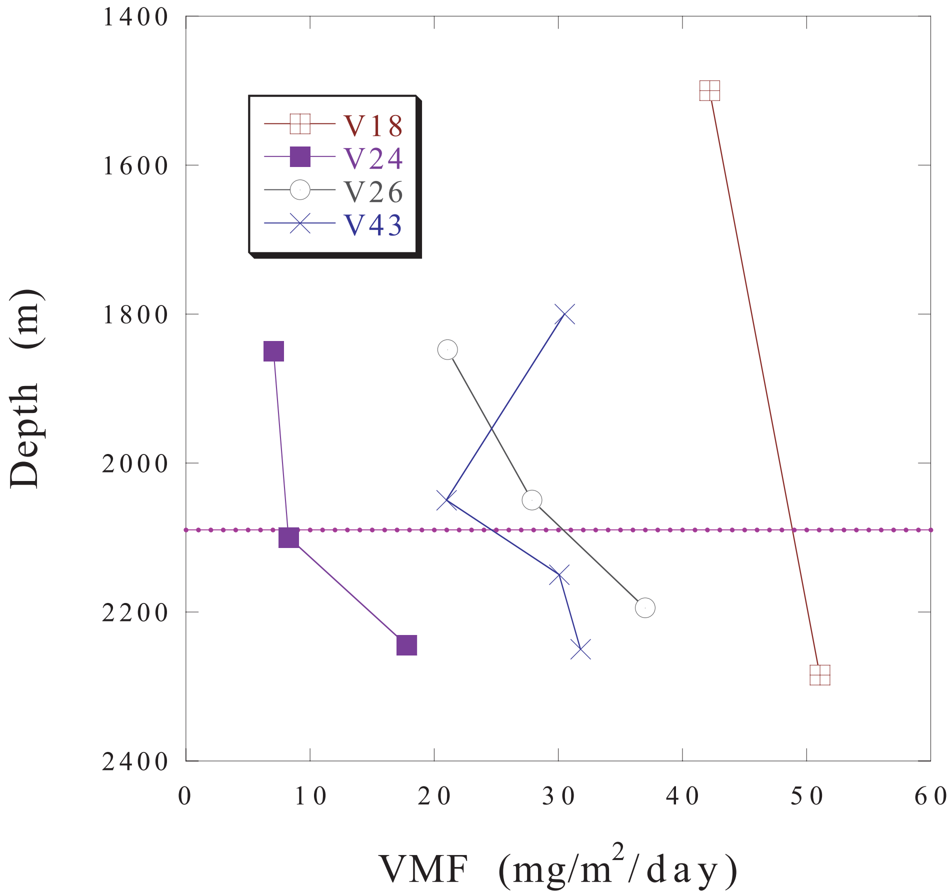

Figure 21: Mean VMF from traps located above the hydrothermal plume (<2100 m) and traps within and below the plume. The data is from moorings V18, V24, V26, and V43. The overall above-plume mean VMF = 25.6 ± 44.6 mg m^{-2} day^{-1}; from within and below the plume, overall mean VMF = 30.4 ± 37.1 mg m^{-2} day^{-1}. The dotted horizontal line indicates the nominal depth of the top of the hydrothermal plume at Cleft segment.

opal, as increases in those species were proportional to those of the total VMF.

4.2 Hydrothermal Flux

Hydrothermal elemental concentrations were measured in samples from V23, V26, V34, and V43. Most of the following discussion pertains to the flux at V34 (short term) and V43 (long term) because they had the most comprehensive depth coverage.

4.2.1 Elemental Flux vs. Time

In general the elemental fluxes measured at V23 (Figs. 10a, b) and V26 (Figs. 12a, b) mimic the total VMF: relatively low and unchanged during midsummer and midwinter with increases during fall and more sharply during spring months.

The elemental flux during the 1990 short-term deployment period at V34 showed two temporal trends (Fig. 19). One trend is the elevated flux of nearly all the measured elements and the total VMF during the first 6-day collection, but only at the 2150 m trap. We have no explanation for this observation and it is possibly the result of a trap malfunction. The other trend was a flux increase of several of the elements after the fourth collection period that peaked during the sixth or seventh collection periods. The flux of Mn and P did not follow the trend and exhibited a rather variable pattern.

Temporal variations in the elemental flux at V43 from 1990 to 1991 (Fig. 15) were consistent within the group of elements analyzed and the temporal flux pattern exhibited is similar to that of the total VMF temporal pattern. In all cases the flux was greatest during the spring and a secondary flux increase generally occurred in the fall. A similar particle flux study at Endeavour segment of the JDFR (Dymond and Roth, 1988) found the greatest hydrothermal elemental fluxes in the fall and slightly smaller fluxes during the spring.

4.2.2 Elemental Flux vs. Depth

Short-term elemental flux variations as a function of depth were noted at V34 (S, Fe, Mn, Zn, Cu, P, Cr, and V) (Fig. 20) and long-term variations at V43 (P, Fe, Al, Cu, Mn, and V) (Fig. 14). In general, elemental fluxes increased progressively with depth but in some cases the maximum flux occurred above the bottom trap. For example, during the short-term experiment at V34 the S, P, and V flux maxima were at 2150 m and during the long-term deployment the maximum Fe flux occurred at 2150 m and the maximum Cu flux was at 2050 m. The increase of elemental flux with depth was considerably greater during the short-term than long-term collection period, i.e., elemental background flux was similar for the most part during both collection periods, but the flux at the bottom traps was quite different. For example, the elemental bottom flux of Mn was twice as high, S was twice as high, Fe was 15 times higher, Cu was 100 times higher, and Zn was 4 times higher. In the discussion above it was pointed out that there was a general increase in total VMF midway through the short-term collection period at most depths and it is clear from Fig. 20 that the mean total VMF is considerably greater in the lower two traps than in the 2050 m trap. It is possible that sinking organic aggregates resulting from a surface bloom entrapped a relative abundance of hydrothermal particles during this time period. This explanation is discussed more thoroughly below under Seasonal Variation (Section 4.3).

The data from the long-term collection is also notably different from elemental fluxes measured at the Endeavour segment of the Juan de Fuca Ridge (Dymond and Roth, 1988) (Table 7). The Cu flux at the 2100 m trap at Endeavour was nearly 1000 times greater than the deep trap on V43; V, Zn, Fe, and Mn were about 500, 100, 30, and 2 times higher at the Endeavour deep trap. Feely *et al.* (1994) reported that Fe flux near Monolith vent on North Cleft was only 2% of that reported by the Dymond and Roth (1988) study. The large differences between the elemental fluxes reported at North

Cleft and Endeavour segments is likely caused principally by differences in the relative locations of vent sources and traps, but also by the total flux of hydrothermal particles discharged at each site, the differences in concentrations of elements in vent fluids at the different sites, and differences in bottom current velocities and trajectories.

The flux of Fe, Cu, Mn, and V was greatest at mid- and below-plume depths at both V34 and V43. These elements are highly enriched in vent fluids or are scavenged from the ambient seawater by hydrothermal particles (Feely *et al.*, 1994; Dymond and Roth, 1988). These observations (moorings V34 and V43) were made about 3 km from the nearest known vent (Pipe Organ). Resuspension of previously sedimented hydrothermal material may also account for higher fluxes of these elements caught in the 2250 m trap. In the study at Endeavour Ridge it was estimated that between 19% (Ba) and 43% (V) of the flux of specified hydrothermal elements resulted from resuspension (Dymond and Roth, 1988). Current meter measurements from moorings V34, V35, and V38, however, suggest current velocities too weak for resuspension during the 1990 short-term experiment.

4.2.3 Hydrothermal Fe

In an attempt to further assess the hydrothermal component of particle flux at the study area, we analyzed Fe flux data from V34 and V43 to evaluate how much Fe in the sediment traps was from hydrothermal input. Non-hydrothermal background particles collected at the Juan de Fuca (Feely *et al.*, 1992) and Gorda (Feely *et al.*, 1998) Ridges were subsequently analyzed for a suite of elemental concentrations including Fe and Al. The Fe/Al ratio was 0.43 at JDFR, and 0.34 and 0.42 at the Gorda Ridge during cruises Great 1 and Great 3, respectively. We used the mean (0.397) of these three data sets to assess hydrothermal Fe enrichment. We proceeded by assuming that any Fe in the sediment traps in excess of this mean value of 0.397 (on a molar basis) was due to hydrothermal enrichment of Fe (see Karlin and Lyle, 1986). On this basis we determined approximate proportions of terrestrial and hydrothermal Fe flux trapped at moorings V34 and V43 (Fig. 22). Accordingly, our calculations indicate that approximately 35%, 83%, and 90% of the Fe flux at 2050 m, 2150 m, and 2250 m, respectively, at V34 is hydrothermally generated. It is also clear that the uppermost trap at 2050 m was well into the hydrothermal plume based on the amount of hydrothermal Fe in the trap. The proportion of hydrothermal to terrestrial Fe at V43 traps is less than that at V34, i.e., the traps at 1800 m, 2050 m, 2150 m, and 2250 m, respectively, had about 1%, 38%, 54%, and 57% hydrothermal Fe. The enrichment of these elements in the sediment trap samples from within and below the plume is confirmation that hydrothermal precipitates were captured in sediment traps within the plume. That 1% of the Fe at 1800 m was denoted as hydrothermal is probably a result of the manner that we used to define the background Fe/Al ratio. Plots of elemental enrichment with depth at mooring V43 (Fig. 14) indicate that hydrothermal enrichment begins beneath 1800 m.

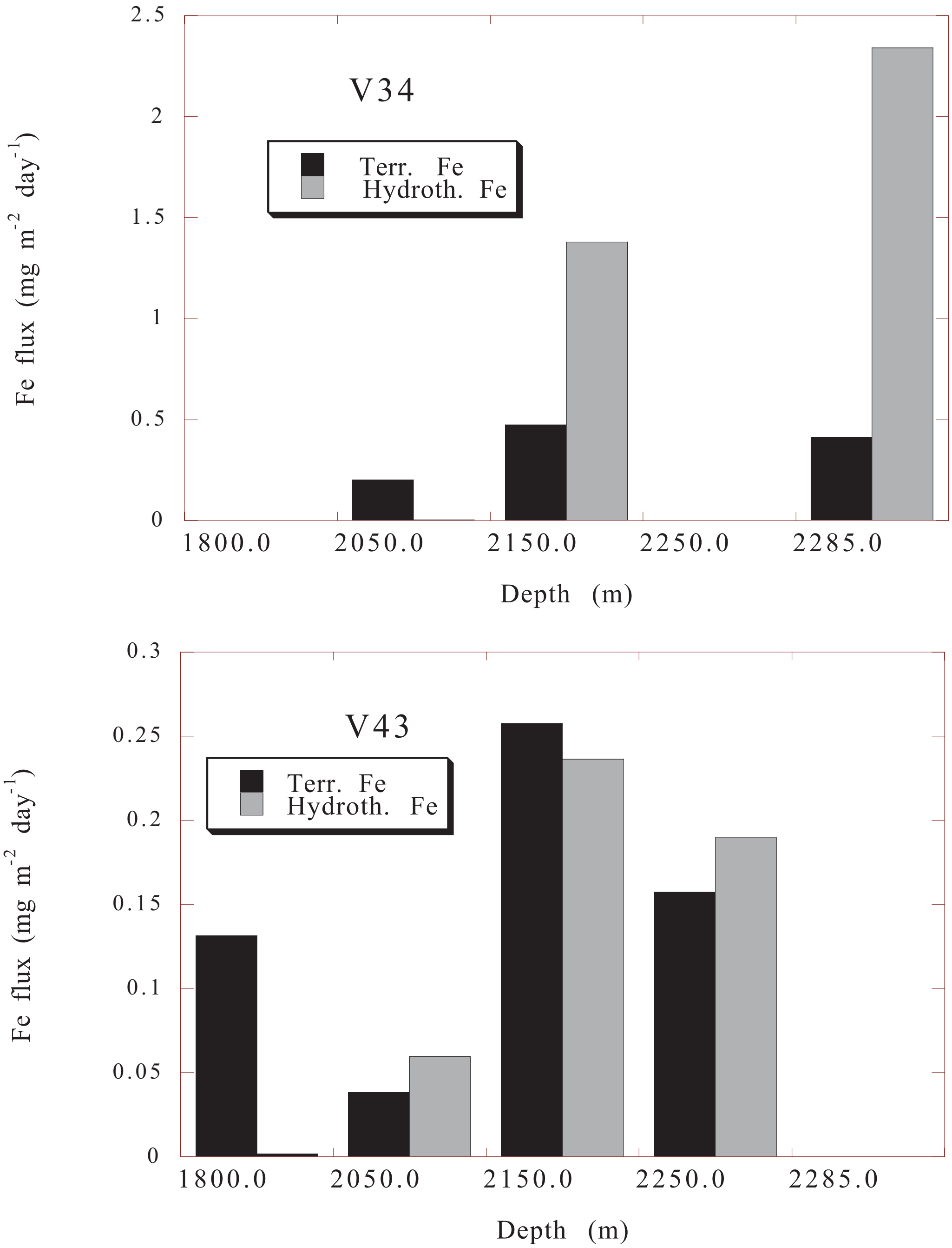

Figure 22: Fe flux partitioned into that having terrestrial and hydrothermal origins at moorings V34 and V43. Flux magnitudes represent the mean Fe flux of the entire sediment trap at the various depths shown.

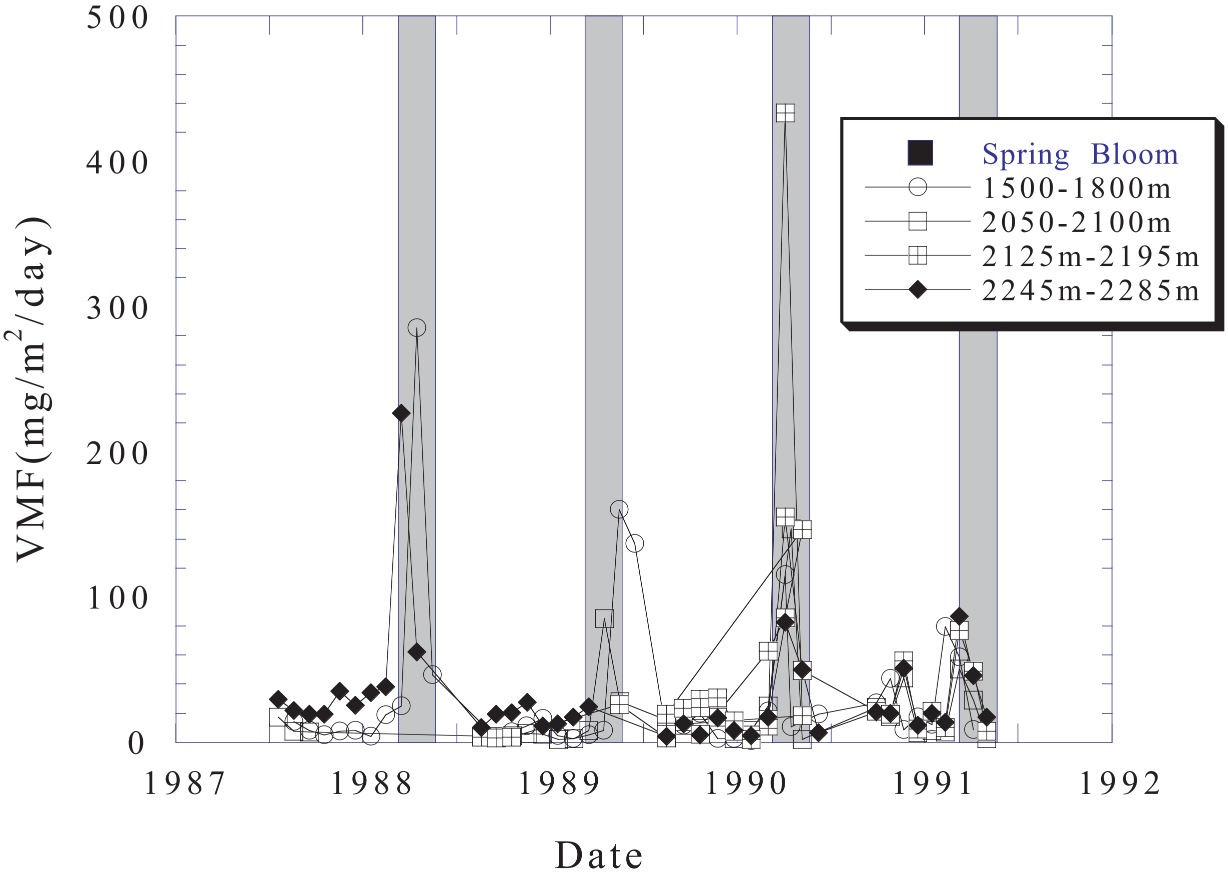

Figure 23: Particle flux from four depth bins from the time series data. Grey bars show approximate timing of the spring bloom (Perry *et al.*, 1989).

4.3 Seasonal Variation

Between 1987 and 1991 several mooring arrays were deployed at north Cleft that were located closely enough together from year to year to construct coherent time series plots of the VMF at those sites. In general, except in cases of malfunction, all the data represent 27- to 33-day collections or nearly a year's worth of data per trap. Several depth horizons are used to show representative flux patterns from throughout the lower water column. The data used to construct the VMF plots were from moorings V18, V23, V24, V25, V26, and V43 (Fig. 23). The periodicity of seasonal phytoplankton blooms off Oregon-Washington and the mechanisms and forces governing the onset and duration of such occurrences have been summarized and reported by Anderson (1964) and Perry *et al.* (1989).

The background VMF throughout the time series study at the selected mooring sites at all depths was about 10–25 mg m^{-2} day^{-1}. The relatively steady sedimentation rate is seen to change abruptly in bursts of increased sedimentation during the spring months every year and, to a lesser degree, during the fall months of some years. The most dramatic increase was measured during the spring of 1990 at the 2150–2175 m depth horizon when the VMF increased to over 400 mg m^{-2} day^{-1}. Other VMF spring peak magnitudes were ~290 mg m^{-2} day^{-1} at the 1500–1800 depth, ~150 mg m^{-2} day^{-1} at the 1500–1800 m depth and ~80 mg m^{-2} day^{-1} at the 2245–2285 m depth during 1988, 1989, and 1991, respectively. Fall peaks of about 40–60 mg m^{-2} day^{-1} appeared during most years of this study. The highest fall peak, about 60 mg m^{-2} day^{-1}, was observed at all depths during 1990.

Many researchers (Deuser and Ross, 1980; Deuser *et al.*, 1981; Honjo, 1982; Smith and Baldwin, 1984; Billet *et al.*, 1983; Lampitt, 1985; Wefer *et al.*, 1988; Deuser, 1986, 1987; Dymond and Roth, 1988) have documented that the annual cycle of primary production is responsible for seasonally regulated pulses of particles to the ocean floor. Surface biogenic material in our samples was routinely inspected under a Wild microscope immediately after filtration. Items that commonly dominated the samples included foraminifera, radiolarians, silicious spicules, diatom tests, and fecal pellets. All of the above-mentioned biogenic parts and pieces were commonly embedded in an amorphous organic matrix (marine snow). These observations support the hypothesis that such macro-aggregates (Shanks and Trent, 1980; Alldredge, 1979; Silver and Alldredge, 1981; Wakeham *et al.*, 1993) and fecal pellets (Turner and Ferrante, 1979 and references therein) provide effective mechanisms for the transfer of particles from the sea surface to the sea floor. Export of materials from the sea surface begins with the aggregation of sinking planktonic carcasses, diatomaceous mucous nets (Smetacek, 1985), fecal pellets, other particulates, and amorphous organic material. The remains of such material were readily identifiable, especially in the spring samples, because of the high concentrations of biogenic components. Such aggregates may provide an effective mechanism for removing the mineral precipitates from hydrothermal plumes as the aggregates sink through them. This mechanism is likely to be especially pronounced during the heavy flux of spring bloom detritus. The results of the total VMF time series analysis and the elemental flux data clearly indicate that both total and hydrothermal elemental particle flux maxima coincided closely in most cases, with the timing of spring phytoplankton blooms (Figs. 15 and 23). We frequently observed secondary fall and early-winter pulses of sedimentation which we presume are mediated by fall plankton blooms. Studies by Lund (1957) and Denny and Walsh (1979) indicated that sinking diatoms carried surface Pb and Zn to the bottom, and others have speculated that such aggregates would scavenge fecal pellets and fine particles (Small *et al.*, 1989; Honjo, 1980; Nozaki *et al.*, 1987; Bishop *et al.*, 1977; Bacon *et al.*, 1985) during descent and sediment them to the bottom. In light of these studies and our observations it is reasonable that sedimentation of hydrothermal particles to the bottom is implemented by such organic aggregates.

This hypothesis is supported by the seasonal pattern of elements with a strong hydrothermal source (e.g., Fe, Mn, P, V, Cu). The sedimentation of these elements consistently showed strong increases during the spring and fall bloom periods (Figs. 10, 12, 15). Moreover, the flux increase from shallow to deep traps was also greatest during the blooms, an increase not seen in the total VMF (Fig. 15). This difference confirms that these elements do not primarily originate in the overlying surface waters but are scavenged out of the hydrothermal plume by bloom-produced biogenic material.

Thus, a pattern emerges from these data which suggests that there is a predictable periodicity to the vertical flux of hydrothermal plume particles and the periodicity appears to be strongly linked to the annual cycles of total VMF, which in turn appears to reflect the annual cycles of primary production in the overlying surface waters. The coincidence of the timing of maximum total flux and maximum hydrothermal flux presents a reasonable argument for seasonal pulses of surface biogenic matter mediating the vertical flux of hydrothermal particulates from the plume to the sea floor. It is possible that the surface aggregates trap and continue to agglomerate with the plume particles as they sink through it, thereby removing them to the bottom.

4.4 Opal

During microscopic examination of samples from the 1990 short-term traps it was noticed that opal fragments (diatom and radiolarian) were ubiquitous and especially abundant. These observations prompted us to quantify the opal concentration in as many samples as possible. Opal comprised 62 $\pm$ 10% of the VMF in the 1990 samples. The opal contribution to the 1988–1989 samples (moorings V23, V24) was $\sim$17%; the Endeavor Ridge samples of the Dymond and Roth study (1988) contained $\sim$31% opal. The 1990 summer opal concentrations were likely high because they coincided with a diatom and radiolarians bloom that typically occurs during July–August in the northeast Pacific (Takahashi, 1986, 1987). Our opal concentration intercomparisons are made with reservation because collection periods were not similar in all cases.

5. Summary

Sediment traps were deployed on subsurface moorings on and about the Juan de Fuca Ridge, generally within 300 m of the bottom, for the purpose of learning more about the vertical flux of particulates near regions of hydrothermal venting and especially the vertical settling of particles from vent generated plumes. During each successful sediment trap deployment period, ten sequential subsamples were collected. Deployment periods lasted from days to nearly a year. The study was conducted continuously from 1984 to 1991; samples were analyzed in all cases for mass and in several cases for a suite of elements including those that are enriched in seawater from hydrothermal venting, and biogenic silica. A summary of the findings of the study include:

1. The mean total VMF (binned data) for on-axis samples from north and south Cleft segment, from 1984–1991, from <2100 m was 25.3 $\pm$ 20.8 mg m^{-2} day^{-1}; at depths from 2100 m to 2150 m the mean was 37.3 $\pm$ 35.0 mg m^{-2} day^{-1}; at depths >2150 m the mean was 44.8 $\pm$ 45.9 mg m^{-2} day^{-1}. The mean flux at the bottom depth bin is

1.8 times greater than in the uppermost depth bin; the difference is significant (95% C.I.). Current meter records suggest that resuspension was at least partially responsible for the increased bottom flux.

2. Elemental analysis of particulates from moorings V34 and V43 shows that elemental flux was generally 2 to 5 times greater below the hydrothermal plume at the JDFR as above the plume. In the case of hydrothermal Fe at V43 the enrichment was more than a hundredfold. In addition, the enrichment of Mn, Cu, and V in our bottommost traps was confirmation that hydrothermal particles are sedimented to the seafloor within 3 km of Pipe Organ Vent.

3. The measured VMF demonstrated a strong seasonal signal as a result of surface phytoplankton blooms. Vertical mass flux increased several hundredfold in some years following the surface bloom. Furthermore, temporal variations of elemental flux was found to trend similarly to the total VMF trends. Increased elemental flux was especially pronounced during the annual spring plankton bloom.

4. Microscopic examination of our samples indicated that organic aggregates comprise a major portion of the vertical particulate flux and they may be responsible for removing hydrothermal particles from the plume, especially following the spring bloom when the rain of surface debris to the seafloor is at a maximum.

6. Acknowledgments

The authors would like to thank the crews of the NOAA vessels R/V *Discoverer* and R/V *Surveyor* for their help, and particularly the deck crew supervised by Herb Padilla of the *Discoverer*.

7. References

Alldredge, A.L. (1979): The chemical composition of macroscopic aggregates in two neritic seas. *Limnol. Oceanogr., 24,* 855–866.

Anderson, G.C. (1964): The seasonal and geographic distribution of primary productivity off the Washington and Oregon coasts. *Limnol. Oceanogr., 9,* 284–302.

Bacon, M.P., C.-A. Huh, A.P. Fleer, and W.G. Deuser (1985): Seasonality in the flux of natural radionuclides and plutonium in the deep Sargasso Sea. *Deep-Sea Res., 32*(3), 273–286.

Baker, E.T. (1994): A 6-year time series of hydrothermal plumes over the Cleft Segment of the Juan de Fuca Ridge. *J. Geophys. Res., 99*(B3), 4889–4904.

Baker, E.T., and S.R. Hammond (1992): Hydrothermal venting and the apparent magmatic budget of the Juan de Fuca Ridge. *J. Geophys. Res., 97*(B3), 3443–3456.

Baker, E.T., J.W. Lavelle, R.A. Feely, G.J. Massoth, and S.L. Walker (1989): Episodic venting of hydrothermal fluids from the Juan de Fuca Ridge. *J. Geophys. Res., 94*(B7), 9237–9250.

Baker, E.T., J.W. Lavelle, and G.J. Massoth (1985): Hydrothermal particle plumes over the southern Juan de Fuca Ridge. *Nature, 316*(6026), 342–344.

Baker, E.T., and G.J. Massoth (1986): Hydrothermal plume measurements: a regional perspective. *Science, 234*, 980–982.

Baker, E.T., G.J. Massoth, and R.A. Feely (1987): Cataclysmic hydrothermal venting on the Juan de Fuca Ridge. *Nature, 6135,* 149–151.

Baker, E.T., and H.B. Milburn (1983): An instrument system for the investigation of particle fluxes. *Cont. Shelf Res., 1*(4), 425–435.

Billett, D.S.M., R.S. Lampitt, A.L. Rice, and R.F.C. Mantoura (1983): Seasonal sedimentation of phytoplankton to the deep-sea benthos. *Nature, 302*(7), 520–522.

Bishop, J.K.B., J.M. Edmond, D.R. Ketten, M.P. Bacon, and W.B. Silker (1977): The chemistry, biology, and vertical flux of particulate maatter from the upper 400 m of the equatorial Atlantic Ocean. *Deep-Sea Res., 24,* 511–548.

Cannon, G., D.J. Pashinski, and M.R. Lemon (1991): Middepth flow near hydrothermal venting sites on the southern Juan de Fuca Ridge. *J. Geophys. Res., 96*(C7), 12,815–12,831.

Delaney, J.R., H.P. Johnson, and J.L. Karsten (1981): The Juan de Fuca Ridge hot spot-propagating rift system: New tectonic, geochemical, and magnetic data. *J. Geophys. Res., 86*(B12), 11,747–11,750.

Denny, P., and R.P. Walsh (1979): Lead accumulation in plankton blooms from Ullswater, the English Lake District. *Environ. Pollut., 18,* 1–9.

Deuser, W.G., and E. H. Ross (1980): Seasonal change in the flux of organic carbon to the deep Sargasso Sea. *Nature, 283*(24), 364–365.

Deuser, W.G., E.H. Ross, and R.F. Anderson (1981): Seasonality in the supply of sediment to the deep Sargasso Sea and implications for the rapid transfer of matter to the deep ocean. *Deep-Sea Res., 28A*(5), 495–505.

Deuser, W.G. (1986): Seasonal and interannual variations in deep-water particle fluxes in the Sargasso Sea and their relation to surface hydrography. *Deep-Sea Res., 33*(2), 225–246.

Deuser, W.G. (1987): Variability of hydrography and particle flux: transient and long-term relationships. In: E.T. Degens, E. Izdar, and S. Honjo (eds.), *Particle Flux in the Ocean: Proceedings of a Workshop Sponsored by the Deutsch Forschungsgemeinschaft (DFG) and the Turkish Research Council (Tübitak), at the Dokuz Eylül University, Izmir, Turkey, June 23–28, 1986.* Im Selgstferlag des Geologisch-Palaöntologischen Institutes der Universität Hamburg, 1987.

Dymond, J., and S. Roth (1988): Plume dispersed hydrothermal particles: A time-series record of settling flux from the Endeavour Ridge using moored sensors. *Geochim. Cosmochim. Acta, 52,* 2525–2536.

Embley, R.W., W. Chadwick, M.R. Perfit, and E.T. Baker (1991): Geology of the northern Cleft Segment, Juan de Fuca Ridge: Recent lava flows, sea-floor spreading, and the formation of megaplumes. *Geology, 19,* 771–775.

Feely, R A., E.T. Baker, G.T. Lebon, J.F. Gendron, G.J. Massoth, and C.W. Mordy (1998): Chemical variations of hydrothermal particles in the 1996 Gorda Ridge event and chronic plumes. *Deep-Sea Res. II, 45*(12), 2637–2664.

Feely, R.A., M.A. Lewison, G.J. Massoth, G. Robert-Baldo, J.W. Lavelle, R.H. Byrne, K.L. Von Damm, and H.C. Curl, Jr. (1987): Composition and dissolution of black smoker particles from active vents on the Juan de Fuca Ridge. *J. Geophys. Res., 92*(11), 11,347–11,363.

Feely, R.A., G.J. Massoth, E.T. Baker, G.T. Lebon, and T.L. Geiselman (1992): Tracking the dispersal of hydrothermal plumes from the Juan de Fuca Ridge using suspended matter composition. *J. Geophys. Res., 97*(B3), 3457–3468.

Feely, R.A., G.J. Massoth, and G.T. Lebon (1991): Sampling of marine particulate matter and analysis by x-ray fluorescence spectrometry. In: *Marine Particles: Analysis and Characterization, Geophys. Monogr. Ser.*, vol. 63, D.C. Hurd and D. W. Spencer (eds.), AGU, Washington, D.C., 251–257.

Feely, R.A., G.J. Massoth, J.H. Trefry, E.T. Baker, A.J. Paulson, and G.T. Lebon (1994): Composition and sedimentation of hydrothermal plume particles from North Cleft segment, Juan de Fuca Ridge. *J. Geophys. Res., 99*(B3), 4985–5006.

Froelich, P.N, G.P. Klinkhammer, M.L. Bender, N.A. Luedtke, G.R. Heath, D. Cullen, P. Dauphin, D. Hammond, B. Hartman, and V. Maynard (1979): Early oxidation of organic matter in pelagic sediments of the eastern equatorial Atlantic: suboxic digenesis. *Geochim. Cosmochim. Acta, 43,* 1075–1090.

Gardner, W.D., J.B. Southard, and C.D. Hollister (1985): Sedimentation, resuspension and chemistry of particles in the northwest Atlantic. *Mar. Geol., 65,* 199–242.

Honjo, S. (1980): Material fluxes and modes of sedimentation in the mesopelagic and bathypelagic zones. *J. Mar. Res., 38,* 53–97.

Honjo, S. (1982): Seasonality and interaction of biogenic and lithogenic particulate flux at the Panama Basin. *Science, 218*(26), 883–884.

Karlin, R., and M. Lyle (1986): Sediment studies on the Gorda Ridge. State of Oregon, Department of Geology and Mineral Industries, Open File Report 0-86-19, 76 pp.

Knauer, G.A., D.M. Darl, J.H. Martin, and C.N. Hunter (1984): In situ effects of selected preservatives on total carbon, nitrogen and metals collected in sediment traps. *J. Mar. Res., 42*(2), 445–462.

Krausse, G.L., C.L. Schelske, and C.O. Davis (1983): Comparison of 2 wet-alkaline methods of disgestion of biogenic silica in water. *Freshwater Biol., 13,* 73–82.

Lampitt, R.S. (1985): Evidence for the seasonal deposition of detritus to the deep-sea floor and its subsequent resuspension. *Deep-Sea Res., 32*(8), 885–897.

Lonsdale, P., and J.B. Southaard (1974): Experimental erosion of North Pacific red clay. *Mar. Geol., 17,* M51–M60.

Lund, J.W. (1957): Chemical analysis in ecology illustrated from Lake District tarns and lakes. 2. Algal differences. *Proc. Linn. Soc. Lond., 167,* 165–171.

Lupton, J.E., J.R. Delaney, H.P. Johnson, and M.K. Tivey (1985): Entrainment and vertical transport of deep-ocean water by buoyant hydrothermal plumes. *Nature, 316,* 621–623.

Martin, J.H., and G.A. Knauer (1983): VERTEX: Manganese transport with $CaCO_3$. *Deep-Sea Res., 30,* 411–425.

Massoth, G.J., E.T. Baker, J.E. Lupton, R.A. Feely, D.A. Butterfield, K. Von Damm, K.K. Roe, and G.T. Lebon (1994): Temporal and spatial variability of hydrothermal manganese and iron at Cleft segment, Juan de Fuca Ridge. *J. Geophys. Res., 99,* 4905–4924.

Normark, W.R., J.L. Morton, R.A. Koski, and D.A. Clague (1983): Active hydrothermal vents and sulfide deposits on the southern Juan de Fuca Ridge. *Geology, 11,* 158–163.

Nozaki, Y., H.-S. Yang, and M. Yamada (1987): Scavenging of thorium in the ocean. *J. Geophys. Res., 92*(C1), 772–778.

Paasche, E. (1973): Silicon and the ecology of marine plankton diatoms. I. *Thalassiosira pseudonana* (*Cyclotella nana*) growth in a chemostat with silicate as limiting nutrient. *Mar. Biol., 198,* 117–126.

Perry, M.J., J.P. Bolger, and D.C. English (1989): Primary production in Washington coastal waters. In: *Coastal Oceanography of Washington and Oregon*, M.R. Landry and B.M. Hickey (eds.), Elsevier, Amsterdam, Netherlands, 117–173.

Rowe, G.T., and W.D. Gardner (1979): Sedimentation rates in the slope water of the northwest Atlantic Ocean measured directly with sediment traps. *J. Mar. Res., 37,* 581–600.

Shanks, A.L., and J.D. Trent (1980): Marine snow: sinking rates and potential role in vertical flux. *Deep-Sea Res., 274,* 137–143.

Silver, M.W., and A.L. Alldredge (1981): Bathypelagic marine snow: Deep-sea algal and detrital community. *J. Mar. Resour., 39,* 501–530.

Small, L.F., H. Pak, D.M. Nelson, and C.S. Weimer (1989): Seasonal dynamics of suspended particulate matter. In: *The Coastal Oceanography of Washington and Oregon,* M.R. Landry and B.M. Hickey (eds.), Elsevier, Amsterdam, 255–285.

Smetacek, V.S. (1985): Role of sinking in diatom life-history cycles: Ecological, evolutionary, and geological significance. *Mar. Biol., 84,* 239–251.

Smith, K.L., and R.J. Baldwin (1984): Seasonal fluctuations in deep-sea sediment community oxygen consumption: Central and eastern North Pacific. *Nature, 307*(16), 624–626.

Southard, J.B., R.A. Young, and C.D. Hollister (1971): Experimental erosion of calcareous ooze. *J. Geophys. Res., 76,* 5903–5909.

Takahashi, K. (1986): Seasonal fluxes of pelagic diatoms in the subarctic Pacific, 1982–1983. *Deep-Sea Res., 33*(9), 1225–1251.

Takahashi, K. (1987): Radiolarian flux and seasonality: Climatic and El Niño response in the subarctic Pacific, 1982–1983. *Global Biogeochem. Cycles, 1*(3), 213–231.

Tennant, D.A., and E.T. Baker (1992): A fast, high-precision splitter for particle suspensions. *Mar. Geol., 108,* 247–252.

Tennant, D.A., S.L. Walker, J.W. Lavelle, and E.T. Baker (1987): A practical manual for determining settling rates of ocean disposed sewage sludge. NOAA Tech. Memo. ERL PMEL-69 (PB87-178273), 29 pp.

Turner, J.T., and J.G. Ferrante (1979): Zooplankton fecal pellets in aquatic ecosystems. *BioScience, 29*(11), 670–677.

Wakeham, S.G., J.I. Hedges, C. Lee, and T.K. Pease (1993): Effects of poisons and preservatives on the composition of organic matter in a sediment trap experiment. *J. Mar. Res., 51*(3), 669–696.

Walsh, I., K. Fischer, D. Murray, and J. Dymond (1988): Evidence for resuspension of rebound particles from near-bottom sediment traps. *Deep-Sea Res., 35,* 59–70.

Wefer, G., G. Fischer, D. Fuetterer, and R. Gersonde (1988): Seasonal particle flux in the Bransfield Strait, Antarctica. *Deep-Sea Res., 35*(6), 891–898.

Tables

Table 1: Sediment trap moorings: location and deployment data.

Mooring designation	Latitude	Longitude	Collection days/ cylinder	Deployment dates	Trap depths
V1	44°38.6′N	130°24.1′W	35	5/85–5/86	2030
V4	44°40.9′N	130°21.6′W	2	5/84–6/84	2178
V5	44°38.8′N	130°25.9′W	10	6/84–9/84	1858,2056,2258,2338
V7	44°41.7′N	130°22.7′W	3.5	6/85–7/85	1950,2195,2230, 2240,2245
V8	44°42.0′N	130°35.3′W	30	6/85–4/86	1348,1698,1948, 2150,2230
V9	44°47.7′N	130°24.5′W	30	8/86–6/87	1805,2205,2405
V10	44°41.42′N	130°21.52′W	1	6/86	2154,2204,2229
V11	44°41.05′N	130°13.91′W	30	8/86–6/87	2200
V12	44°41.4′N	130°21.0′W	30	8/86–6/87	2152,2202,2227
V17	44°59.1′N	130°59.5′W	30	7/87–5/88	1500,2100,2500
V18	44°53.4′N	130°15.6′W	30	7/87–5/88	1500,2100,2285
V19	44°41.3′N	130°21.6′W	30	7/87–5/88	2000,2245
V20	44°59.5′N	130°11.4′W	2	9/87	1655,2155,2205,2225
V23	44°48.14′N	130°18.38′W	30	7/88–5/89	1850,2050,2125,2195
V24	45°09.99′N	130°10.17′W	30	7/88–5/89	1850,2100,2175,2245
V25	45°06.0′N	130°10.0′W	33	8/89–7/90	1848,2100,2175,2245
V26	44°48.0′N	130°18.8′W	33	8/89–7/90	1848,2050,2125,2195 2195
V32	44°54.4′N	130°07.8′W	6	7/90–9/90	1800,2250
V33	44°56.0′N	130°12.35′W	6	7/90–9/90	2150
V34	44°56.3′N	130°14.7′W	6	7/90–9/90	2050,2150,2150,2285
V35	44°56.7′N	130°15.4′W	6	7/90–9/90	2150
V36	44°57.7′N	130°20.4′W	6	7/90–9/90	1500,1800,1800,2250
V37	44°57.0′N	130°10.6′W	6	7/90–9/90	2200
V38	44°58.8′N	130°13.1′W	6	7/90–9/90	2050,2150
V39	44°58.8′N	130°16.4′W	6	7/90–9/90	2200
V40	44°53.6′N	130°11.8′W	6	7/90–9/90	2200
V41	44°53.8′N	130°15.7′W	6	7/90–9/90	2050,2150
V42	44°53.3′N	130°18.5′W	6	7/90–9/90	2200
V43	44°56.3′N	130°14.7′W	27	9/90–6/91	1800,2050,2150,2250

Table 2: Total VMF and biogenic opal concentrations (when analyzed) from mooring V1 to V26 and V43.

Mooring ID	Latitude	Longitude	Collection period (days)	Completion date	Depth (m)	mab	Mass (g)	VMF (mg/m^2/day)	Mean flux ± 1 std dev	% Opal
V1/28-1	44°38.6′N	130°24.1′W	35	1984.400	2030	100				
V1/28-2	44°38.6′N	130°24.1′W	35	1984.496	2030	100				
V1/28-3	44°38.6′N	130°24.1′W	35	1984.592	2030	100				
V1/28-4	44°38.6′N	130°24.1′W	35	1984.688	2030	100				
V1/28-5	44°38.6′N	130°24.1′W	35	1984.784	2030	100				
V1/28-6	44°38.6′N	130°24.1′W	35	1984.880	2030	100				
V1/28-7	44°38.6′N	130°24.1′W	35	1984.975	2030	100				
V1/28-8	44°38.6′N	130°24.1′W	35	1985.071	2030	100				
V1/28-9	44°38.6′N	130°24.1′W	35	1985.167	2030	100				
V1/28-10	44°38.6′N	130°24.1′W	35	1985.263	2030	100				
V4/33-1	44°40.9′N	130°21.6′W	2	1984.400	2178	60			110 ± 40	
V4/33-2	44°40.9′N	130°21.6′W	2	1984.406	2178	60				
V4/33-3	44°40.9′N	130°21.6′W	2	1984.411	2178	60				
V4/33-4	44°40.9′N	130°21.6′W	2	1984.416	2178	60				
V4/33-5	44°40.9′N	130°21.6′W	2	1984.422	2178	60				
V4/33-6	44°40.9′N	130°21.6′W	2	1984.427	2178	60				
V4/33-7	44°40.9′N	130°21.6′W	2	1984.433	2178	60				
V4/33-8	44°40.9′N	130°21.6′W	2	1984.438	2178	60				
V4/33-9	44°40.9′N	130°21.6′W	2	1984.444	2178	60				
V4/33-10	44°40.9′N	130°21.6′W	2	1984.449	2178	60				
V5/30-1	44°38.8′N	130°25.9′W	10	1984.400	1858	500	0.0	0.0	37.4 ± 33	
V5/30-2	44°38.8′N	130°25.9′W	10	1984.427	1858	500	34.4	105.7		
V5/30-3	44°38.8′N	130°25.9′W	10	1984.455	1858	500	21.4	65.7		
V5/30-4	44°38.8′N	130°25.9′W	10	1984.482	1858	500	11.6	35.6		
V5/30-5	44°38.8′N	130°25.9′W	10	1984.510	1858	500	16.0	49.2		
V5/30-6	44°38.8′N	130°25.9′W	10	1984.537	1858	500	5.1	15.6		
V5/30-7	44°38.8′N	130°25.9′W	10	1984.564	1858	500	4.4	13.4		
V5/30-8	44°38.8′N	130°25.9′W	10	1984.592	1858	500	12.0	37.0		
V5/30-9	44°38.8′N	130°25.9′W	10	1984.619	1858	500	2.8	8.6		
V5/30-10	44°38.8′N	130°25.9′W	10	1984.647	1858	500	1.6	4.8		

Table 2: (continued).

Mooring ID	Latitude	Longitude	Collection period (days)	Completion date	Depth (m)	mab	Mass (g)	VMF ($mg/m^2/day$)	Mean flux ± 1 std dev	% Opal
V5/35-1	44°38.8′N	130°25.9′W	10	1984.400	2056	301	0.0	0.0	40 ± 33	
V5/35-2	44°38.8′N	130°25.9′W	10	1984.427	2056	301	23.9	73.6		
V5/35-3	44°38.8′N	130°25.9′W	10	1984.455	2056	301	27.6	84.8		
V5/35-4	44°38.8′N	130°25.9′W	10	1984.482	2056	301	17.1	52.5		
V5/35-5	44°38.8′N	130°25.9′W	10	1984.510	2056	301	26.9	82.8		
V5/35-6	44°38.8′N	130°25.9′W	10	1984.537	2056	301	7.2	22.3		
V5/35-7	44°38.8′N	130°25.9′W	10	1984.564	2056	301	5.2	16.1		
V5/35-8	44°38.8′N	130°25.9′W	10	1984.592	2056	301	4.4	13.5		
V5/35-9	44°38.8′N	130°25.9′W	10	1984.619	2056	301	2.5	7.8		
V5/35-10	44°38.8′N	130°25.9′W	10	1984.647	2056	301	1.6	5.0		
V5/27-1	44°38.8′N	130°25.9′W	10	1984.400	2258	100	0.0	0.0	80.7 ± 78	
V5/27-2	44°38.8′N	130°25.9′W	10	1984.427	2258	100	39.6	121.7		
V5/27-3	44°38.8′N	130°25.9′W	10	1984.455	2258	100	40.4	124.4		
V5/27-4	44°38.8′N	130°25.9′W	10	1984.482	2258	100	27.4	84.3		
V5/27-5	44°38.8′N	130°25.9′W	10	1984.510	2258	100	83.0	255.5		
V5/27-6	44°38.8′N	130°25.9′W	10	1984.537	2258	100	15.1	46.5		
V5/27-7	44°38.8′N	130°25.9′W	10	1984.564	2258	100	9.6	29.4		
V5/27-8	44°38.8′N	130°25.9′W	10	1984.592	2258	100	9.6	29.5		
V5/27-9	44°38.8′N	130°25.9′W	10	1984.619	2258	100	7.0	21.5		
V5/27-10	44°38.8′N	130°25.9′W	10	1984.647	2258	100	4.2	12.8		
V5/25-1	44°38.8′N	130°25.9′W	10	1984.400	2338	20				
V5/25-2	44°38.8′N	130°25.9′W	10	1984.427	2338	20	54.0	166.1	110.8 ± 67	
V5/25-3	44°38.8′N	130°25.9′W	10	1984.455	2338	20	61.4	188.9		
V5/25-4	44°38.8′N	130°25.9′W	10	1984.482	2338	20	57.7	177.4		
V5/25-5	44°38.8′N	130°25.9′W	10	1984.510	2338	20	0.0	0.0		
V5/25-6	44°38.8′N	130°25.9′W	10	1984.537	2338	20	37.9	116.6		
V5/25-7	44°38.8′N	130°25.9′W	10	1984.564	2338	20	22.3	68.5		
V5/25-8	44°38.8′N	130°25.9′W	10	1984.592	2338	20	25.2	77.6		
V5/25-9	44°38.8′N	130°25.9′W	10	1984.619	2338	20	16.2	49.8		
V5/25-10	44°38.8′N	130°25.9′W	10	1984.647	2338	20	13.2	40.6		

Table 2: (continued).

Mooring ID	Latitude	Longitude	Collection period (days)	Completion date	Depth (m)	mab	Mass (g)	VMF ($mg/m^2/day$)	Mean flux ± 1 std dev	% Opal
V7/6-1	44°41.7′N	130°22.7′W	4	1985.445	2195	55	1.0	9.2	33.7 ± 27	
V7/6-2	44°41.7′N	130°22.7′W	4	1985.455	2195	55	1.5	13.8		
V7/6-3	44°41.7′N	130°22.7′W	4	1985.464	2195	55	6.5	58.7		
V7/6-4	44°41.7′N	130°22.7′W	4	1985.474	2195	55	1.5	14.0		
V7/6-5	44°41.7′N	130°22.7′W	4	1985.484	2195	55	1.3	11.7		
V7/6-6	44°41.7′N	130°22.7′W	4	1985.493	2195	55	1.6	14.2		
V7/6-7	44°41.7′N	130°22.7′W	4	1985.503	2195	55	9.6	87.2		
V7/6-8	44°41.7′N	130°22.7′W	4	1985.512	2195	55	3.2	28.8		
V7/6-9	44°41.7′N	130°22.7′W	4	1985.522	2195	55	3.7	33.8		
V7/6-10	44°41.7′N	130°22.7′W	4	1985.532	2195	55	7.3	66.1		
V7/15-1	44°41.7′N	130°22.7′W	4	1985.445	2230	20	1.8	16.5	28.0 ± 13	
V7/15-2	44°41.7′N	130°22.7′W	4	1985.455	2230	20	2.0	18.1		
V7/15-3	44°41.7′N	130°22.7′W	4	1985.464	2230	20	3.3	29.7		
V7/15-4	44°41.7′N	130°22.7′W	4	1985.474	2230	20	2.2	20.4		
V7/15-5	44°41.7′N	130°22.7′W	4	1985.484	2230	20	2.5	22.9		
V7/15-6	44°41.7′N	130°22.7′W	4	1985.493	2230	20	1.7	15.7		
V7/15-7	44°41.7′N	130°22.7′W	4	1985.503	2230	20	2.5	22.4		
V7/15-8	44°41.7′N	130°22.7′W	4	1985.512	2230	20	5.1	46.3		
V7/15-9	44°41.7′N	130°22.7′W	4	1985.522	2230	20	4.2	37.9		
V7/15-10	44°41.7′N	130°22.7′W	4	1985.532	2230	20	5.7	52.0		
V7/29-1	44°41.7′N	130°22.7′W	4	1985.445	2245	5	1.3	12.0	32.4 ± 16	
V7/29-2	44°41.7′N	130°22.7′W	4	1985.455	2245	5	3.1	28.2		
V7/29-3	44°41.7′N	130°22.7′W	4	1985.465	2245	5	2.7	24.6		
V7/29-4	44°41.7′N	130°22.7′W	4	1985.474	2245	5	2.6	23.4		
V7/29-5	44°41.7′N	130°22.7′W	4	1985.484	2245	5	2.6	23.8		
V7/29-6	44°41.7′N	130°22.7′W	4	1985.493	2245	5	3.9	35.7		
V7/29-7	44°41.7′N	130°22.7′W	4	1985.503	2245	5	3.2	29.4		
V7/29-8	44°41.7′N	130°22.7′W	4	1985.513	2245	5	4.2	38.3		
V7/29-9	44°41.7′N	130°22.7′W	4	1985.522	2245	5	7.8	70.6		
V7/29-10	44°41.7′N	130°22.7′W	4	1985.532	2245	5	4.1	37.6		

Table 2: (continued).

Mooring ID	Latitude	Longitude	Collection period (days)	Completion date	Depth (m)	mab	Mass (g)	VMF (mg/m^2/day)	Mean flux ± 1 std dev	% Opal
V8/30-1	44°42.0′N	130°35.3′W	30	1985.521	1348	902	49.5	50.9	46.1 ± 26	
V8/30-2	44°42.0′N	130°35.3′W	30	1985.603	1348	902	21.7	22.3		
V8/30-3	44°42.0′N	130°35.3′W	30	1985.685	1348	902	23.6	24.2		
V8/30-4	44°42.0′N	130°35.3′W	30	1985.768	1348	902	40.7	41.8		
V8/30-5	44°42.0′N	130°35.3′W	30	1985.850	1348	902	50.2	51.7		
V8/30-6	44°42.0′N	130°35.3′W	30	1985.932	1348	902	59.3	60.9		
V8/30-7	44°42.0′N	130°35.3′W	30	1986.014	1348	902	83.3	85.6		
V8/30-8	44°42.0′N	130°35.3′W	30	1986.096	1348	902	21.1	21.7		
V8/30-9	44°42.0′N	130°35.3′W	30	1986.179	1348	902	15.7	16.2		
V8/30-10*	44°42.0′N	130°35.3′W	170	1986.643	1348	902	474.6	86.4		
V8/31-1	44°42.0′N	130°35.3′W	30	1985.521	1698	552	25.1	25.8	42.5 ± 31	
V8/31-2	44°42.0′N	130°35.3′W	30	1985.603	1698	552	16.4	16.8		
V8/31-3	44°42.0′N	130°35.3′W	30	1985.685	1698	552	19.5	20.4		
V8/31-4	44°42.0′N	130°35.3′W	30	1985.768	1698	552	51.7	53.2		
V8/31-5	44°42.0′N	130°35.3′W	30	1985.850	1698	552	44.6	45.9		
V8/31-6	44°42.0′N	130°35.3′W	30	1985.932	1698	552	50.6	52.0		
V8/31-7	44°42.0′N	130°35.3′W	30	1986.014	1698	552	116.4	119.7		
V8/31-8	44°42.0′N	130°35.3′W	30	1986.096	1698	552	18.7	19.2		
V8/31-9	44°42.0′N	130°35.3′W	30	1986.179	1698	552	13.3	13.7		
V8/31-10	44°42.0′N	130°35.3′W	30	1986.261	1698	552	56.2	57.8		
V8/32-1	44°42.0′N	130°35.3′W	30	1985.521	1948	302	3.2	3.3	12.6 ± 8.3	
V8/32-2	44°42.0′N	130°35.3′W	30	1985.603	1948	302	26.1	26.9		
V8/32-3	44°42.0′N	130°35.3′W	30	1985.685	1948	302	7.7	7.9		
V8/32-4	44°42.0′N	130°35.3′W	30	1985.768	1948	302	9.4	9.6		
V8/32-5	44°42.0′N	130°35.3′W	30	1985.850	1948	302	10.8	11.1		
V8/32-6*	44°42.0′N	130°35.3′W	290	1986.259	1948	302	16.7	16.7		

Table 2: (continued).

Mooring ID	Latitude	Longitude	Collection period (days)	Completion date	Depth (m)	mab	Mass (g)	VMF ($mg/m^2/day$)	Mean flux ± 1 std dev	% Opal
V8/33-1	44°42.0′N	130°35.3′W	30	1985.521	2150	100	17.9	18.4		
V8/33-2	44°42.0′N	130°35.3′W	30	1985.603	2150	100	16.6	17.1		
V8/33-3	44°42.0′N	130°35.3′W	30	1985.685	2150	100	17.3	17.8		
V8/33-4	44°42.0′N	130°35.3′W	350	1986.643	2150	100	57.3	57.3		
V8/36-1	44°42.0′N	130°35.3′W	30	1985.521	2230	20	83.7	86.1	52.7 ± 29	
V8/36-2	44°42.0′N	130°35.3′W	30	1985.603	2230	20	21.7	22.3		
V8/36-3	44°42.0′N	130°35.3′W	30	1985.685	2230	20	14.2	14.6		
V8/36-4	44°42.0′N	130°35.3′W	30	1985.768	2230	20	28.8	29.6		
V8/36-5	44°42.0′N	130°35.3′W	30	1985.850	2230	20	44.8	46.1		
V8/36-6	44°42.0′N	130°35.3′W	30	1985.932	2230	20	57.9	59.6		
V8/36-7	44°42.0′N	130°35.3′W	30	1986.014	2230	20	89.4	91.9		
V8/36-8	44°42.0′N	130°35.3′W	30	1986.643	2230	20	519.9	72.0		
V9/12-1	44°47.7′N	130°24.5′W	30	1986.712	1805	800	25.3	25.3	28.8 ± 37	
V9/12-2	44°47.7′N	130°24.5′W	30	1986.794	1805	800	14.8	14.8		
V9/12-3	44°47.7′N	130°24.5′W	30	1986.877	1805	800	4.6	4.6		
V9/12-4	44°47.7′N	130°24.5′W	30	1986.959	1805	800	9.6	9.6		
V9/12-5	44°47.7′N	130°24.5′W	30	1987.041	1805	800				
V9/12-6	44°47.7′N	130°24.5′W	30	1987.123	1805	800	4.2	4.2		
V9/12-7	44°47.7′N	130°24.5′W	30	1987.205	1805	800	4.2	4.2		
V9/12-8	44°47.7′N	130°24.5′W	30	1987.288	1805	800	51.2	51.2		
V9/12-9	44°47.7′N	130°24.5′W	30	1987.370	1805	800	119.9	119.9		
V9/12-10	44°47.7′N	130°24.5′W	30	1987.452	1805	800	25.5	25.5		

Table 2: (continued).

Mooring ID	Latitude	Longitude	Collection period (days)	Completion date	Depth (m)	mab	Mass (g)	VMF (mg/m^2/day)	Mean flux ± 1 std dev	% Opal
V9/13-1	44°47.7′N	130°24.5′W	30	1986.712	2205	400	53.1	56.4	51.1 ± 35	
V9/13-2	44°47.7′N	130°24.5′W	30	1986.794	2205	400	48.8	51.8		
V9/13-3	44°47.7′N	130°24.5′W	30	1986.877	2205	400	90.5	96.1		
V9/13-4	44°47.7′N	130°24.5′W	30	1986.959	2205	400	22.2	23.6		
V9/13-5	44°47.7′N	130°24.5′W	30	1987.041	2205	400	8.1	8.6		
V9/13-6	44°47.7′N	130°24.5′W	30	1987.123	2205	400	14.4	15.3		
V9/13-7	44°47.7′N	130°24.5′W	30	1987.205	2205	400	31.6	33.6		
V9/13-8	44°47.7′N	130°24.5′W	30	1987.288	2205	400	58.7	62.4		
V9/13-9	44°47.7′N	130°24.5′W	30	1987.370	2205	400	105.2	111.7		
V9/13-10	44°47.7′N	130°24.5′W	30	1987.452	2205	400				
V9/14-1	44°47.7′N	130°24.5′W	30	1986.712	2405	200	63.9	67.9		
V9/14-2	44°47.7′N	130°24.5′W	30	1986.794	2405	200	46.6	49.5		
V9/14-3	44°47.7′N	130°24.5′W	30	1986.877	2405	200	56.8	60.4		
V9/14-4	44°47.7′N	130°24.5′W	30	1986.959	2405	200	8.0	8.5		
V9/14-5	44°47.7′N	130°24.5′W	30	1987.041	2405	200				
V9/14-6	44°47.7′N	130°24.5′W	30	1987.123	2405	200				
V9/14-7	44°47.7′N	130°24.5′W	30	1987.205	2405	200				
V9/14-8	44°47.7′N	130°24.5′W	30	1987.288	2405	200				
V9/14-9	44°47.7′N	130°24.5′W	30	1987.370	2405	200				
V9/14-10	44°47.7′N	130°24.5′W	30	1987.452	2405	200				
V11/25-1	44°41.05 ′N	130°13.91 ′W	30	1986.729	2200	50	158.1	167.8	64.7 ± 55	
V11/25-2	44°41.05 ′N	130°13.91 ′W	30	1986.811	2200	50	82.6	87.7		
V11/25-3	44°41.05 ′N	130°13.91 ′W	30	1986.893	2200	50	81.5	86.6		
V11/25-4	44°41.05 ′N	130°13.91 ′W	30	1986.975	2200	50	31.6	33.5		
V11/25-5	44°41.05 ′N	130°13.91 ′W	30	1987.058	2200	50	8.4	8.9		
V11/25-6	44°41.05 ′N	130°13.91 ′W	30	1987.140	2200	50	26.7	28.3		
V11/25-7	44°41.05 ′N	130°13.91 ′W	30	1987.222	2200	50	6.8	7.2		
V11/25-8	44°41.05 ′N	130°13.91 ′W	30	1987.304	2200	50	134.5	142.8		
V11/25-9	44°41.05 ′N	130°13.91 ′W	30	1987.386	2200	50	42.0	44.6		
V11/25-10	44°41.05 ′N	130°13.91 ′W	30	1987.469	2200	50	37.5	39.8		

Table 2: (continued).

Mooring ID	Latitude	Longitude	Collection period (days)	Completion date	Depth (m)	mab	Mass (g)	VMF (mg/m^2/day)	Mean flux ± 1 std dev	% Opal
V12/16-1	44°41.4 ′N	130°21.0 ′W	30	1986.729	2152	100	165.0	175.2	73.0 ± 68	
V12/16-2	44°41.4 ′N	130°21.0 ′W	30	1986.811	2152	100	140.5	149.2		
V12/16-3	44°41.4 ′N	130°21.0 ′W	30	1986.893	2152	100	75.9	80.6		
V12/16-4	44°41.4 ′N	130°21.0 ′W	30	1986.975	2152	100	143.2	152.0		
V12/16-5	44°41.4 ′N	130°21.0 ′W	30	1987.058	2152	100	18.4	19.6		
V12/16-6	44°41.4 ′N	130°21.0 ′W	30	1987.140	2152	100	18.6	19.8		
V12/16-7	44°41.4 ′N	130°21.0 ′W	30	1987.222	2152	100	5.1	4.5		
V12/16-8	44°41.4 ′N	130°21.0 ′W	30	1987.304	2152	100	29.0	30.8		
V12/16-9	44°41.4 ′N	130°21.0 ′W	30	1987.386	2152	100	25.8	27.4		
V12/16-10	44°41.4 ′N	130°21.0 ′W	30	1987.469	2152	100				
V12/18-1	44°41.4 ′N	130°21.0 ′W	30	1986.729	2227	25	206.3	219.1	110 ± 68	
V12/18-2	44°41.4 ′N	130°21.0 ′W	30	1986.811	2227	25	158.3	168.1		
V12/18-3	44°41.4 ′N	130°21.0 ′W	30	1986.893	2227	25	108.7	115.5		
V12/18-4	44°41.4 ′N	130°21.0 ′W	30	1986.975	2227	25	201.0	213.4		
V12/18-5	44°41.4 ′N	130°21.0 ′W	30	1987.058	2227	25	69.9	74.3		
V12/18-6	44°41.4 ′N	130°21.0 ′W	30	1987.140	2227	25	53.7	57.1		
V12/18-7	44°41.4 ′N	130°21.0 ′W	30	1987.222	2227	25	34.8	37.0		
V12/18-8	44°41.4 ′N	130°21.0 ′W	30	1987.304	2227	25	87.3	92.7		
V12/18-9	44°41.4 ′N	130°21.0 ′W	30	1987.386	2227	25	67.8	72.0		
V12/18-10	44°41.4 ′N	130°21.0 ′W	30	1987.469	2227	25	44.8	47.6		
V17/7-1	44°59.1′N	130°59.5′W	30	1987.548	1500	1350	15.3	16.3	36.7 ± 51	
V17/7-2	44°59.1′N	130°59.5′W	30	1987.630	1500	1350	8.8	9.4		
V17/7-3	44°59.1′N	130°59.5′W	30	1987.712	1500	1350	8.0	8.5		
V17/7-4	44°59.1′N	130°59.5′W	30	1987.795	1500	1350	14.3	15.1		
V17/7-5	44°59.1′N	130°59.5′W	30	1987.877	1500	1350	16.1	17.1		
V17/7-6	44°59.1′N	130°59.5′W	30	1987.959	1500	1350	3.3	3.5		
V17/7-7	44°59.1′N	130°59.5′W	30	1988.041	1500	1350	5.9	6.2		
V17/7-8	44°59.1′N	130°59.5′W	30	1988.123	1500	1350	66.9	71.0		
V17/7-9	44°59.1′N	130°59.5′W	30	1988.205	1500	1350	157.8	167.5		
V17/7-10	44°59.1′N	130°59.5′W	30	1988.288	1500	1350	49.7	52.7		

Table 2: (continued).

Mooring ID	Latitude	Longitude	Collection period (days)	Completion date	Depth (m)	mab	Mass (g)	VMF (mg/m^2/day)	Mean flux ± 1 std dev	% Opal
V17/6-1	44°59.1′N	130°59.5′W	30	1987.548	2100	750	21.6	22.9	31.4 ± 77	
V17/6-2	44°59.1′N	130°59.5′W	30	1987.630	2100	750	13.5	14.3		
V17/6-3	44°59.1′N	130°59.5′W	30	1987.712	2100	750	10.8	11.5		
V17/6-4	44°59.1′N	130°59.5′W	30	1987.795	2100	750	5.4	5.7		
V17/6-5	44°59.1′N	130°59.5′W	30	1987.877	2100	750	1.6	1.7		
V17/6-6	44°59.1′N	130°59.5′W	30	1987.959	2100	750	0.3	0.3		
V17/6-7	44°59.1′N	130°59.5′W	30	1988.041	2100	750	0.4	0.4		
V17/6-8	44°59.1′N	130°59.5′W	30	1988.123	2100	750	0.3	0.3		
V17/6-9	44°59.1′N	130°59.5′W	30	1988.206	2100	750	234.7	249.1		
V17/6-10	44°59.1′N	130°59.5′W	30	1988.288	2100	750	6.8	7.2		
V17/11-1	44°59.1′N	130°59.5′W	30	1987.548	2500	350	17.7	18.7		
V17/11-2	44°59.1′N	130°59.5′W	30	1987.630	2500	350	9.1	9.7		
V17/11-3	44°59.1′N	130°59.5′W	30	1987.712	2500	350	4.8	5.1		
V17/11-4	44°59.1′N	130°59.5′W	30	1987.795	2500	350	2.6	2.8		
V17/11-5	44°59.1′N	130°59.5′W	30	1988.288	2500	350	210.0	44.6		
V18/15-1	44°53.4′N	130°15.6′W	30	1987.548	1500	800	13.2	14.0	42.2 ± 86	
V18/15-2	44°53.4′N	130°15.6′W	30	1987.630	1500	800	7.4	7.9		
V18/15-3	44°53.4′N	130°15.6′W	30	1987.712	1500	800	4.8	5.1		
V18/15-4	44°53.4′N	130°15.6′W	30	1987.795	1500	800	7.0	7.4		
V18/15-5	44°53.4′N	130°15.6′W	30	1987.877	1500	800	7.7	8.2		
V18/15-6	44°53.4′N	130°15.6′W	30	1987.959	1500	800	1.9	4.0		
V18/15-7	44°53.4′N	130°15.6′W	30	1988.041	1500	800	8.7	18.5		
V18/15-8	44°53.4′N	130°15.6′W	30	1988.123	1500	800	23.5	25.0		
V18/15-9	44°53.4′N	130°15.6′W	30	1988.206	1500	800	268.8	285.4		
V18/15-10	44°53.4′N	130°15.6′W	30	1988.288	1500	800	43.6	46.3		
V18/26-1	44°53.4′N	130°15.6′W	30	1987.548	2100	200	16.2	17.2		
V18/26-2	44°53.4′N	130°15.6′W	30	1987.630	2100	200	7.2	7.7		
V18/26-3	44°53.4′N	130°15.6′W	30	1987.712	2100	200	6.3	6.7		
V18/26-4	44°53.4′N	130°15.6′W	30	1988.288	2100	200				

Table 2: (continued).

Mooring ID	Latitude	Longitude	Collection period (days)	Completion date	Depth (m)	mab	Mass (g)	VMF (mg/m^2/day)	Mean flux ± 1 std dev	% Opal
V18/27-1	44°53.4′N	130°15.6′W	30	1987.548	2285	5	28.0	29.8	51.1 ± 63	
V18/27-2	44°53.4′N	130°15.6′W	30	1987.630	2285	5	20.4	21.6		
V18/27-3	44°53.4′N	130°15.6′W	30	1987.712	2285	5	18.0	19.1		
V18/27-4	44°53.4′N	130°15.6′W	30	1987.795	2285	5	18.1	19.2		
V18/27-5	44°53.4′N	130°15.6′W	30	1987.877	2285	5	33.2	35.2		
V18/27-6	44°53.4′N	130°15.6′W	30	1987.959	2285	5	23.8	25.3		
V18/27-7	44°53.4′N	130°15.6′W	30	1988.041	2285	5	32.0	33.9		
V18/27-8	44°53.4′N	130°15.6′W	30	1988.123	2285	5	35.8	38.0		
V18/27-9	44°53.4′N	130°15.6′W	30	1988.206	2285	5	213.7	226.8		
V18/27-10	44°53.4′N	130°15.6′W	30	1988.288	2285	5	58.6	62.2		
V19/28-1	44°41.3′N	130°21.6′W	30	1987.548	2000	250	10.1	10.7		
V19/28-2	44°41.3′N	130°21.6′W	30	1987.630	2000	250	5.8	6.1		
V19/28-3	44°41.3′N	130°21.6′W	30	1987.712	2000	250	6.9	7.3		
V19/28-4	44°41.3′N	130°21.6′W	30	1987.795	2000	250	18.6	19.7		
V19/28-5	44°41.3′N	130°21.6′W	30	1988.288	2000	250	248.7	44.0		
V19/2-1	44°41.3′N	130°21.6′W	30	1987.548	2245	5	21.2	22.5	36.8 ± 41	
V19/2-2	44°41.3′N	130°21.6′W	30	1987.630	2245	5	15.6	16.6		
V19/2-3	44°41.3′N	130°21.6′W	30	1987.712	2245	5	10.4	11.0		
V19/2-4	44°41.3′N	130°21.6′W	30	1987.795	2245	5	16.5	17.5		
V19/2-5	44°41.3′N	130°21.6′W	30	1987.877	2245	5	10.7	11.3		
V19/2-6	44°41.3′N	130°21.6′W	30	1987.959	2245	5	13.4	14.2		
V19/2-7	44°41.3′N	130°21.6′W	30	1988.041	2245	5	12.8	13.6		
V19/2-8	44°41.3′N	130°21.6′W	30	1988.123	2245	5	63.8	67.8		
V19/2-9	44°41.3′N	130°21.6′W	30	1988.205	2245	5	133.1	141.3		
V19/2-10	44°41.3′N	130°21.6′W	30	1988.288	2245	5	48.8	51.8		

Table 2: (continued).

Mooring ID	Latitude	Longitude	Collection period (days)	Completion date	Depth (m)	mab	Mass (g)	VMF (mg/m^2/day)	Mean flux ± 1 std dev	% Opal
V20/30-1	44°59.5′N	130°11.4′W	2	1987.685	1655	600	1.8		29.2	
V20/30(2-9)	44°59.5′N	130°11.4′W	2	1987.685	1655	600				
V20/30-2	44°59.5′Nv	130°11.4′W	2	1987.690	1655	600				
V20/30-3	44°59.5′N	130°11.4′W	2	1987.696	1655	600				
V20/30-4	44°59.5′N	130°11.4′W	2	1987.701	1655	600				
V20/30-5	44°59.5′N	130°11.4′W	2	1987.707	1655	600				
V20/30-6	44°59.5′N	130°11.4′W	2	1987.712	1655	600				
V20/30-7	44°59.5′Nv	130°11.4′W	2	1987.718	1655	600				
V20/30-8	44°59.5′N	130°11.4′W	2	1987.723	1655	600				
V20/30-9	44°59.5′N	130°11.4′W	2	1987.729	1655	600				
V20/30-10	44°59.5′N	130°11.4′W	2	1987.734	1655	600				
V20/31-1	44°59.5′N	130°11.4′W	2	1987.685	2155	100	9.7		154.2	
V20/31(2-9)	44°59.5′N	130°11.4′W	2	1987.685	2155	100				
V20/31-2	44°59.5′Nv	130°11.4′W	2	1987.690	2155	100				
V20/31-3	44°59.5′N	130°11.4′W	2	1987.696	2155	100				
V20/31-4	44°59.5′N	130°11.4′W	2	1987.701	2155	100				
V20/31-5	44°59.5′N	130°11.4′W	2	1987.707	2155	100				
V20/31-6	44°59.5′N	130°11.4′W	2	1987.712	2155	100				
V20/31-7	44°59.5′N	130°11.4′W	2	1987.718	2155	100				
V20/31-8	44°59.5′N	130°11.4′W	2	1987.723	2155	100				
V20/31-9	44°59.5′N	130°11.4′W	2	1987.729	2155	100				
V20/31-10	44°59.5′N	130°11.4′W	2	1987.734	2155	100				
V20/32-1	44°59.5′N	130°11.4′W	2	1987.685	2205	50	10.2		161.7	
V20/32(2-9)	44°59.5′N	130°11.4′W	2	1987.685	2205	50				
V20/32-2	44°59.5′Nv	130°11.4′W	2	1987.690	2205	50				
V20/32-3	44°59.5′N	130°11.4′W	2	1987.696	2205	50				
V20/32-4	44°59.5′N	130°11.4′W	2	1987.701	2205	50				
V20/32-5	44°59.5′N	130°11.4′W	2	1987.707	2205	50				
V20/32-6	44°59.5′N	130°11.4′W	2	1987.712	2205	50				
V20/32-7	44°59.5′Nv	130°11.4′W	2	1987.718	2205	50				
V20/32-8	44°59.5′N	130°11.4′W	2	1987.723	2205	50				
V20/32-9	44°59.5′N	130°11.4′W	2	1987.729	2205	50				
V20/32-10	44°59.5′N	130°11.4′W	2	1987.734	2205	50				

Table 2: (continued).

Mooring ID	Latitude	Longitude	Collection period (days)	Completion date	Depth (m)	mab	Mass (g)	VMF (mg/m^2/day)	Mean flux ± 1 std dev	% Opal
V20/33-1	44°59.5′N	130°11.4′W	2	1987.685	2225	25	7.5		118.7	
V20/33(2-9)	44°59.5′N	130°11.4′W	2	1987.685	2225	25				
V20/33-2	44°59.5′Nv	130°11.4′W	2	1987.690	2225	25				
V20/33-3	44°59.5′N	130°11.4′W	2	1987.696	2225	25				
V20/33-4	44°59.5′N	130°11.4′W	2	1987.701	2225	25				
V20/33-5	44°59.5′N	130°11.4′W	2	1987.707	2225	25				
V20/33-6	44°59.5′N	130°11.4′W	2	1987.712	2225	25				
V20/33-7	44°59.5′Nv	130°11.4′W	2	1987.718	2225	25				
V20/33-8	44°59.5′N	130°11.4′W	2	1987.723	2225	25				
V20/33-9	44°59.5′N	130°11.4′W	2	1987.729	2225	25				
V20/33-10	44°59.5′N	130°11.4′W	2	1987.734	2225	25				
V23/13-1	44°48.14′N	130°18.38′W	30	1988.633	2050	175	526.0			
V23/13-2	44°48.14′N	130°18.38′W	30	1988.715	2050	175	4.0	4.1	16.1 ± 27	17.1
V23/13-3	44°48.14′N	130°18.38′W	30	1988.797	2050	175	4.5	4.7		2.3
V23/13-4	44°48.14′N	130°18.38′W	30	1988.880	2050	175	5.6	5.7		18.3
V23/13-5	44°48.14′N	130°18.38′W	30	1988.962	2050	175	5.2	5.3		19.3
V23/13-6	44°48.14′N	130°18.38′W	30	1989.044	2050	175	1.9	2.0		25.9
V23/13-7	44°48.14′N	130°18.38′W	30	1989.126	2050	175	2.6	2.7		14.3
V23/13-8	44°48.14′N	130°18.38′W	30	1989.208	2050	175	7.8	8.1		29.8
V23/13-9	44°48.14′N	130°18.38′W	30	1989.291	2050	175	82.6	85.0		17.7
V23/13-10	44°48.14′N	130°18.38′W	30	1989.373	2050	175	27.1	27.8		16.8
V23/14-1	44°48.14′N	130°18.38′W	30	1988.633	2125	100	6.5	6.7		15.9
V23/14-2	44°48.14′N	130°18.38′W	30	1988.715	2125	100	7.0	7.3		15.2
V23/14-3	44°48.14′N	130°18.38′W	30	1988.797	2125	100				
V23/14-4	44°48.14′N	130°18.38′W	30	1988.880	2125	100				
V23/14-5	44°48.14′N	130°18.38′W	30	1988.962	2125	100				
V23/14-6	44°48.14′N	130°18.38′W	30	1989.044	2125	100				
V23/14-7	44°48.14′N	130°18.38′W	30	1989.126	2125	100				
V23/14-8	44°48.14′N	130°18.38′W	30	1989.208	2125	100				
V23/14-9	44°48.14′N	130°18.38′W	30	1989.291	2125	100				
V23/14-10	44°48.14′N	130°18.38′W	30	1989.373	2125	100				

Table 2: (continued).

Mooring ID	Latitude	Longitude	Collection period (days)	Completion date	Depth (m)	mab	Mass (g)	VMF (mg/m^2/day)	Mean flux ± 1 std dev	% Opal
V23/16-1	44°48.14′N	130°18.38′W	30	1988.633	2195	30	1.8	1.8		15.9
V23/16-2	44°48.14′N	130°18.38′W	30	1988.715	2195	30				15.2
V23/16-3	44°48.14′N	130°18.38′W	30	1988.797	2195	30				
V23/16-4	44°48.14′N	130°18.38′W	30	1988.880	2195	30				
V23/16-5	44°48.14′N	130°18.38′W	30	1988.962	2195	30				
V23/16-6	44°48.14′N	130°18.38′W	30	1989.044	2195	30				
V23/16-7	44°48.14′N	130°18.38′W	30	1989.126	2195	30				
V23/16-8	44°48.14′N	130°18.38′W	30	1989.208	2195	30				
V23/16-9	44°48.14′N	130°18.38′W	30	1989.291	2195	30				
V23/16-10	44°48.14′N	130°18.38′W	30	1989.373	2195	30				
V24/17-1	45°09.99′N	130°10.17′W	30	1988.630	1850	425	3.0	3.1	35.4 ± 60	10.4
V24/17-2	45°09.99′N	130°10.17′W	30	1988.712	1850	425	6.6	6.8		12.2
V24/17-3	45°09.99′N	130°10.17′W	30	1988.795	1850	425	10.8	11.1		
V24/17-4	45°09.99′N	130°10.17′W	30	1988.877	1850	425	15.6	16.1		40.0
V24/17-5	45°09.99′N	130°10.17′W	30	1988.959	1850	425	4.4	4.5		31.3
V24/17-6	45°09.99′N	130°10.17′W	30	1989.041	1850	425	2.1	2.2		16.5
V24/17-7	45°09.99′N	130°10.17′W	30	1989.123	1850	425	4.8	4.9		13.0
V24/17-8	45°09.99′N	130°10.17′W	30	1989.205	1850	425	7.8	8.1		14.6
V24/17-9	45°09.99′N	130°10.17′W	30	1989.288	1850	425	155.6	160.1		4.5
V24/17-10	45°09.99′N	130°10.17′W	30	1989.370	1850	425	133.1	137.0		5.0
V24/18-1	45°09.99′N	130°10.17′W	30	1988.630	2100	175	3.7	3.9	23.7 ± 46.9	16.1
V24/18-2	45°09.99′N	130°10.17′W	30	1988.712	2100	175	3.6	3.7		10.3
V24/18-3	45°09.99′N	130°10.17′W	30	1988.795	2100	175	7.4	7.6		27.9
V24/18-4	45°09.99′N	130°10.17′W	30	1988.877	2100	175	12.4	12.7		33.5
V24/18-5	45°09.99′N	130°10.17′W	30	1988.959	2100	175	5.1	5.3		14.7
V24/18-6	45°09.99′N	130°10.17′W	30	1989.041	2100	175	1.7	1.8		12.6
V24/18-7	45°09.99′N	130°10.17′W	30	1989.123	2100	175	2.9	3.0		20.7
V24/18-8	45°09.99′N	130°10.17′W	30	1989.205	2100	175	28.4	29.2		3.3
V24/18-9	45°09.99′N	130°10.17′W	30	1989.288	2100	175	142.5	146.7		1.0
V24/18-10	45°09.99′N	130°10.17′W	30	1989.370	2100	175				

Table 2: (continued).

Mooring ID	Latitude	Longitude	Collection period (days)	Completion date	Depth (m)	mab	Mass (g)	VMF (mg/m^2/day)	Mean flux ± 1 std dev	% Opal
V24/25-1	45°09.99′N	130°10.17′W	30	1988.630	2175	100	3.3	3.4		10.2
V24/25-2	45°09.99′N	130°10.17′W	30	1988.712	2175	100	2.9	3.0		9.3
V24/25-3	45°09.99′N	130°10.17′W	30	1988.795	2175	100	3.3	3.4		4.0
V24/25-4	45°09.99′N	130°10.17′W	30	1988.877	2175	100				
V24/25-5	45°09.99′N	130°10.17′W	30	1988.959	2175	100				
V24/25-6	45°09.99′N	130°10.17′W	30	1989.041	2175	100				
V24/25-7	45°09.99′N	130°10.17′W	30	1989.123	2175	100				
V24/25-8	45°09.99′N	130°10.17′W	30	1989.205	2175	100				
V24/25-9	45°09.99′N	130°10.17′W	30	1989.288	2175	100				
V24/25-10	45°09.99′N	130°10.17′W	30	1989.370	2175	100	25.3	26.0		2.9
V24/31-1	45°09.99′N	130°10.17′W	30	1988.630	2245	30	9.6	9.9	17.8 ± 6.3	12.2
V24/31-2	45°09.99′N	130°10.17′W	30	1988.712	2245	30	18.6	19.1		10.4
V24/31-3	45°09.99′N	130°10.17′W	30	1988.795	2245	30	19.8	20.4		16.3
V24/31-4	45°09.99′N	130°10.17′W	30	1988.877	2245	30	26.7	27.5		35.6
V24/31-5	45°09.99′N	130°10.17′W	30	1988.959	2245	30	11.1	11.4		19.4
V24/31-6	45°09.99′N	130°10.17′W	30	1989.041	2245	30	12.3	12.7		21.6
V24/31-7	45°09.99′N	130°10.17′W	30	1989.123	2245	30	17.0	17.5		11.9
V24/31-8	45°09.99′N	130°10.17′W	30	1989.205	2245	30	23.6	24.2		27.1
V24/31-9	45°09.99′N	130°10.17′W	30	1989.288	2245	30				
V24/31-10	45°09.99′N	130°10.17′W	30	1989.370	2245	30				
V25/7-1	45°06.0′N	130°10.0′W	33	1989.622	1848	427	4.8	5.4	10.3 ± 4.4	
V25/7-2	45°06.0′N	130°10.0′W	33	1989.712	1848	427	11.0	12.5		
V25/7-3	45°06.0′N	130°10.0′W	33	1989.803	1848	427	13.6	15.3		
V25/7-4	45°06.0′N	130°10.0′W	33	1989.893	1848	427	7.0	8.0		
V25/7-5	45°06.0′N	130°10.0′W	33	1989.984	1848	427				
V25/7-6	45°06.0′N	130°10.0′W	33	1990.074	1848	427				
V25/7-7	45°06.0′N	130°10.0′W	33	1990.164	1848	427				
V25/7-8	45°06.0′N	130°10.0′W	33	1990.255	1848	427				
V25/7-9	45°06.0′N	130°10.0′W	33	1990.345	1848	427				
V25/7-10	45°06.0′N	130°10.0′W	33	1990.436	1848	427				

Table 2: (continued).

Mooring ID	Latitude	Longitude	Collection period (days)	Completion date	Depth (m)	mab	Mass (g)	VMF (mg/m^2/day)	Mean flux ± 1 std dev	% Opal
V25/11-1	45°06.0′N	130°10.0′W	33	1989.622	2100	175	4.8	5.5		
V25/11-2	45°06.0′N	130°10.0′W	33	1989.712	2100	175	9.9	11.2		
V25/11-3	45°06.0′N	130°10.0′W	33	1989.803	2100	175	9.5	10.7		
V25/11-4	45°06.0′N	130°10.0′W	33	1989.893	2100	175				
V25/11-5	45°06.0′N	130°10.0′W	33	1989.984	2100	175				
V25/11-6	45°06.0′N	130°10.0′W	33	1990.074	2100	175				
V25/11-7	45°06.0′N	130°10.0′W	33	1990.164	2100	175				
V25/11-8	45°06.0′N	130°10.0′W	33	1990.255	2100	175				
V25/11-9	45°06.0′N	130°10.0′W	33	1990.345	2100	175				
V25/11-10	45°06.0′N	130°10.0′W	33	1990.436	2100	175				
V25/15-1	45°06.0′N	130°10.0′W	33	1989.622	2175	100	2.7	3.0	60.0 ± 140	
V25/15-2	45°06.0′N	130°10.0′W	33	1989.712	2175	100	12.6	14.2		
V25/15-3	45°06.0′N	130°10.0′W	33	1989.803	2175	100	26.2	29.5		
V25/15-4	45°06.0′N	130°10.0′W	33	1989.893	2175	100	15.4	17.4		
V25/15-5	45°06.0′N	130°10.0′W	33	1989.984	2175	100	6.7	7.6		
V25/15-6	45°06.0′N	130°10.0′W	33	1990.074	2175	100	4.3	4.8		
V25/15-7	45°06.0′N	130°10.0′W	33	1990.164	2175	100	10.0	11.3		
V25/15-8	45°06.0′N	130°10.0′W	33	1990.255	2175	100	384.1	433.5		
V25/15-9	45°06.0′N	130°10.0′W	33	1990.345	2175	100	16.3	18.4		
V25/15-10	45°06.0′N	130°10.0′W	33	1990.436	2175	100				
V25/27-1	45°06.0′N	130°10.0′W	33	1989.622	2245	30	3.4	3.8	20.7 ± 25.7	
V25/27-2	45°06.0′N	130°10.0′W	33	1989.712	2245	30	11.1	12.5		
V25/27-3	45°06.0′N	130°10.0′W	33	1989.803	2245	30	4.2	4.8		
V25/27-4	45°06.0′N	130°10.0′W	33	1989.893	2245	30	15.0	16.9		
V25/27-5	45°06.0′N	130°10.0′W	33	1989.984	2245	30	7.3	8.2		
V25/27-6	45°06.0′N	130°10.0′W	33	1990.074	2245	30	4.1	4.7		
V25/27-7	45°06.0′N	130°10.0′W	33	1990.164	2245	30	15.2	17.2		
V25/27-8	45°06.0′N	130°10.0′W	33	1990.255	2245	30	73.3	82.8		
V25/27-9	45°06.0′N	130°10.0′W	33	1990.345	2245	30	44.1	49.8		
V25/27-10	45°06.0′N	130°10.0′W	33	1990.436	2245	30	5.8	6.5		

Table 2: (continued).

Mooring ID	Latitude	Longitude	Collection period (days)	Completion date	Depth (m)	mab	Mass (g)	VMF ($mg/m^2/day$)	Mean flux ± 1 std dev	% Opal
V26/30-1	44°48.0′N	130°18.8′W	33	1989.707	1848	377	4.1	4.6	21.1 ± 36	
V26/30-2	44°48.0′N	130°18.8′W	33	1989.797	1848	377	10.5	11.9		
V26/30-3	44°48.0′N	130°18.8′W	33	1989.888	1848	377	17.8	20.0		
V26/30-4	44°48.0′N	130°18.8′W	33	1989.978	1848	377	2.2	2.4		
V26/30-5	44°48.0′N	130°18.8′W	33	1990.069	1848	377	2.1	2.4		
V26/30-6	44°48.0′N	130°18.8′W	33	1990.159	1848	377	0.8	0.9		
V26/30-7	44°48.0′N	130°18.8′W	33	1990.250	1848	377	18.8	21.2		
V26/30-8	44°48.0′N	130°18.8′W	33	1990.340	1848	377	102.2	115.3		
V26/30-9	44°48.0′N	130°18.8′W	33	1990.430	1848	377	9.6	10.8		
V26/30-10	44°48.0′N	130°18.8′W	33	1990.521	1848	377				
V26/32-1	44°48.0′N	130°18.8′W	33	1989.707	2050	175	13.4	15.1	27.9 ± 45	
V26/32-2	44°48.0′N	130°18.8′W	33	1989.797	2050	175	10.4	11.7		
V26/32-3	44°48.0′N	130°18.8′W	33	1989.888	2050	175	19.4	21.8		
V26/32-4	44°48.0′N	130°18.8′W	33	1989.978	2050	175	16.1	18.2		
V26/32-5	44°48.0′N	130°18.8′W	33	1990.069	2050	175	2.0	2.3		
V26/32-6	44°48.0′N	130°18.8′W	33	1990.159	2050	175	7.3	8.2		
V26/32-7	44°48.0′N	130°18.8′W	33	1990.250	2050	175	22.1	25.0		
V26/32-8	44°48.0′N	130°18.8′W	33	1990.340	2050	175	130.3	147.1		
V26/32-9	44°48.0′N	130°18.8′W	33	1990.430	2050	175	1.5	1.7		
V26/32-10	44°48.0′N	130°18.8′W	33	1990.521	2050	175				
V26/33-1	44°48.0′N	130°18.8′W	33	1989.707	2125	100	10.5	11.8	55.5 ± 54	
V26/33-2	44°48.0′N	130°18.8′W	33	1989.797	2125	100	18.7	21.1		
V26/33-3	44°48.0′N	130°18.8′W	33	1989.888	2125	100	4.7	5.3		
V26/33-4	44°48.0′N	130°18.8′W	33	1989.978	2125	100				
V26/33-5	44°48.0′N	130°18.8′W	33	1990.069	2125	100				
V26/33-6	44°48.0′N	130°18.8′W	33	1990.159	2125	100				
V26/33-7	44°48.0′N	130°18.8′W	33	1990.250	2125	100	55.7	62.9		
V26/33-8	44°48.0′N	130°18.8′W	33	1990.340	2125	100	75.8	85.5		
V26/33-9	44°48.0′N	130°18.8′W	33	1990.430	2125	100	129.6	146.3		
V26/33-10	44°48.0′N	130°18.8′W	33	1990.521	2125	100				

Table 2: (continued).

Mooring ID	Latitude	Longitude	Collection period (days)	Completion date	Depth (m)	mab	Mass (g)	VMF ($mg/m^2/day$)	Mean flux ± 1 std dev	% Opal
V26/36-1	44°48.0′N	130°18.8′W	33	1989.707	2195	30	16.8	19.0	37.0 ± 46	
V26/36-2	44°48.0′N	130°18.8′W	33	1989.797	2195	30	20.7	23.3		
V26/36-3	44°48.0′N	130°18.8′W	33	1989.888	2195	30	21.3	24.1		
V26/36-4	44°48.0′N	130°18.8′W	33	1989.978	2195	30	26.9	30.4		
V26/36-5	44°48.0′N	130°18.8′W	33	1990.069	2195	30	12.9	14.5		
V26/36-6	44°48.0′N	130°18.8′W	33	1990.159	2195	30	1.5	1.6		
V26/36-7	44°48.0′N	130°18.8′W	33	1990.250	2195	30	14.1	15.9		
V26/36-8	44°48.0′N	130°18.8′W	33	1990.340	2195	30	137.3	155.0		
V26/36-9	44°48.0′N	130°18.8′W	33	1990.430	2195	30	43.9	49.5		
V26/36-10	44°48.0′N	130°18.8′W	33	1990.521	2195	30				
V43/17-1	44°56.3′N	130°14.7′W	27	1990.743	1800	490	16.9	19.3	30.5 ± 25	
V43/17-2	44°56.3′N	130°14.7′W	27	1990.817	1800	490	23.7	27.1		
V43/17-3	44°56.3′N	130°14.7′W	27	1990.890	1800	490	38.5	44.0		
V43/17-4	44°56.3′N	130°14.7′W	27	1990.965	1800	490	7.6	8.6		
V43/17-5	44°56.3′N	130°14.7′W	27	1991.039	1800	490	15.0	17.1		
V43/17-6	44°56.3′N	130°14.7′W	27	1991.112	1800	490	10.5	12.0		
V43/17-7	44°56.3′N	130°14.7′W	27	1991.187	1800	490	69.4	79.3		
V43/17-8	44°56.3′N	130°14.7′W	27	1991.261	1800	490	51.5	58.9		
V43/17-9	44°56.3′N	130°14.7′W	27	1991.335	1800	490	7.4	8.5		
V43/17-10	44°56.3′N	130°14.7′W	27	1991.408	1800	490				
V43/30-1	44°56.3′N	130°14.7′W	27	1990.743	2050	240	20.9	23.9	21.0 ± 17.5	
V43/30-2	44°56.3′N	130°14.7′W	27	1990.817	2050	240	15.5	17.7		
V43/30-3	44°56.3′N	130°14.7′W	27	1990.890	2050	240	38.9	44.5		
V43/30-4	44°56.3′N	130°14.7′W	27	1990.965	2050	240	5.6	6.4		
V43/30-5	44°56.3′N	130°14.7′W	27	1991.039	2050	240	7.0	8.0		
V43/30-6	44°56.3′N	130°14.7′W	27	1991.112	2050	240	.2	7.0		
V43/30-7	44°56.3′N	130°14.7′W	27	1991.187	2050	240	44.3	50.6		
V43/30-8	44°56.3′N	130°14.7′W	27	1991.261	2050	240	25.5	29.1		
V43/30-9	44°56.3′N	130°14.7′W	27	1991.335	2050	240	1.9	2.2		
V43/30-10	44°56.3′N	130°14.7′W	27	1991.408	2050	240				

Table 2: (continued).

Mooring ID	Latitude	Longitude	Collection period (days)	Completion date	Depth (m)	mab	Mass (g)	VMF (mg/m^2/day)	Mean flux ± 1 std dev	% Opal
V43/33-1	44°56.3′N	130°14.7′W	27	1990.743	2150	140	18.8	21.5	30.1 ± 24.6	
V43/33-2	44°56.3′N	130°14.7′W	27	1990.817	2150	140	16.9	19.3		
V43/33-3	44°56.3′N	130°14.7′W	27	1990.890	2150	140	48.9	55.9		
V43/33-4	44°56.3′N	130°14.7′W	27	1990.965	2150	140	7.9	9.0		
V43/33-5	44°56.3′N	130°14.7′W	27	1991.039	2150	140	18.7	21.4		
V43/33-6	44°56.3′N	130°14.7′W	27	1991.112	2150	140	8.7	10.0		
V43/33-7	44°56.3′N	130°14.7′W	27	1991.187	2150	140	67.4	77.1		
V43/33-8	44°56.3′N	130°14.7′W	27	1991.261	2150	140	43.0	49.1		
V43/33-9	44°56.3′N	130°14.7′W	27	1991.335	2150	140	6.9	7.8		
V43/33-10	44°56.3′N	130°14.7′W	27	1991.408	2150	140				
V43/34-1	44°56.3′N	130°14.7′W	27	1990.743	2250	40	18.1	20.7	31.8 ± 25	
V43/34-2	44°56.3′N	130°14.7′W	27	1990.817	2250	40	17.4	19.9		
V43/34-3	44°56.3′N	130°14.7′W	27	1990.890	2250	40	44.5	50.9		
V43/34-4	44°56.3′N	130°14.7′W	27	1990.965	2250	40	10.4	11.9		
V43/34-5	44°56.3′N	130°14.7′W	27	1991.039	2250	40	17.4	19.9		
V43/34-6	44°56.3′N	130°14.7′W	27	1991.112	2250	40	11.8	13.5		
V43/34-7	44°56.3′N	130°14.7′W	27	1991.187	2250	40	75.9	86.8		
V43/34-8	44°56.3′N	130°14.7′W	27	1991.261	2250	40	40.0	45.7		
V43/34-9	44°56.3′N	130°14.7′W	27	1991.335	2250	40	15.0	17.2		
V43/34-10	44°56.3′N	130°14.7′W	27	1991.408	2250	40				

Table 3: Elemental fluxes from moorings V23 and V26.

Mooring/ Sed. Trap	Completion date	Corr. VMF	Al flux	Corr. Sl flux	Corr. P flux	S flux	Corr. Mn flux	Corr. Fe flux	Cu flux	Zn flux	Cr flux
		(mg/m^2/day)									
V23/2050m	1988.715	4.3384	0.080	0.56	0.030	0.031	0.095	0.086	0.00005	0.0016	0.0005
V23/2050m	1988.797	5.5715	0.060	1.43	0.008	0.036	0.049	0.068	0.00022	0.0010	0.0004
V23/2050m	1988.880	6.1902	0.080	1.09	0.037	0.052	0.033	0.105	0.00012	0.0014	0.0005
V23/2050m	1988.962	5.9759	0.060	1.14	0.034	0.033	0.024	0.082	0	0.0016	0.0005
V23/2050m	1989.044	2.2312	0.050	0.57	–0.002	0.020	0.018	0.044	0.00006	0.0010	0.0003
V23/2050m	1989.126	2.7996	0.080	0.43	0.030	0.146	0.011	0.067	0.00059	0.0013	0.0005
V23/2050m	1989.208	8.8760	0.300	2.66	0.004	0.060	0.012	0.175	0	0.0023	0.0006
V23/2050m	1989.291	86.576	0.580	13.05	0.086	0.892	0.064	0.408	0.00043	0.0224	0.0024
V23/2050m	1989.373	28.884	0.320	3.83	0.029	0.147	0.025	0.286	0	0.0059	0.0017
V26/1848m	1989.707	5.0100	0.095	0.94	0.015	0.064	0.007	0.085	0.00001	0.0017	0.0002
V26/1848m	1989.797	14.220	0.130	3.44	0.083	0.144	0.008	0.078	0	0.0072	0.0003
V26/1848m	1989.888	23.850	0.230	6.35	0.105	0.222	0.013	0.135	0.00048	0.0068	0.0006
V26/1848m	1989.978	4.4400	0.140	2.62	0.011	0.046	0.002	0.021	0.00015	0.0023	0.0001
V26/1848m	1990.069	3.1600	0.001	1.00	0.025	0.018	0.000	0.005	0	0.0004	0.0000
V26/1848m	1990.159	1.0100	0.001	0.15	0.080	0.005	0.000	0.008	0.00001	0.0003	0.0000
V26/1848m	1990.250	24.490	0.430	5.87	0.108	0.452	0.103	0.594	0.00146	0.0133	0.0011
V26/1848m	1990.340	119.72	0.520	24.89	0.191	1.049	0.050	0.461	0.00519	0.0227	0.0016
V26/1848m	1990.430	13.800	0.095	4.45	0.028	0.113	0.007	0.052	0.00005	0.0040	0.0003
V26/2050m	1989.707	16.580	0.260	3.32	0.124	0.148	0.079	1.855	0.00214	0.0183	0.0031
V26/2050m	1989.797	13.880	0.142	3.33	0.099	0.124	0.035	0.874	0.00151	0.0100	0.0014
V26/2050m	1989.888	25.680	0.211	5.88	0.132	0.194	0.048	0.761	0.00218	0.0123	0.0015
V26/2050m	1989.978	21.740	0.127	7.64	0.037	0.160	0.017	0.174	0.00075	0.0082	0.0004
V26/2050m	1990.069	2.8900	0.015	1.09	0.026	0.019	0.003	0.022	0.00008	0.0007	0.0001
V26/2050m	1990.159	9.6800	0.071	2.35	0.036	0.092	0.008	0.149	0.00057	0.0055	0.0005
V26/2050m	1990.250	28.110	0.347	6.56	0.117	0.247	0.066	0.627	0.00183	0.0077	0.0016
V26/2050m	1990.340	151.59	0.706	27.48	0.199	1.442	0.155	1.313	0	0.0382	0.0044
V26/2050m	1990.430	2.8500	0.003	1.29	0.021	0.008	0.001	0.005	0	0.0002	0.0000

Table 4: Elemental fluxes from mooring V43.

Sample No.	Dec. date	Depth. (m)	VMF	Al	Si	P	S	Cr	Mn	Fe	Cu	Zn	Ca	V
			(mg/m^2/day)											
V43-17-1	1990.743	1800.0	19.276	0.093274	2.3728	0.026	0.082923	0.00041737	0.0059884	0.0662	0.0000	0.010586	3.1229	0.00056
V43-17-2	1990.817	1800.0	27.089	0.11044	4.4330	0.177	0.20247	0.00062708	0.0073350	0.0728	0.0000	0.0090833	0.97524	0.00078
V43-17-3	1990.891	1800.0	43.962	0.29649	11.886	0.065	0.31046	0.0014098	0.014217	0.2122	0.0000	0.015667	1.1431	0.00168
V43-17-4	1990.965	1800.0	8.641	0.10474	2.3310	0.022	0.093388	0.00028935	0.0079352	0.0814	0.00051264	0.0040579	0.057039	0.00032
V43-17-5	1991.039	1800.0	17.104	0.11999	4.9319	0.048	0.11882	0.00042287	0.0062528	0.0852	0.0000	0.0055604	0.14199	0.00042
V43-17-6	1991.113	1800.0	12.016	0.096923	2.6550	0.022	0.093273	0.00048407	0.0077881	0.0707	0.00038534	0.0051410	0.28841	0.00029
V43-17-7	1991.187	1800.0	79.299	0.33798	16.440	0.051	0.44787	0.0020988	0.025807	0.2957	0.0000	0.017315	9.0405	0.00185
V43-17-8	1991.261	1800.0	58.900	0.36138	11.352	0.028	0.29738	0.0020670	0.022354	0.2656	0.0000	0.014012	6.3023	0.00198
V43-17-9	1991.335	1800.0	8.512	0.074460	1.4318	0.000	0.10975	0.00023719	0.0011679	0.0483	5.1440e-05	0.0024114	0.46819	0.00033
V43-30-1	1990.743	2050.0	23.851	0.13093	2.7000	0.028	0.095576	0.0016756	0.017725	0.3203	0.00096789	0.0088862	5.1058	0.00099
V43-30-2	1990.817	2050.0	17.690	0.11158	3.0704	0.037	0.16480	0.0013366	0.012812	0.2086	0.00046550	0.0081679	1.5217	0.00072
V43-30-3	1990.891	2050.0	44.499	0.25322	8.0562	0.050	0.26235	0.0026221	0.023625	0.0547	0.0068841	0.013884	0.93458	0.00125
V43-30-4	1990.965	2050.0	6.422	0.057421	0.87582	0.019	0.064616	0.00042833	0.0098061	0.0979	0.0013437	0.0046171	0.043697	0.00037
V43-30-5	1991.039	2050.0	7.965	0.085789	2.2757	0.019	0.075494	0.00056250	0.012620	0.1275	0.00035945	0.0030730	0.044635	0.00039
V43-30-6	1991.113	2050.0	7.046	0.087383	2.1193	0.014	0.076652	0.00047780	0.010403	0.1078	0.00033081	0.0026906	0.050049	0.00033
V43-30-7	1991.187	2050.0	50.624	0.21632	10.146		0.32212	0.0025717	0.024667	0.2616	0.0000	0.0094313	6.3280	0.00123
V43-30-8	1991.261	2050.0	29.108	0.19110	5.7148	0.023	0.17354	0.0026424	0.018343	0.1945	0.00011665	0.0092694	3.2313	0.00109
V43-30-9	1991.335	2050.0	2.201	0.027377	0.39334	0.013	0.019789	0.00019584	0.0026274	0.0297	0.0000	0.0013498	0.018711	0.00010
V43-33-1	1990.743	2150.0	21.458	0.15927	2.6277	0.040	0.13057	0.00096144	0.0027774	0.4500	0.00031382	0.0075077	1.7012	0.00108
V43-33-2	1990.817	2150.0	19.306	0.11375	2.5874	0.039	0.10955	0.00081749	0.026719	0.4322	4.5727e-05	0.010090	0.86904	0.00126
V43-33-3	1990.891	2150.0	55.917	0.61527	20.284	0.128	0.55503	0.0022057	0.097427	0.8689	0.00043428	0.014811	1.7337	0.00296
V43-33-4	1990.965	2150.0	8.979	0.13766	2.0088	0.048	0.13628	0.00059143	0.0014423	0.2534	0.00090537	0.0029864	0.060293	0.00073
V43-33-5	1991.039	2150.0	21.423	0.24222	6.3807	0.036	0.15399	0.0010412	0.045854	0.3811	0.00011836	0.0092814	0.49284	0.00091
V43-33-6	1991.113	2150.0	9.960	0.14829	2.7945	0.024	0.089292	0.00063676	0.026485	0.2535	0.00027929	0.0063219	0.17929	0.00063
V43-33-7	1991.187	2150.0	77.068	0.43091	15.277	0.039	0.35533	0.0033818	0.079558	0.7697	0.0000	0.014378	8.0932	0.00247
V43-33-8	1991.261	2150.0	49.090	0.35259	8.5465	0.018	0.21115	0.0017301	0.052350	0.4382	0.00079923	0.015540	6.1370	0.00174
V43-33-9	1991.335	2150.0	7.847	0.083291	0.91069		0.063359	0.00096272	0.010800	0.1219	3.8103e-06	0.0042893	1.4674	0.00035
V43-34-1	1990.743	2250.0	20.654	0.20674	1.4803	0.075	0.30804	0.00043415	0.051892	0.6631	0.00018607	0.0066157	0.15506	0.00364
V43-34-2	1990.817	2250.0	19.847	0.021840	0.087362	0.085	0.20848	0.0000	0.0031768	0.0772	0.0012906	0.0054998	0.10523	0.00000
V43-34-3	1990.891	2250.0	50.902	0.44800	2.6065	0.185	0.69745	0.0000	0.050756	0.5977	0.0000	0.0085527	0.32073	0.00402
V43-34-4	1990.965	2250.0	11.872	0.064141	0.31714	0.105	0.098587	0.0000	0.014622	0.1762	0.0000	0.0038722	0.11284	0.00069
V43-34-5	1991.039	2250.0	19.863	0.19471	1.3014	0.053	0.19073	0.00027815	0.056167	0.4505	0.00049670	0.0041127	0.10331	0.00123
V43-34-6	1991.113	2250.0	13.463	0.11717	0.79596	0.039	0.13603	0.0000	0.033764	0.2639	5.3872e-05	0.0016431	0.082155	0.00096
V43-34-7	1991.187	2250.0	86.773	0.22561	1.9090	0.169	1.0673	0.0000	0.014231	0.2793	0.0015619	0.077490	0.35578	0.00174
V43-34-8	1991.261	2250.0	45.678	0.32434	2.3297	0.077	0.55731	0.0000	0.18058	0.4463	0.0000	0.0085880	0.25125	0.00123
V43-34-9	1991.335	2250.0	17.182	0.020627	0.12204	0.045	0.15126	0.0000	0.0025268	0.0347	0.0000	0.0010313	0.077350	0.00000

Table 5: Total VMF and biogenic opal concentrations from moorings V32–V42.

Mooring ID	Latitude	Longitude	Coll. intvl. (days)	Compl. date	Depth (m)	MAB	Total mass (mg)	Opal free mass (g)	Total VMF (mg/m^2/day)	Opal free VMF (mg/m^2/day)	% opal	Mean VMF (mg/m^2/day)
V32/12-1	44°54.4′N	130°07.8′W	6.0	1990.5640	1800.0	695	1.550	0.613	7.9679	3.151	60.457	22.600
V32/12-2	44°54.4′N	130°07.8′W	6.0	1990.5804	1800.0	695		1.429	17.340	7.352	57.602	
V32/12-3	44°54.4′N	130°07.8′W	6.0	1990.5969	1800.0	695		3.196	38.572	16.435	57.390	
V32/12-4	44°54.4′N	130°07.8′W	6.0	1990.6133	1800.0	695		2.458	32.283	12.641	60.843	
V32/12-5	44°54.4′N	130°07.8′W	6.0	1990.6298	1800.0	695		2.610	36.561	13.424	63.283	
V32/12-6	44°54.4′N	130°07.8′W	6.0	1990.6462	1800.0	695		3.022	33.383	15.541	53.447	
V32/12-7	44°54.4′N	130°07.8′W	6.0	1990.6626	1800.0	695		0.587	13.094	3.019	76.943	
V32/12-8	44°54.4′N	130°07.8′W	6.0	1990.6791	1800.0	695		1.435	25.707	7.383	71.278	
V32/12-9	44°54.4′N	130°07.8′W	6.0	1990.6956	1800.0	695		0.887	15.424	4.561	70.429	
V32/12-10	44°54.4′N	130°07.8′W	6.0	1990.7119	1800.0	695		0.390	5.6966	2.004	64.824	
V32/24-1	44°54.4′N	130°07.8′W	6.0	1990.5640	2250.0	245						0.0000
V32/24-2	44°54.4′N	130°07.8′W	6.0	1990.5804	2250.0	245						
V32/24-3	44°54.4′N	130°07.8′W	6.0	1990.5969	2250.0	245						
V32/24-4	44°54.4′N	130°07.8′W	6.0	1990.6133	2250.0	245						
V32/24-5	44°54.4′N	130°07.8′W	6.0	1990.6298	2250.0	245						
V32/24-6	44°54.4′N	130°07.8′W	6.0	1990.6462	2250.0	245						
V32/24-7	44°54.4′N	130°07.8′W	6.0	1990.6626	2250.0	245						
V32/24-8	44°54.4′N	130°07.8′W	6.0	1990.6791	2250.0	245						
V32/24-9	44°54.4′N	130°07.8′W	6.0	1990.6956	2250.0	245						
V32/24-10	44°54.4′N	130°07.8′W	6.0	1990.7119	2250.0	245						
V33/26-1	44°56.0′N	130°12.35′W	6.0	1990.5640	2150.0	120		0.599	6.1941	3.083	50.227	19.700
V33/26-2	44°56.0′N	130°12.35′W	6.0	1990.5804	2150.0	120		0.897	11.703	4.615	60.561	
V33/26-3	44°56.0′N	130°12.35′W	6.0	1990.5969	2150.0	120		1.193	15.526	6.135	60.486	
V33/26-4	44°56.0′N	130°12.35′W	6.0	1990.6133	2150.0	120		0.757	10.208	3.895	61.845	
V33/26-5	44°56.0′N	130°12.35′W	6.0	1990.6298	2150.0	120		2.831	33.087	14.561	55.992	
V33/26-6	44°56.0′N	130°12.35′W	6.0	1990.6462	2150.0	120		1.647	28.180	8.472	69.937	
V33/26-7	44°56.0′N	130°12.35′W	6.0	1990.6626	2150.0	120		2.408	30.973	12.384	60.017	
V33/26-8	44°56.0′N	130°12.35′W	6.0	1990.6791	2150.0	120		1.179	20.094	6.063	69.826	
V33/26-9	44°56.0′N	130°12.35′W	6.0	1990.6956	2150.0	120		0.941	12.551	4.840	61.438	
V33/26-10	44°56.0′N	130°12.35′W	6.0	1990.7119	2150.0			2.891	28.662	14.868	48.128	

Table 5: (continued).

Mooring ID	Latitude	Longitude	Coll. intvl. (days)	Compl. date	Depth (m)	MAB	Total mass (mg)	Opal free mass (g)	Total VMF (mg/m^2/day)	Opal free VMF (mg/m^2/day)	% opal	Mean VMF (mg/m^2/day)
V34/15-1	44°56.3′N	130°14.7′W	6.0	1990.5640	2050.0	243		0.875	18.043	4.500	75.062	28.600
V34/15-2	44°56.3′N	130°14.7′W	6.0	1990.5804	2050.0	243		0.956	15.136	4.915	67.526	
V34/15-3	44°56.3′N	130°14.7′W	6.0	1990.5969	2050.0	243		2.123	27.845	10.917	60.793	
V34/15-4	44°56.3′N	130°14.7′W	6.0	1990.6133	2050.0	243		1.597	31.829	8.214	74.192	
V34/15-5	44°56.3′N	130°14.7′W	6.0	1990.6298	2050.0	243		3.035	50.240	15.607	68.934	
V34/15-6	44°56.3′N	130°14.7′W	6.0	1990.6462	2050.0	243		3.416	52.462	17.568	66.513	
V34/15-7	44°56.3′N	130°14.7′W	6.0	1990.6626	2050.0	243		1.315	31.725	6.766	78.673	
V34/15-8	44°56.3′N	130°14.7′W	6.0	1990.6791	2050.0	243		1.505	32.417	7.741	76.121	
V34/15-9	44°56.3Nv	130°14.7′W	6.0	1990.6956	2050.0	243		0.833	19.817	4.283	78.388	
V34/15-10	44°56.3′N	130°14.7′W	6.0	1990.7119	2050.0	243		0.438	6.8148	2.252	66.954	
V34/30-1	44°56.3′N	130°14.7′W	6.0	1990.5640	2150.0	143		6.701	149.480	34.464	76.944	51.600
V34/30-2	44°56.3′N	130°14.7′W	6.0	1990.5804	2150.0	143		2.656	34.147	13.659	59.999	
V34/30-3	44°56.3′N	130°14.7′W	6.0	1990.5969	2150.0	143		1.724	24.591	8.869	63.934	
V34/30-4	44°56.3′N	130°14.7′W	6.0	1990.6133	2150.0	143		2.812	43.982	14.461	67.121	
V34/30-5	44°56.3′N	130°14.7′W	6.0	1990.6298	2150.0	143		3.890	60.465	20.005	66.914	
V34/30-6	44°56.3′N	130°14.7′W	6.0	1990.6462	2150.0	143		3.666	72.828	18.857	74.108	
V34/30-7	44°56.3′N	130°14.7′W	6.0	1990.6626	2150.0	143		2.611	52.482	13.429	74.412	
V34/30-8	44°56.3′N	130°14.7′W	6.0	1990.6791	2150.0	143		1.926	33.515	9.906	70.443	
V34/30-9	44°56.3′N	130°14.7′W	6.0	1990.6956	2150.0	143		0.716	16.409	3.683	77.557	
V34/30-10	44°56.3Nv	130°14.7′W	6.0	1990.7119	2150.0	143		2.191	27.934	11.269	59.659	
V34/20-1	44°56.3′N	130°14.7′W	6.0	1990.5640	2150.0	143						0.0000
V34/20-2	44°56.3′N	130°14.7′W	6.0	1990.5804	2150.0	143						
V34/20-3	44°56.3′N	130°14.7′W	6.0	1990.5969	2150.0	143						
V34/20-4	44°56.3′N	130°14.7′W	6.0	1990.6133	2150.0	143						
V34/20-5	44°56.3′N	130°14.7′W	6.0	1990.6298	2150.0	143						
V34/20-6	44°56.3′N	130°14.7′W	6.0	1990.6462	2150.0	143						
V34/20-7	44°56.3′N	130°14.7′W	6.0	1990.6626	2150.0	143						
V34/20-8	44°56.3′N	130°14.7′W	6.0	1990.6791	2150.0	143						
V34/20-9	44°56.3′N	130°14.7′W	6.0	1990.6956	2150.0	143						
V34/20-10	44°56.3′N	130°14.7′W	6.0	1990.7119	2150.0	143						

Table 5: (continued).

Mooring ID	Latitude	Longitude	Coll. intvl. (days)	Compl. date	Depth (m)	MAB	Total mass (mg)	Opal free mass (g)	Total VMF (mg/m^2/day)	Opal free VMF (mg/m^2/day)	% opal	Mean VMF (mg/m^2/day)
V34/27-1	44°56.3′N	130°14.7′W	6.0	1990.5640	2285.0	5.00		2.403	26.938	12.361	54.112	42.200
V34/27-2	44°56.3′N	130°14.7′W	6.0	1990.5804	2285.0	5.00		1.534	22.769	7.892	65.341	
V34/27-3	44°56.3′N	130°14.7′W	6.0	1990.5969	2285.0	5.00		2.492	30.607	12.819	58.117	
V34/27-4	44°56.3′N	130°14.7′W	6.0	1990.6133	2285.0	5.00		2.949	34.616	15.169	56.179	
V34/27-5	44°56.3′N	130°14.7′W	6.0	1990.6298	2285.0	5.00		5.016	70.266	25.798	63.285	
V34/27-6	44°56.3′N	130°14.7′W	6.0	1990.6462	2285.0	5.00		5.160	75.860	26.542	65.012	
V34/27-7	44°56.3′N	130°14.7′W	6.0	1990.6626	2285.0	5.00		4.633	51.682	23.829	53.893	
V34/27-8	44°56.3′N	130°14.7′W	6.0	1990.6791	2285.0	5.00		4.108	60.578	21.130	65.119	
V34/27-9	44°56.3′N	130°14.7′W	6.0	1990.6956	2285.0	5.00		2.191	28.507	11.268	60.472	
V34/27-10	44°56.3′N	130°14.7′W	6.0	1990.7119	2285.0	5.00		2.184	20.111	11.230	44.159	
V35/11-1	44°56.7′N	130°15.4′W	6.0	1990.5640	2150.0	18.0		2.612	26.682	13.436	49.643	41.200
V35/11-2	44°56.7′N	130°15.4′W	6.0	1990.5804	2150.0	18.0		2.759	28.396	14.188	50.035	
V35/11-3	44°56.7′N	130°15.4′W	6.0	1990.5969	2150.0	18.0		3.206	30.432	16.491	45.812	
V35/11-4	44°56.7′N	130°15.4′W	6.0	1990.6133	2150.0	18.0		3.829	40.307	19.692	51.145	
V35/11-5	44°56.7′N	130°15.4′W	6.0	1990.6298	2150.0	18.0		6.626	69.084	34.080	50.669	
V35/11-6	44°56.7′N	130°15.4′W	6.0	1990.6462	2150.0	18.0		7.140	79.011	36.723	53.522	
V35/11-7	44°56.7′N	130°15.4′W	6.0	1990.6626	2150.0	18.0		3.107	40.351	15.979	60.401	
V35/11-8	44°56.7′N	130°15.4′W	6.0	1990.6791	2150.0	18.0		4.158	43.519	21.385	50.860	
V35/11-9	44°56.7′N	130°15.4′W	6.0	1990.6956	2150.0	18.0		2.808	26.764	14.440	46.047	
V35/11-10	44°56.7′N	130°15.4′W	6.0	1990.7119	2150.0	18.0		3.455	26.963	17.769	34.098	
V36/29-1	44°57.7′N	130°20.4′W	6.0	1990.5640	1500.0	955		1.345	17.793	6.920	61.110	30.000
V36/29-2	44°57.7′N	130°20.4′W	6.0	1990.5804	1500.0	955		1.192	21.118	6.133	70.960	
V36/29-3	44°57.7′N	130°20.4′W	6.0	1990.5969	1500.0	955		3.167	41.304	16.289	60.563	
V36/29-4	44°57.7′N	130°20.4′W	6.0	1990.6133	1500.0	955		4.413	55.759	22.696	59.296	
V36/29-5	44°57.7′N	130°20.4′W	6.0	1990.6298	1500.0	955		2.188	38.512	11.256	70.773	
V36/29-6	44°57.7′N	130°20.4′W	6.0	1990.6462	1500.0	955		0.881	19.100	4.534	76.263	
V36/29-7	44°57.7′N	130°20.4′W	6.0	1990.6626	1500.0	955		1.733	33.622	8.912	73.493	
V36/29-8	44°57.7′N	130°20.4′W	6.0	1990.6791	1500.0	955		1.273	18.819	6.547	65.210	
V36/29-9	44°57.7′N	130°20.4′W	6.0	1990.6956	1500.0	955		2.138	23.611	10.996	53.429	
V36/29-10	44°57.7′N	130°20.4′W	6.0	1990.7119	1500.0	955						

Table 5: (continued).

Mooring ID	Latitude	Longitude	Coll. intvl. (days)	Compl. date	Depth (m)	MAB	Total mass (mg)	Opal free mass (g)	Total VMF (mg/m^2/day)	Opal free VMF (mg/m^2/day)	% opal	Mean VMF (mg/m^2/day)
V36/32-1	44°57.7′N	130°20.4′W	6.0	1990.5640	1800.0	655						
V36/32-2	44°57.7′N	130°20.4′W	6.0	1990.5804	1800.0	655						
V36/32-3	44°57.7′N	130°20.4′W	6.0	1990.5969	1800.0	655			9.4825			
V36/32-4	44°57.7′N	130°20.4′W	6.0	1990.6133	1800.0	655		1.272	22.151	6.544	70.459	
V36/32-5	44°57.7′N	130°20.4′W	6.0	1990.6298	1800.0	655		0.992	20.783	5.102	75.453	
V36/32-6	44°57.7′N	130°20.4′W	6.0	1990.6462	1800.0	655		0.683	16.061	3.515	78.116	
V36/32-7	44°57.7′N	130°20.4′W	6.0	1990.6626	1800.0	655		0.327	8.7762	1.684	80.815	
V36/32-8	44°57.7′N	130°20.4′W	6.0	1990.6791	1800.0	655		0.000	7.9764	0.000	100.00	
V36/32-9	44°57.7′N	130°20.4′W	6.0	1990.6956	1800.0	655						
V36/32-10	44°57.7′N	130°20.4′W	6.0	1990.7119	1800.0	655						
V36/33-1	44°57.7′N	130°20.4′W	6.0	1990.5640	1800.0	655		2.224	26.308	11.437	56.525	17.600
V36/33-2	44°57.7′N	130°20.4′W	6.0	1990.5804	1800.0	655						
V36/33-3	44°57.7′N	130°20.4′W	6.0	1990.5969	1800.0	655		1.298	22.885	6.675	70.833	
V36/33-4	44°57.7′N	130°20.4′W	6.0	1990.6133	1800.0	655		0.928	12.315	4.774	61.238	
V36/33-5	44°57.7′N	130°20.4′W	6.0	1990.6298	1800.0	655		2.757	38.086	14.179	62.772	
V36/33-6	44°57.7′N	130°20.4′W	6.0	1990.6462	1800.0	655		0.401	10.380	2.064	80.120	
V36/33-7	44°57.7′N	130°20.4′W	6.0	1990.6626	1800.0	655		1.205	22.407	6.196	72.346	
V36/33-8	44°57.7′N	130°20.4′W	6.0	1990.6791	1800.0	655		0.504	10.356	2.592	74.969	
V36/33-9	44°57.7′N	130°20.4′W	6.0	1990.6956	1800.0	655		0.394	7.0874	2.026	71.410	
V36/33-10	44°57.7′N	130°20.4′W	6.0	1990.7119	1800.0	655		1.204	8.5772	6.194	27.788	
V36/36-1	44°57.7′N	130°20.4′W	6.0	1990.5640	2250.0	205						
V36/36-2	44°57.7′N	130°20.4′W	6.0	1990.5804	2250.0	205		1.356	21.318	6.974	67.287	
V36/36-3	44°57.7′N	130°20.4′W	6.0	1990.5969	2250.0	205		3.280	53.176	16.872	68.271	
V36/36-4	44°57.7′N	130°20.4′W	6.0	1990.6133	2250.0	205		2.869	56.961	14.753	74.099	
V36/36-5	44°57.7′N	130°20.4′W	6.0	1990.6298	2250.0	205		2.810	53.144	14.454	72.803	
V36/36-6	44°57.7′N	130°20.4′W	6.0	1990.6462	2250.0	205		2.219	36.266	11.414	68.527	
V36/36-7	44°57.7′N	130°20.4′W	6.0	1990.6626	2250.0	205		2.706	47.311	13.915	70.587	
V36/36-8	44°57.7′N	130°20.4′W	6.0	1990.6791	2250.0	205		2.294	44.797	11.797	73.665	
V36/36-9	44°57.7′N	130°20.4′W	6.0	1990.6956	2250.0	205		2.121	33.026	10.911	66.964	
V36/36-10	44°57.7′N	130°20.4′W	6.0	1990.7119	2250.0	205		1.636	26.507	8.413	68.263	

Table 5: (continued).

Mooring ID	Latitude	Longitude	Coll. intvl. (days)	Compl. date	Depth (m)	MAB	Total mass (mg)	Opal free mass (g)	Total VMF ($mg/m^2/day$)	Opal free VMF ($mg/m^2/day$)	% opal	Mean VMF ($mg/m^2/day$)
V37/6-1	44°57.0′N	130°10.6′W	6.0	1990.5640	2200.0	175		1.968	18.275	10.124	44.601	28.800
V37/6-2	44°57.0′N	130°10.6′W	6.0	1990.5804	2200.0	175		1.707	20.326	8.779	56.810	
V37/6-3	44°57.0′N	130°10.6′W	6.0	1990.5969	2200.0	175		1.885	23.124	9.693	58.081	
V37/6-4	44°57.0′N	130°10.6′W	6.0	1990.6133	2200.0	175		2.752	30.731	14.155	53.941	
V37/6-5	44°57.0′N	130°10.6′W	6.0	1990.6298	2200.0	175		6.007	58.440	30.898	47.130	
V37/6-6	44°57.0′N	130°10.6′W	6.0	1990.6462	2200.0	175		2.676	38.830	13.764	64.553	
V37/6-7	44°57.0′N	130°10.6′W	6.0	1990.6626	2200.0	175		2.480	37.143	12.758	65.653	
V37/6-8	44°57.0′N	130°10.6′W	6.0	1990.6791	2200.0	175		0.860	15.023	4.425	70.549	
V37/6-9	44°57.0′N	130°10.6′W	6.0	1990.6956	2200.0	175		1.342	17.034	6.900	59.491	
V37/6-10	44°57.0′N	130°10.6′W	6.0	1990.7119	2200.0	175						
V38/18-1	44°58.8′N	130°13.1′W	6.0	1990.5640	2050.0	232						
V38/18-2	44°58.8′N	130°13.1′W	6.0	1990.5804	2050.0	232						
V38/18-3	44°58.8′N	130°13.1′W	6.0	1990.5969	2050.0	232						
V38/18-4	44°58.8′N	130°13.1′W	6.0	1990.6133	2050.0	232						
V38/18-5	44°58.8′N	130°13.1′W	6.0	1990.6298	2050.0	232						
V38/18-6	44°58.8′N	130°13.1′W	6.0	1990.6462	2050.0	232						
V38/18-7	44°58.8′N	130°13.1′W	6.0	1990.6626	2050.0	232						
V38/18-8	44°58.8′N	130°13.1′W	6.0	1990.6791	2050.0	232						
V38/18-9	44°58.8′N	130°13.1′W	6.0	1990.6956	2050.0	232						
V38/18-10	44°58.8′N	130°13.1′W	6.0	1990.7119	2050.0	232						
V38/34-1	44°58.8′N	130°13.1′W	6.0	1990.5640	2150.0	132		1.643	21.297	8.449	60.325	32.600
V38/34-2	44°58.8′N	130°13.1′W	6.0	1990.5804	2150.0	132		1.929	19.653	9.923	49.506	
V38/34-3	44°58.8′N	130°13.1′W	6.0	1990.5969	2150.0	132		4.165	34.823	21.423	38.482	
V38/34-4	44°58.8′N	130°13.1′W	6.0	1990.6133	2150.0	132		2.147	20.636	11.045	46.477	
V38/34-5	44°58.8′N	130°13.1′W	6.0	1990.6298	2150.0	132		5.887	61.081	30.280	50.425	
V38/34-6	44°58.8′N	130°13.1′W	6.0	1990.6462	2150.0	132		5.138	60.007	26.428	55.959	
V38/34-7	44°58.8′N	130°13.1′W	6.0	1990.6626	2150.0	132		1.902	30.895	9.783	68.334	
V38/34-8	44°58.8′N	130°13.1′W	6.0	1990.6791	2150.0	132		2.094	29.776	10.768	63.838	
V38/34-9	44°58.8′N	130°13.1′W	6.0	1990.6956	2150.0	132		0.724	15.207	3.723	75.520	
V38/34-10	44°58.8′N	130°13.1′W	6.0	1990.7119	2150.0	132		0.347	5.4523	1.784	67.276	

Table 5: (continued).

Mooring ID	Latitude	Longitude	Coll. intvl. (days)	Compl. date	Depth (m)	MAB	Total mass (mg)	Opal free mass (g)	Total VMF ($mg/m^2/day$)	Opal free VMF ($mg/m^2/day$)	% opal	Mean VMF ($mg/m^2/day$)
V39/17-1	44°58.8′N	130°16.4′W	6.0	1990.5640	2200.0	85.0		1.443	16.466	7.420	54.939	29.900
V39/17-2	44°58.8′N	130°16.4′W	6.0	1990.5804	2200.0	85.0		2.044	22.718	10.512	53.729	
V39/17-3	44°58.8′N	130°16.4′W	6.0	1990.5969	2200.0	85.0		2.201	23.469	11.320	51.766	
V39/17-4	44°58.8′N	130°16.4′W	6.0	1990.6133	2200.0	85.0		1.807	20.683	9.295	55.060	
V39/17-5	44°58.8′N	130°16.4′W	6.0	1990.6298	2200.0	85.0		2.270	35.752	11.677	67.338	
V39/17-6	44°58.8′N	130°16.4′W	6.0	1990.6462	2200.0	85.0		4.010	54.759	20.624	62.337	
V39/17-7	44°58.8′N	130°16.4′W	6.0	1990.6626	2200.0	85.0		2.050	32.300	10.544	67.356	
V39/17-8	44°58.8′N	130°16.4′W	6.0	1990.6791	2200.0	85.0		4.906	56.386	25.235	55.246	
V39/17-9	44°58.8′N	130°16.4′W	6.0	1990.6956	2200.0	85.0		2.168	30.296	11.151	63.194	
V39/17-10	44°58.8′N	130°16.4′W	6.0	1990.7119	2200.0	85.0		0.384	6.0917	1.974	67.587	
V40/31-1	44°53.6′N	130°11.8′W	6.0	1990.5640	2200.0	165		2.043	23.279	10.507	54.864	32.100
V40/31-2	44°53.6′N	130°11.8′W	6.0	1990.5804	2200.0	165		1.756	23.276	9.031	61.201	
V40/31-3	44°53.6′N	130°11.8′W	6.0	1990.5969	2200.0	165		6.542	63.254	33.648	46.804	
V40/31-4	44°53.6′N	130°11.8′W	6.0	1990.6133	2200.0	165		1.601	28.404	8.235	71.009	
V40/31-5	44°53.6′N	130°11.8′W	6.0	1990.6298	2200.0	165		3.904	51.022	20.080	60.645	
V40/31-6	44°53.6′N	130°11.8′W	6.0	1990.6462	2200.0	165		2.038	34.627	10.480	69.734	
V40/31-7	44°53.6′N	130°11.8′W	6.0	1990.6626	2200.0	165		1.907	31.219	9.809	68.579	
V40/31-8	44°53.6′N	130°11.8′W	6.0	1990.6791	2200.0	165		1.429	26.340	7.350	72.097	
V40/31-9	44°53.6′N	130°11.8′W	6.0	1990.6956	2200.0	165		1.582	24.986	8.135	67.442	
V40/31-10	44°53.6′N	130°11.8′W	6.0	1990.7119				1.166	14.503	5.998	58.640	
V41/13-1	44°53.8′N	130°15.7′W	6.0	1990.5640	2050.0	247		1.247	15.137	6.414	57.628	31.100
V41/13-2	44°53.8′N	130°15.7′W	6.0	1990.5804	2050.0	247		1.131	16.673	5.817	65.115	
V41/13-3	44°53.8′N	130°15.7′W	6.0	1990.5969	2050.0	247		4.629	51.414	23.808	53.693	
V41/13-4	44°53.8′N	130°15.7′W	6.0	1990.6133	2050.0	247		2.884	31.750	14.834	53.279	
V41/13-5	44°53.8′N	130°15.7′W	6.0	1990.6298	2050.0	247		7.817	88.204	40.205	54.418	
V41/13-6	44°53.8′N	130°15.7′W	6.0	1990.6462	2050.0	247		2.934	40.178	15.091	62.439	
V41/13-7	44°53.8′N	130°15.7′W	6.0	1990.6626	2050.0	247		1.979	27.247	10.177	62.647	
V41/13-8	44°53.8′N	130°15.7′W	6.0	1990.6791	2050.0	247		1.279	18.018	6.578	63.495	
V41/13-9	44°53.8′N	130°15.7′W	6.0	1990.6956	2050.0	247		0.763	10.028	3.923	60.876	
V41/13-10	44°53.8′N	130°15.7′W	6.0	1990.7119	2050.0	247		1.299	12.363	6.680	45.969	

Table 5: (continued).

Mooring ID	Latitude	Longitude	Coll. intvl. (days)	Compl. date	Depth (m)	MAB	Total mass (mg)	Opal free mass (g)	Total VMF (mg/m^2/day)	Opal free VMF (mg/m^2/day)	% opal	Mean VMF (mg/m^2/day)
V41/14-1	44°53.8′N	130°15.7′W	6.0	1990.5640	2150.0	147		1.252	21.758	6.441	70.397	32.800
V41/14-2	44°53.8′N	130°15.7′W	6.0	1990.5804	2150.0	147		2.151	26.802	11.060	58.732	
V41/14-3	44°53.8′N	130°15.7′W	6.0	1990.5969	2150.0	147		5.010	46.841	25.768	44.989	
V41/14-4	44°53.8′N	130°15.7′W	6.0	1990.6133	2150.0	147		2.287	33.238	11.763	64.609	
V41/14-5	44°53.8′N	130°15.7′W	6.0	1990.6298	2150.0	147		6.345	66.242	32.634	50.735	
V41/14-6	44°53.8′N	130°15.7′W	6.0	1990.6462	2150.0	147		3.363	46.792	17.296	63.036	
V41/14-7	44°53.8′N	130°15.7′W	6.0	1990.6626	2150.0	147		2.054	33.635	10.564	68.593	
V41/14-8	44°53.8′N	130°15.7′W	6.0	1990.6791	2150.0	147		0.799	16.607	4.107	75.267	
V41/14-9	44°53.8′N	130°15.7′W	6.0	1990.6956	2150.0	147		0.482	8.2456	2.480	69.919	
V41/14-10	44°53.8′N	130°15.7′W	6.0	1990.7119	2150.0	147		2.968	27.697	15.265	44.886	
V42/7-1	44°53.3′N	130°18.5′W	6.0	1990.5640	2200.0	130		0.700	9.1619	3.599	60.716	25.300
V42/7-2	44°53.3′N	130°18.5′W	6.0	1990.5804	2200.0	130		1.505	16.609	7.743	53.378	
V42/7-3	44°53.3′N	130°18.5′W	6.0	1990.5969	2200.0	130		2.106	21.743	10.831	50.185	
V42/7-4	44°53.3′N	130°18.5′W	6.0	1990.6133	2200.0	130		3.105	38.200	15.971	58.192	
V42/7-5	44°53.3′N	130°18.5′W	6.0	1990.6298	2200.0	130		4.663	52.890	23.985	54.651	
V42/7-6	44°53.3′N	130°18.5′W	6.0	1990.6462	2200.0	130		2.352	34.716	12.098	65.152	
V42/7-7	44°53.3′N	130°18.5′W	6.0	1990.6626	2200.0	130		1.544	24.325	7.942	67.348	
V42/7-8	44°53.3′N	130°18.5′W	6.0	1990.6791	2200.0	130		3.201	42.813	16.463	61.546	
V42/7-9	44°53.3′N	130°18.5′W	6.0	1990.6956	2200.0	130		0.797	12.565	4.100	67.371	
V42/7-10	44°53.3′N	130°18.5′W	6.0	1990.7119	2200.0	130		0.479	5.9544	2.465	58.600	

Table 6: Elemental fluxes from mooring V34.

Mooring	Depth (m)	Compl. date	Uncor. VMF	Remob. Si	Remob. Opal	Corr. VMF	Al flux	Corr. Si flux	Corr. P flux	S flux	V flux	Cr flux	Corr. Mn flux	Corr. total Fe flux	Hyd. Fe	Terr. Fe	Cu flux	Zn flux
			(mg/m^2/day)															
V34/15-1	2050	1990.564	18.000	3.4400	7.3616	25.362	0.13719	8.7447	0.046601	0.17212	0.0018001	0.00069998	0.0087281	0.16667	0.0000	0.16667	0.00056016	0.0051912
V34/15-2	2050	1990.580	15.100	2.1800	4.6652	19.765	0.12012	4.2009	0.035086	0.11344	0.00047314	0.00085743	0.0085330	0.20275	0.053833	0.14891	0.00053617	0.0071231
V34/15-3	2050	1990.597	27.800	4.6200	9.8868	37.687	0.18012	7.8230	0.24829	0.24035	0.0014698	0.0013723	0.0089596	0.20257	0.0000	0.20257	0.016370	0.017470
V34/15-4	2050	1990.613	31.800	6.8200	14.595	46.395	0.21626	12.186	0.087571	0.15906	0.0018955	0.0016846	0.011607	0.25810	0.0000	0.25810	0.0000	0.020551
V34/15-5	2050	1990.630	50.200	0.0005	0.0010700	50.201	0.25754	11.104	0.029343	0.46783	0.0024209	0.00070262	0.014800	0.49174	0.17292	0.31881	0.0041517	0.023551
V34/15-6	2050	1990.646	52.500	7.8100	16.713	69.213	0.25631	16.905	0.11428	0.26186	0.0021689	0.0012304	0.010855	0.25539	0.0000	0.25539	0.0000	0.012092
V34/15-7	2050	1990.663	31.700	3.5300	7.5542	39.254	0.17746	8.5978	0.13810	0.23929	0.0026254	0.0012748	0.014290	0.20317	0.0000	0.20317	0.0000	0.017700
V34/15-8	2050	1990.679	32.400	6.5300	13.974	46.374	0.23256	15.057	0.13599	0.29414	0.0033339	0.0020498	0.010550	0.26725	0.0000	0.26725	0.0017350	0.022264
V34/15-9	2050	1990.696	19.800	4.0700	8.7098	28.510	0.15723	8.5954	0.036589	0.15545	0.0021090	0.00091874	0.0070566	0.16339	0.0000	0.16339	8.5081e-05	0.010273
V34/15-10	2050	1990.712	6.8000	0.7600	1.6264	8.4264	0.029205	1.1617	0.018171	0.030369	0.0000	0.00024295	0.0014946	0.026645	0.0000	0.026645	0.0000	0.0022748
V34/30-1	2150	1990.564	149.50	14.1800	30.345	179.85	0.81858	65.234	0.16818	1.8271	0.012856	0.0095314	0.038611	1.9052	0.89240	1.0128	0.022430	0.067340
V34/30-2	2150	1990.580	34.100	4.3200	9.2448	43.345	0.30444	12.689	0.076107	0.45488	0.0042254	0.0022285	0.048511	1.6538	1.2766	0.37720	0.010405	0.027495
V34/30-3	2150	1990.597	24.600	7.1300	15.258	39.858	0.29293	14.007	0.065828	0.76152	0.0044018	0.0018738	0.023280	2.1081	1.7450	0.36305	0.054163	0.047300
V34/30-4	2150	1990.613	44.000	6.6100	14.145	58.145	0.38202	18.453	0.094989	1.1560	0.0061944	0.0036039	0.063152	1.8438	1.3703	0.47348	0.013291	0.053487
V34/30-5	2150	1990.630	60.500	0.0000	0.0000	60.500	0.43161			1.0128	0.0060639	0.0024365		2.6672	2.1334	0.53376	0.010528	0.092503
V34/30-6	2150	1990.646	72.800	7.4000	15.836	88.636	0.49372	30.598	0.13218	0.88654	0.0087889	0.0057255	0.058849	2.4882	1.8776	0.61057	0.0071735	0.038193
V34/30-7	2150	1990.663	52.500	6.2500	13.375	65.875	0.48611	22.971	0.11822	0.83676	0.0062302	0.0032074	0.056835	2.6833	2.0821	0.60115	0.19822	0.043268
V34/30-8	2150	1990.679	33.500	4.5700	9.7798	43.280	0.32490	13.312	0.10627	0.47150	0.0051801	0.0017093	0.045111	1.7503	1.3485	0.40179	0.041545	0.049609
V34/30-9	2150	1990.696	16.400	1.9000	4.0660	20.466	0.11571	5.3695	0.44419	0.22078	0.0012239	0.00062750	0.0096893	0.49078	0.34633	0.14445	0.026682	0.017488
V34/30-10	2150	1990.712	27.900	5.2900	11.321	39.221	0.19076	10.100	0.083219	0.49186	0.0025695	0.0018075	0.036881	0.99197	0.75605	0.23591	0.0089201	0.025887
V34/27-1	2250	1990.564	26.900	3.0400	6.5056	33.406	0.17973	8.1931	0.11918	0.41713	0.0060503	0.0013647	0.19063	4.7573	4.5351	0.22227	0.0048541	0.024647
V34/27-2	2250	1990.580	22.800	3.8400	8.2176	31.018	0.24786	8.2383	0.081148	0.29024	0.0033483	0.0017515	0.049126	1.3165	1.0095	0.30703	0.0026360	0.044456
V34/27-3	2250	1990.597	30.600	4.8500	10.379	40.979	0.29986	9.1536	0.073792	0.30589	0.0023588	0.0016246	0.031898	0.83020	0.45780	0.37240	0.0049403	0.013499
V34/27-4	2250	1990.613	34.600	4.6000	9.8440	44.444	0.19182	7.9015	0.085046	0.29292	0.0047890	0.0011303	0.10083	2.2680	2.0305	0.23756	0.0030117	0.015806
V34/27-5	2250	1990.630	70.300	12.7500	27.285	97.585	0.46931	23.046	0.17529	1.3614	0.0064698	0.0033558	0.17989	3.7935	3.2131	0.58038	0.012382	0.14362
V34/27-6	2250	1990.646	75.900	6.5400	13.996	89.896	0.37645	17.025	0.12858	1.9200	0.0067004	0.0038311	0.063880	3.4423	2.9768	0.46554	0.023842	0.044570
V34/27-7	2250	1990.663	51.700	4.7600	10.186	61.886	0.58830	16.021	0.11045	1.6203	0.0062300	0.0021910	0.072009	4.5661	3.8385	0.72753	0.33381	0.094343
V34/27-8	2250	1990.679	60.600	7.3700	15.772	76.372	0.44377	15.912	0.095555	0.76839	0.0049288	0.0026595	0.18118	2.9587	2.4099	0.54880	0.10199	0.060407
V34/27-9	2250	1990.696	28.500	3.5700	7.6398	36.140	0.27528	8.4878	0.12158	0.26327	0.0037892	0.0012624	0.091392	1.9970	1.6566	0.34043	0.011055	0.013854
V34/27-10	2250	1990.712	20.100	2.4800	5.3072	25.407	0.26631	5.3706	0.080609	0.46819	0.0022726	0.0017152	0.062329	1.6355	1.3062	0.32933	0.017619	0.057750

Table 7: Comparison of elemental fluxes at north Cleft and Endeavour segments of the JDFR.

	Dec. date	depth	Total flux	Al flux	Si flux	S flux	Mn flux	Fe flux	Cu flux	Zn flux	Ca flux	Va
			(mg/m^2/day)									
This study V34	1990.56-1990.71	2050	28.60			0.213	0.0096900	0.22400	0.0023400	0.013800		0.0018300
	1990.56-1990.7	2150	51.60			0.812	0.042300	1.8600	0.039300	0.046300		0.0057700
	1990.56-1990.7	2285	42.20			0.771	0.10200	2.7600	0.051600	0.051300		0.0046900
This study V43	1990.74-1991.34	1800	30.50	0.177	6.43	0.195	0.011000	0.0017300	0.00010500	0.0093000	2.39	0.00091000
	1990.74-1991.34	2050	21.04	0.129	3.93	0.139	0.014700	0.059500	0.0011600	0.0068200	1.92	0.00072000
	1990.74-1991.34	2150	30.11	0.254	6.82	0.201	0.038200	0.23600	0.00032200	0.0094700	2.30	0.0013500
	1990.74-1991.34	2250	31.80	0.180	1.22	0.379	0.045300	0.19000	0.00039900	0.013000	0.17	0.0015000
Dymond and Roth; 1988	1984.77-1985.44	1700	72.38	0.638	11.23	n.d.	0.0086800	0.40820	0.0020800	0.0052055	14.06	0.0089600
	1984.77-1985.44	1950	34.55	0.419	4.30	4.11	0.021500	2.0411	0.11780	0.32055	4.99	0.021600
	1984.77-1985.44	2100	66.90	0.860	7.53	12.5	0.092500	5.9726	0.40000	1.2301	7.86	0.096160

Appendix

Table A1: Time of recovery, splitting, and processing for sediment traps in which remobilization rates were calculated.

			Remobilization in Supernate						Remobilization in Splitting Solution						
Mooring	Date Trap Opened	Date Recovered	Date Sampled	Vol. (liters)	Duration	Label	Elements Sampled	Equations	Date Split	Dilution	Date Processed	Duration	Label	Elements Sampled	Equations
V23	18 Aug 88	12 Sep 89	22 Jan 90	0.18	Deployment & Storage	RF_{su}	Sal, Si, P, Fe, Mn	1–5 5	22 Jan 90	unknown	Aug 91	Remobilization in splitting solution unknown		not sampled	
V26	15 Aug 89	9 Jul 90	21 Mar 91	0.18	Deployment & Storage	RF_{su}	Sal, Si, P, Fe, Mn	1–5 5	21 Mar 91	unknown	Aug 91	Remobilization in splitting solution unknown		not sampled	
V34	18 Jul 90	17 Sep 90	9 Nov 90	0.18	Deployment & Storage	RF_{su}	Sal, Si, P, Fe, Mn	1–5 5	9 Nov 90	4–15	Aug 91	In splitting solution between Nov. 90 and Aug. 91	RF_{spl}	Sal, Si, P	7–8
V43	28 Sep 90	10 Jun 91	10 Jun 91	0.18	Deployment	RF_{su}	Sal, Si, P, Fe, Mn	1–5 5	29 Sep 91	unknown	immediately upon splitting	No remobilization in splitting solution assumed		not sampled	
			29 Sep 91	~0.06	Storage	RF_{st}	Fe, Mn	6							

Table A2a: Concentrations of salinity, Si, P, Fe, and Mn in the supernates of the sediment trap cylinders for trap 13 on mooring V23 at the time of sample splitting.

Mooring/ Trap	Sampling Jar	Supernate at Recovery Sal ppt	Si (μM)	P (μM)	Fe (nM)	Mn (nM)
V23/13	1					
V23/13	2	38.70	201	6.900	74	8946
V23/13	3	43.02	327	3.192	82	4613
V23/13	4	44.49	254	7.306	0	2235
V23/13	5	43.35	289	6.570	952	2240
V23/13	6	42.98	214	1.865	0	1600
V23/13	7	44.98	183	7.000	452	942
V23/13	8	42.32	317	2.512	0	754
V23/13	9	46.56	457	7.643	0	687
V23/13	10	47.64	366	5.919	0	494
Fill		88.30	122	2.06		
Ambient SW		34.60	183	2.96		

Table A2b: Concentrations of salinity, Si, P, Fe, and Mn in the supernates of the sediment trap cylinders for traps 30, 32, and 36 on mooring V26 at the time of sample splitting.

Mooring/ Trap	Sampling Jar	Supernate at Recovery				
		Sal ppt	Si μM	P μM	Fe nM	Mn nM
V26/30	1		247	4.32	2865	220
V26/30	2	43.13	603	14.1	269	38
V26/30	3	41.05	892	15.9	752	27
V26/30	4	40.35	555	4.04	310	0
V26/30	5	64.13	290	6.63	0	0
V26/30	6	36.77	199	16.28	403	0
V26/30	7	37.65	790	14.12	0	368
V26/30	8	41.55	996	22.81	0	215
V26/30	9	48.81	724	6.08	0	0
V26/30	10	no sample			0	0
V26/32	1	39.21	451	8.02	430	0
V26/32	2	41.84	579	9.82	609	0
V26/32	3		894	19.5	7395	626
V26/32	4	49.44	825	7.27	1056	87
V26/32	5	46.84	278	6.87	358	58
V26/32	6	37.93	454	6.54	0	22
V26/32	7		752	13.48	0	46
V26/32	8		1008	18.7	430	26
V26/32	9		386	6.35	0	0
V26/32	10				0	0
V26/36	1		480	5.04	1343	0
V26/36	2	39.10	645	4.41	895	0
V26/36	3		795	4.38	5694	448
V26/36	4	40.97	835	14.35	127	0
V26/36	5		823	4.28	2793	157
V26/36	6		281	4.4	174	0
V26/36	7		814	6.04	412	0
V26/36	8	39.10	964	16.14	7395	1438
V26/36	9	40.50	881	19.25	14414	1183
V26/36	10				0	0
Fill Sol.		88.30	122	2.06		
Ambient SW		34.60	181	2.97		

Table A2c: Concentrations of salinity, Si, P, Fe, and Mn in the supernates of the sediment trap cylinders for traps 15, 30, and 27 on mooring V34 at the time of sample splitting, and the concentrations of salinity, Si, and P in the diluted splitting solution just prior to processing particles onto filters.

		Supernate at Recovery					Splitting Solution at Processing (t2)		
Mooring/	Sampling	Sal	Si	P	Fe	Mn	Sal	Si	P
Trap	Jar	ppt	μM		nM		ppt	μM	
V34/15	1	77.30	210	4.38	0	43.5	9.97	124	0.08
V34/15	2	72.30	183	3.19	10.1	30.6	16.70	130	0.98
V34/15	3	70.53	236	9.9	17.5	28.9	7.06	131	1.66
V34/15	4	68.41	242	4.09	29.1	36.6	13.30	236	1.72
V34/15	5	67.33	281	4.19	9.3	34.8			
V34/15	6	68.79	255	6	0	34.4	14.33	243	1.10
V34/15	7	66.40	178	6.84	120	56.4	5.85	199	0.45
V34/15	8	67.30	241	5.77	21	0	10.35	207	1.26
V34/15	9	68.88	200	3.02	0	0	14.05	169	0.95
V34/15	10	66.74	181	3.12	0	0	13.64	74	0.82
V34/30	1	76.37	367	2.96	17.5	13.5	8.43	299	0.59
V34/30	2	62.74	242	3.38	59	209	7.44	119	0.06
V34/30	3	76.74	216	2.56	87	106	8.21	234	0.36
V34/30	4	72.84	251	2.79	76	123	18.47	264	1.06
V34/30	5						10.25	348	1.28
V34/30	6	69.11	238	3.24	0	121	16.39	283	0.59
V34/30	7	72.88	236	3.37	0	87	11.84	243	0.70
V34/30	8	74.09	206	3.46	0	60	14.94	175	0.82
V34/30	9	71.23	193	18.42	86	46	5.65	76	0.03
V34/30	10	73.53	219	4.34	0	77	10.73	156	0.65
V34/27	1	46.48	218	2.73	0		7.10	125	0.30
V34/27	2	61.63	250	3.69	42	57.8	8.90	121	0.53
V34/27	3	62.69	262	3.73	66	89	9.48	132	0.61
V34/27	4	64.99	257	3.11	60	89	9.21	139	0.18
V34/27	5		322	3.75	0	0	8.75	345	1.23
V34/27	6		288	3.72	0	104	4.03	150	0.06
V34/27	7		269	3.25	0	84	7.30	127	0.06
V34/27	8		271	3.27	0	50	8.80	203	0.06
V34/27	9		247	4.45	0	118	4.40	111	0.01
V34/27	10		193	3.48	0	26.4	9.12	112	0.59
Fill Sol.		88.30	193	2.61					
Ambient SW 1800 m		34.60	181	2.88					
Ambient SW Blw 1800 m				2.97					

Table A2d: Concentrations of salinity, Si, P, Fe, and Mn in the supernates of the sediment trap cylinders for traps 17, 30, and 34 on mooring V43 at the time of recovery on board ship; and the volumes of the remaining supernates and the concentrations of Fe and Mn in the remaining supernates just prior to processing particles onto filters.

		Supernate at Recovery					Splitting Solution at Processing (t2)		
Mooring/ Trap	Sampling Jar	Sal ppt	Si µM	P µM	Fe nM	Mn nM	Sal ppt	Si µM	P µM
V43/17	1	54.98	168	5.84	<61	<21	0.059	177	26
V43/17	2	56.24	207	26.55	<61	43	0.054	367	117
V43/17	3	45.35	330	6.84	107	43	0.076	661	91
V43/17	4	36.45	230	4.33	<61	63	0.051	371	72
V43/17	5	54.21	139	5.61	<61	63	0.070	645	45
V43/17	6	56.39	248	4.53	<61	57	0.067	260	63
V43/17	7	50.05	226	6.85	<61	37	0.052	1107	151
V43/17	8	56.10	233	4.67	<61	<21	0.072	65	<21
V43/17	9	35.36	255	1.35	<61	<21	0.049	54	<21
V43/17	10	no sample							
V43/30	1	45.91	223	4.68	815	<21	0.078	445	<21
V43/30	2	47.21	226		435	<21	0.073	289	<21
V43/30	3	51.33	338		431	88	0.098	399	32
V43/30	4	49.71	220	3.29	303	127	0.078	406	67
V43/30	5	53.26	223	3.29	305	90	0.058	947	163
V43/30	6	60.23	214	3.13	235	82	0.068	276	127
V43/30	7	37.99	48	3.43	370	41	0.065	459	52
V43/30	8	49.41	154	4.26	293	<21	0.057	233	<21
V43/30	9	56.03	163	3.92	<34	57		<34	32
V43/30	10								
V43/33	1	36.61	263	5.16	1205	910	0.082	12641	5692
V43/33	2	54.82	293	4.74	850	116	0.084	163	84
V43/33	3	54.33	346	7.54	830	164	0.079	727	220
V43/33	4	35.35	210	7.87	1913	2902	0.072	1419	4491
V43/33	5	46.10	260	3.63	523	196	0.083	400	
V43/33	6	51.00	205	3.62	<34	200	0.087	<34	132
V43/33	7	54.30	303	4.43	1221	210	0.074	384	242
V43/33	8	49.22	246	3.43	738	140	0.072	107	87
V43/33	9								
V43/33	10								
V43/34	1	53.10	223	5.43	417		0.057	1741	93
V43/34	2	44.13	201	4.65	936	<21	0.048	3838	115
V43/34	3	56.10	195	8.74	234	85	0.072	1288	212
V43/34	4	54.30	212	15.24	473	140	0.058	897	108
V43/34	5	55.34	181	5.48	370	174	0.057	915	119
V43/34	6	60.21	181	4.91	302	100	0.059	788	181
V43/34	7	52.18	171	1.53	110	107	0.062	1107	182
V43/34	8	56.54	183	2.72	241	107	0.059	420	99
V43/34	9	59.03	160	3.47	249	110	0.054	340	38
V43/34	10								
Filling		88.30	122	2.06					
Ambient		34.60	181	2.97					

Table A3: Si, P, Fe, and Mn in sediment trap supernates expressed as flux (mg m^{-2} day^{-1}).

		Si	P	Fe	Mn
Mooring	Sample No.	(mg/m^2/day)			
V23/13	2	0.12	0.0237	0.0008	0.0939
V23/13	3	0.82	0.0022	0.0009	0.0484
V23/13	4	0.44	0.0267	0	0.0235
V23/13	5	0.62	0.0222	0.0102	0.0235
V23/13	6	0.22	–0.0056	0	0.0168
V23/13	7	0.06	0.0249	0.0048	0.0099
V23/13	8	0.77	–0.0019	0	0.0079
V23/13	9	1.54	0.0289	0	0.0072
V23/13	10	1.06	0.0188	0	0.0052
V26/30	1	0.41	0.0089	0.0278	
V26/30	2	2.32	0.0667	0.0026	0.0004
V26/30	3	3.85	0.0772	0.0073	0.0003
V26/30	4	2.04	0.0069	0.0030	0
V26/30	5	0.76	0.0246	0	0
V26/30	6	0.11	0.0790	0.0039	0
V26/30	7	3.29	0.0663	0	0.0035
V26/30	8	4.42	0.1181	0	0.0020
V26/30	9	3	0.0198	0	0
V26/32	1	1.48	0.0303	0.0042	0
V26/32	2	2.18	0.0413	0.0059	0
V26/32	3	3.88	0.0987	0.0717	0.0060
V26/32	4	3.54	0.0269	0.0102	0.0008
V26/32	5	0.59	0.0243	0.0035	0.0006
V26/32	6	1.48	0.0215	0	0.0002
V26/32	7	3.11	0.0630	0	0.0004
V26/32	8	4.49	0.0939	0.0042	0.0002
V26/32	9	1.15	0.0208	0	0
V26/36	1	1.64	0.0128	0.0130	0
V26/36	2	2.52	0.0090	0.0087	0
V26/36	3	3.33	0.0089	0.0552	0.0043
V26/36	4	3.55	0.0680	0.0012	0
V26/36	5	3.48	0.0083	0.0271	0.0015
V26/36	6	0.57	0.0090	0.0017	0
V26/36	7	3.43	0.0187	0.0040	0
V26/36	8	4.23	0.0784	0.0717	0.0137
V26/36	9	3.79	0.0969	0.1398	0.0113
V34/15	1	3.44	0.0340	0	0.0023
V34/15	2	2.18	0.0210	0.0005	0.0016
V34/15	3	4.62	0.2350	0.0009	0.0015
V34/15	4	6.82	0.0690	0.0016	0.0019
V34/15	5	0.0005	0.0018		
V34/15	6	7.81	0.0910	0	0.0018
V34/15	7	3.53	0.1170	0.0064	0.0030
V34/15	8	6.53	0.1020	0.0011	0
V34/15	9	4.07	0.0190	0	0
V34/15	10	0.76	0.0160	0	0

Table A3: (continued)

Mooring	Sample No.	Si	P	Fe	Mn
		(mg/m^2/day)			
V34/30	1	14.18	0.019	0.0009	0.0007
V34/30	2	4.32	0.007	0.0031	0.0110
V34/30	3	7.13	0	0.0046	0.0056
V34/30	4	6.61	0.013	0.0041	0.0065
V34/30	5	0			
V34/30	6	7.40	0.011	0	0.0064
V34/30	7	6.25	0.024	0	0.0046
V34/30	8	4.57	0.027	0	0.0031
V34/30	9	1.90	0.418	0.0046	0.0024
V34/30	10	5.29	0.049	0	0.0040
V34/27	1	3.04	–0.006	0	0
V34/27	2	3.84	0.028	0.0022	0.0030
V34/27	3	4.85	0.031	0.0035	0.0047
V34/27	4	4.60	0.004	0.0032	0.0047
V34/27	5	12.75	0.054	0	0
V34/27	6	6.54	0.023	0	0.0055
V34/27	7	4.76	0.006	0	0.0044
V34/27	8	7.37	0.002	0	0.0026
V34/27	9	3.57	0.044	0	0.0062
V34/27	10	2.48	0.023	0.0014	
V43/17	1	0.06	0.0211	0.0007	1.00E-04
V43/17	2	0.30	0.1575	0.0013	0.0009
V43/17	3	0.96	0.0266	0.0046	0.0009
V43/17	4	0.30	0.0091	0.0012	0.0010
V43/17	5	–0.12	0.0195	0.0030	0.0009
V43/17	6	0.54	0.0127	0.0011	0.0009
V43/17	7	0.37	0.0272	0.0038	0.0009
V43/17	8	0.45	0.0136	0.0003	0
V43/17	9	0.45	–0.0106	0.0002	0
V43/30	1	0.32	0.0125	0.0120	0
V43/30	2	0.35	0.0065	0	0
V43/30	3	1.05	0.0077	0.0012	0.0012
V43/30	4	0.33	0.0038	0.0057	0.0018
V43/30	5	0.37	0.0042	0.0072	0.0017
V43/30	6	0.36	0.0039	0.0040	0.0015
V43/30	7	–0.77	0.0034	0.0064	0.0007
V43/30	8	–0.06	0.0101	0.0043	0
V43/30	9	0.03	0.0086		
V43/33	1	0.50	0.0146	0.0826	0.0409
V43/33	2	0.80	0.0139	0.0110	0.0018
V43/33	3	1.11	0.0322	0.0136	0.0030
V43/33	4	0.18	0.0323	0.0294	0.0548
V43/33	5	0.55	0.0056	0.0084	0.0023
V43/33	6	0.25	0.0061	0	0.0031
V43/33	7	0.86	0.0118	0.0164	0.0036
V43/33	8	0.48	0.0047	0.0093	0.0020
V43/33	9				

Table A3: (continued)

		Si	P	Fe	Mn
Mooring	Sample No.	(mg/m^2/day)			
V43/34	1	0.37	0.0182	0.0115	0.0003
V43/34	2	0.18	0.0121	0.0232	0.0004
V43/34	3	0.22	0.0403	0.0089	0.0020
V43/34	4	0.31	0.0829	0.0090	0.0020
V43/34	5	0.14	0.0188	0.0078	0.0025
V43/34	6	0.17	0.0156	0.0066	0.0019
V43/34	7	0.06	–0.0075	0.0058	0.0020
V43/34	8	0.16	0.0008	0.0045	0.0016
V43/34	9	0.03	0.0060	0.0042	0.0014